Detecting, Identifying, and Disrupting Protein–Protein Interactions

by

Sang-Hyun Park

A dissertation submitted in partial fulfillment

of the requirements for the degree of

Doctor of Philosophy

(Biochemistry)

at the

UNIVERSITY OF WISCONSIN – MADISON

1999

A dissertation entitled

Detecting, Identifying, and Disrupting Protein–Protein Interactions

submitted to the Graduate School of the
University of Wisconsin-Madison
in partial fulfillment of the requirements for the
degree of Doctor of Philosophy

by

Sang-Hyun Park

Date of Final Oral Examination: December 13, 1999

Month & Year Degree to be awarded: **December** 1999 **May** **August**

Approval Signatures of Dissertation Readers:

Signature, Dean of Graduate School

Virginia S. Hinshaw / EH

Readers' Page: This page is not to be hand-written except for the signatures

ACKNOWLEDGMENTS

I am grateful to James Hu, Jordan Tang and Martin Chalfie for providing bacterial strains and plasmids. I also thank Chiwook Park for providing the wild-type RNase A used in Chapter 3. Ronald Raines has been a superior advisor. I thank Ron for his support for my study. He allowed for the freedom of creativity and the freedom of work hour. Genetic selection and screens developed in this thesis owes a lot to frustrations with the yeast two-hybrid screening on which I spent the first two years of my graduate study. This thesis was partially supported by a Korean Government Fellowship for Overseas Study.

I must thank my family for their patience and support for my studying abroad. I cannot thank enough my wife, Nam-Sook Baik, who has endured a great deal of agony and joy together with me throughout the days in Madison. I want to say sorry to my son, Albert (건우), for my occasional absence from him when he needed me. Finally, I thank my mother for her enthusiasm in life, her endless love of family, and who I am. Without support from my family, this thesis would not have existed.

이 논문을 나로하여금 존재하게 해주신, 나의 어머니께 드립니다. 이 논문이 어머님이 보여주신 이해와 사랑에 대한 미미한 보답이라도 되기를 바랍니다. 그리고 지난 6 년간 여러 어려움 속에서도 꿋꿋이 인내해준 나의 아내 백남숙에게 감사를 보냅니다. 아내의 인내와 이해없이는 이 논문은 존재하지 않았을 겁니다.

일천구백구십구년 겨울 매디슨에서, 박상현 씀.

ABSTRACT

Protein–protein interactions have critical roles in many biological processes. We describe here the development of new approaches to detect, identify, and disrupt specific protein–protein interactions. First, for the disruption of the interactions, a genetic selection was developed to select for dissociative inhibitors of dimeric enzymes from a genetically encoded combinatorial peptide library. The validity of the approach was confirmed by identification of an inhibitor of HIV-1 protease. A peptide selected by *in vivo* screening demonstrated the true dissociative inhibition by both kinetic and biochemical analyses. Second, a genetic screen is described to analyze the interaction between ribonuclease A (RNase A) and the ribonuclease inhibitor (RI) protein. An epitope library of RNase A was created and screened for epitopes that interact with RI. Third, green fluorescent protein fusions were used to detect and assess the strength of a protein–protein interaction. Two methods, fluorescence gel retardation and fluorescence polarization, are described to study the interaction of S-protein and S-peptide in ribonuclease S. Combined together, these new approaches provide powerful tools to study protein–protein interactions and to discover therapeutic agents targeting specific protein–protein interactions.

TABLE OF CONTENTS

LIST OF FIGURES

LIST OF TABLES

ABBREVIATIONS

Ac	acetyl
ATP	adenosine triphosphate
ATPγS	adenosine 5'-O-(3-thiotriphosphate)
BSA	bovine serum albumin
bp	base pairs
CAPS	3-(cyclohexylamino)-1-propanesulfonic acid
dATP	deoxyadenosine triphosphate
DABCYL	4-(4'-dimethylaminophenylazo)benzoic acid
DMF	dimethyl formamide
DTT	dithiothreitol
dTTP	deoxythymidine triphosphate
EDANS	5-(2'-aminoethylamino)naphthalene-sulfonic acid
EDTA	ethylenediaminetetraacetic acid
ELISA	enzyme-linked immunosorbent assay
F-moc	9-fluorenylmethoxycarbonyl
HBVS	1,6-hexane-*bis*-vinylsulfone
HEPES	N-(2-hydroxyethyl)piperazine-N'-(2-ethanesulfonic acid)
HPLC	high-performance liquid chromatography
FPLC	fast protein liquid chromatography
5-IAF	5-iodoacetamidofluorescein

IgG	immunoglobulin G
IPTG	isopropyl β-D-thiogalactoside
LB	Lauria-Bertani
MES	2-(N-morpholino)ethanesulfonic acid
PAGE	polyacrylamide gel electrophoresis
PBS	phosphate buffered saline
PCR	polymerase chain reaction
PEG	polyethylene glycol
pfu	plaque-forming unit
PMSF	phenylmethylsulfonyl fluoride
poly(C)	polycytidylic acid
poly(dI-dC)	polydeoxyinosinic-polydeoxycytidylic acid
PR	protease
SDS	sodium dodecyl sulfate
TBE	tris-borate-EDTA
TCEP	Tris(2-carboxyethyl)phosphine
TFA	trifluoroacetic acid
Tris	tris(hydroxymethyl)aminomethane
Trx	thioredoxin
UV	ultraviolet
X-Gal	5-bromo-4-chloro-3-indolyl-β-D-galactoside

Chapter 1

Introduction

1.1 OVERVIEW

Interactions between biopolymers play critical roles in cellular processes. In particular, protein–protein interactions provide a widespread mechanism by which the flow of inter- and intracellular information is governed. Such interactions and their roles are well characterized for many biological processes, including signal transduction, cell-cycle regulation, gene regulation, viral assembly and replication, and the formation of hormone–receptor and antibody–antigen complexes. Furthermore, many enzymes exert and regulate their catalytic activities by forming quaternary complexes assembled from monomeric subunits. Intersubunit interactions are vital to the function of allosteric proteins, as demonstrated in the binding of oxygen by hemoglobin.

Abnormal protein–protein interactions are also important in various disease processes. The conversion of the *neu* gene into an oncogene apparently occurs when mutations in the Neu receptor protein favor dimerization, which activates the tyrosine kinase domain of the protein (Sternberg & Gullick, 1989). The impact of an unwanted protein–protein interaction is also apparent in the classical example of the variant hemoglobin in patients with sickle cell anemia (Ingram, 1957; Watowich et al., 1993). Less specific protein–protein interactions occur when proteins aggregate. Amyloid fibrils composed of aggregated protein form in the tissues in several diseases including Alzheimer's and rheumatoid arthritis (Sipe, 1992; Cohen, 1994).

The loss of a protein–protein interaction can have undesirable consequences as well. The oxidation of a specific methionine in R-1-proteinase inhibitor (also known as R-1-

antitrypsin) obstructs its binding to various proteases, including elastase, which in turn appears to lead to the development of adult respiratory distress syndrome and emphysema (Johnson & Travis, 1979; Evans & Pryor, 1994). Signal transfer among neurons is operated by neurotransmitters released by synaptic vesicles. Both synaptic vesicle trafficking and neurotransmitter release are mediated by a series of specific interactions among cytoskeletal, synaptic vesicle, presynaptic membrane, and cytosolic proteins. The majority of these interactions are mediated by specific protein modules and domains that are found in many proteins (Benfenati et al., 1999).

1.2 CHARACTERISTICS OF PROTEIN INTERFACES

The interaction of proteins with small-molecule ligands typically occurs in small clefts in a key-and-lock fashion. In contrast, protein–protein interactions occur over a large surface area, which is relatively flat. The molecular interfaces of protein complexes often compromise a substantial fraction of the surface area of the monomers involved in the complexes. For example, the size of interface area per subunit in dimeric proteins has been found to vary from 368 $Å^2$ to 4761 $Å^2$ (Jones & Thornton, 1995) and to correlate with the surface area and the molecular weight of the subunits.

The secondary structure of interface regions has been analyzed. It is known that there is an approximately equal proportion of helical, strand, and turn structures involved (Tsai et al., 1996). Some interfaces contain only one type of structure, but most are mixed.

Interestingly, the distribution of secondary structures in interfaces more closely resembles the distribution found in the exterior rather than the interior of proteins (Argos, 1988). The interfaces involving β-sheets fall into three categories: those that interact by extending the sheet through classic backbone–backbone hydrogen bonds (as in HIV-1 protease), those in which sheets stack on top of one another as in subtilisin inhibitor homodimer (Mitsui et al., 1979), and mixed structures of extended and stacked conformation as in superoxide dismutase (Tainer et al., 1982).

It is often assumed that proteins associate through hydrophobic patches on their surfaces. The abundance of hydrophobic amino acid residues at interfaces could give an indication of the role of hydrophobicity in the stability of a complex. It has been revealed that hydrophobic residues are found more commonly at the interfaces of homodimers than at those of heterocomplexes (Jones & Thornton, 1996). The lower abundance of hydrophobic residues in heterocomplex (for example, antibody–protein antigen) interfaces is balanced by a high abundance of polar residues. One possible explanation for this difference is that most homodimers rarely occur or function as monomers. In contrast, monomers in heterocomplexes must be able to maintain a stable native fold. Interfaces are more hydrophobic than protein exteriors in general, yet more polar than protein interiors (Tsai et al., 1996).

The number of hydrogen bonds and Coulombic interactions in protein–protein interfaces is quite variable, though roughly proportional to the interface size. On average, one hydrogen bond is found in each 200 $Å^2$ of interface surface (Janin et al., 1988). The nature of these hydrogen bonds differs, however, depending on the type of complex. For

example, the interfaces of oligomeric proteins, including antibody–protein antigen complexes carry hydrogen bonds mostly between sidechains. Yet, two-thirds of hydrogen bonds in protease–inhibitor complexes involve mainchain atoms (Janin & Chothia, 1990).

1.3 METHODS TO DETECT PROTEIN–PROTEIN INTERACTIONS

Many problems in modern biology involve complex networks of interacting proteins. As some of these interactions are weak and transient and may involve the formation of multiprotein complexes, the strength of individual interactions can vary greatly. This variation makes the detection of protein–protein interactions inherently more difficult than that of other macromolecular interactions. The ability to detect and identify protein–protein interactions is desirable because the identification of an interacting partner of a protein can reveal the biological function of the protein as well as its place in the network of protein–protein interactions. To this end, a variety of biochemical and genetic approaches have been developed for detection and identification of such interactions.

Traditional biochemical approaches to identify protein–protein interactions involve techniques such as immunocoprecipitation, chemical crosslinking, and affinity copurification. Immunocoprecipitation experiments using antibodies can reveal an affinity between two proteins, albeit *in vitro* following cell lysis under conditions that cannot determine whether two proteins were within the same cellular compartment. Methods for crosslinking proteins within the cell and cofractionating them by affinity

chromatography have also proven useful. Nonetheless, purification, sequencing and identification of the crosslinked proteins can be difficult because of the small quantities obtainable. Expression screening of cDNA libraries allows for identification of interacting proteins (Sambrook et al., 1989). Generally, proteins encoded from cDNAs are immobilized onto a filter, which is then probed with the target protein. Detection of the target protein can be done by either immunochemical or radioisotopic methods. All of these traditional methods can be time-consuming and labor-intensive.

In contrast to the biochemical screens, the yeast two-hybrid system has been useful for detecting and identifying protein–protein interactions *in vivo* (Fields & Song, 1989). The approach takes advantage of the characteristics of a transcriptional activator protein, GAL4, from the yeast *Saccharomyces cerevisiae*. The GAL4 protein contains two distinct and separate domains: a DNA-binding domain and a transcription activation domain (Keegan et al., 1986). When two interacting proteins X and Y are fused to the DNA-binding domain and transcription activation domain, a functional transcription activator is reconstructed through the interaction between X and Y. The reconstructed activator triggers transcription of reporter genes such as *lacZ*, whose phenotype is easily detectable. The initial study by Fields and Song merely demonstrated an interaction between two known proteins (SNF1 and SNF4), but the method has proven more popular as a tool to screen libraries in order to identify and isolate genes encoding proteins that interact with a protein of interest (Chien et al., 1991). Traditionally, this process has required extensive biochemical assays and genetic screens. Using reporter genes required for the growth of yeast (such as *LEU2* and *HIS3*) has enabled the creation of powerful

growth selections to screen large libraries (Durfee et al., 1993; Gyuris et al., 1993). Over the past ten years, the two-hybrid system has been used extensively to detect and identify a number of protein–protein interactions, most of which were previously unknown. Several variations of the original two-hybrid system have been made to broaden its ability to detect protein–DNA interactions (one-hybrid system) (Li & Herskowitz, 1993), and protein–RNA interactions (three-hybrid system) (SenGupta et al., 1996; Zhang et al., 1999). Although the two-hybrid system is a useful genetic technique to detect protein–protein interactions, it has limitations. Because the hybrid proteins are targeted to the nucleus, interactions that require post-translational modifications are not likely to be detected. Two-hybrid screens often generate a number of false positives that must be eliminated by time-consuming processes if they can be eliminated at all. More general problem is to determine whether interaction identified by genetic methods are actually due to the biochemical association of the encoded proteins *in vivo*.

A powerful approach to identify small peptide ligands to a known protein *in vitro* uses a filamentous bacteriophage, and is called the phage display system (Smith, 1985). This method exploits the fact that peptides or small proteins may be incorporated on the surface of phage molecules as fusions to coat proteins. In the method, small peptides from a random or an epitope library are fused to a phage coat protein, (pVIII) or a tail protein (pIII) and displayed on phage particles. Next, a phage library is enriched for members that bind to an immobilized target by panning. Multiple rounds of amplification and panning enable the enrichment of ligands by orders of magnitudes, making this approach very powerful. Target molecules that can be used in phage display system are

not limited to proteins or polypeptides. Screens can be directed against DNA, RNA, or organic molecules as well (Rebar & Pabo, 1994). Monovalent phage display is an advance in this technology that enables the isolation of ligands with higher affinity (Lowman et al., 1991; Matthews & Wells, 1993). Another application of the method is the display of proteins encoded by a cDNA library to identify proteins that interact with a target protein (Crameri et al., 1994). In addition to identifying protein–protein interactions, the method can be used to identify protease substrates. Foe example, sequences with high specificity to subtilisin and factor Xa were discovered using a library of random peptides located between phage particle and affinity tag (Matthews & Wells, 1993).

A few other methods have been developed to identify interacting partners. These approaches sought ways to physically couple a gene to its encoded peptide or protein to facilitate cloning after screening. For instance, tight binding *lac* repressor (Cull et al., 1992) and polysomes (Mattheakis et al., 1994) were used to display polypeptides and to isolate ligands to target proteins of interest.

In this thesis, I developed novel approaches to explore protein–protein interactions. Chapter 2 describes a genetic selection for dissociative inhibitors of designated protein–protein interactions from an encoded combinatorial peptide library. The homologous dimerization of HIV-1 protease was chosen as a target. Chapter 3 describes an *in vivo* method to dissect a known protein–protein interaction. Interaction of ribonuclease A and the ribonuclease inhibitor protein was used as an example. Chapter 4 describes two *in vitro* approaches to monitor protein–protein interactions using green fluorescent protein.

Complex formation of S-protein and S-peptide from ribonuclease S was analyzed using the methods.

1.4 HIV-1 PROTEASE DIMER

The human immunodeficiency virus type 1 (HIV-1), an etiological agent of acquired immunodeficiency syndromes (AIDS), is a member of the Retroviridae family (Gallo et al., 1984; Wong-Staal & Gallo, 1985). The HIV-1 genome is comprised of the same overall *gag-pol-env* genes as seen in other retroviruses, and these genes are necessary for viral replication (Ratner et al., 1985; Wain-Hobson et al., 1985). During viral replication, these genes are translated into polyproteins that undergo enzymatic cleavage to generate 15 viral proteins including protease, reverse transcriptase, integrase, and other structural or regulatory proteins (Frankel & Young, 1998). A protease is responsible for autoproteolytic release of itself from a *gag-pol* polyprotein and proteolytic maturation of the other viral proteins. This protease, HIV-1 protease, is essential to the maturation and infectivity of HIV as indicated by the production of non-infectious, replication-deficient virions by virus variants with inactive protease (Kohl et al., 1988). The critical role of the protease in virus infectivity has made it a prime target for development of antiviral agents and one of the most extensively characterized proteins to date.

HIV-1 protease (HIVPR) is a dimeric enzyme of two identical subunits, which consist of 99 amino acid residues. The active site is formed at the dimer interface with each

monomer contributing a catalytically essential aspartic acid (Asp25). The amino acid sequence around the active site contains a triad of residues, Asp-Thr-Gly, which is well conserved in the aspartyl protease family (Katoh et al., 1987). HIV-1 protease and other retroviral proteases also exhibit other characteristics of aspartic proteases, such as inhibition by pepstatin (Seelmeier et al., 1988) and inactivation by replacement of the active-site aspartate residues (Katoh et al., 1985; Kohl et al., 1988).

Numerous inhibitors to HIVPR have been designed and developed for the purpose of treating AIDS. The main strategy in the development of HIVPR inhibitors has been the design of inhibitors that compete with natural substrates for the same active site and substrate-binding pocket. Several drugs have already been approved by the US Food and Drug Administration (FDA), including ritonavir (Abbott), saquinavir (Hoffman-La Roche), and indinavir (Merck). Many others are in advanced clinical trials. Yet, high rates of viral turnover in HIV infection and the inability of HIV reverse transcriptase (RT) to correct transcriptional errors result in viral strains that are resistant to the inhibitors (Condra, 1998). It has been shown that the clinical use of RT inhibitors leads to the rapid development of drug resistance and cross-resistance against different RT inhibitors (Schinazi et al., 1997).

The structures of many liganded or unliganded HIVPR's have been determined at atomic resolution and resulted in a huge collection of data for structure-function relationships of the protease (Vondrasek & Wlodawer, 1997). The atomic structures of native HIVPR are known for both recombinant and synthetic enzymes, and confirm that the molecule is homodimer and that its active site resembles closely that of other aspartic

proteases (Lapatto et al., 1989; Wlodawer et al., 1989). Figure 1.1 shows a schematic view of the three-dimensional structure of HIVPR with labeled elements of secondary structure.

The general topology of the HIVPR monomer is similar to that of a single domain in pepsin-like aspartic proteases, with the main difference being that the dimer interface in the former is made up of four short strands, rather than the six long strands present in the pepsins. Each subunit of protease consists of nine β-strands and one α-helix (Table 1.1). Most of structure of HIVPR consists of β-strands arranged in a simple, symmetrical way. The N-terminal β-strand *a* (residues 1–4) forms the outer part of the interface β-sheet. The β-strand *b* (residues 9–15) continues through a turn into β-strand *c*, which terminates at the active-site triad (Asp25-Thr26-Gly27). Following the active-site loop is β-strand *d*, containing residues 30–35. The second half of subunit is topologically related to the first half by an approximate intramolecular two-fold axis. Residues 43–49 form β-strand *a′*, which, as in pepsin-like proteases, belongs to the flap. The other strand in the flap (residues 52–58) forms a part of the long β-chain *b′* (residues 52–66). The β-chain *c′* comprises residues 69–78 and, after a loop at residues 79–82, continues as strand *d′* (residues 83–85), which leads directly to the well-defined helix *h′* (residues 86–94). Strand *a* and a terminal strand *q* (residues 95–99) form a four-stranded anti-parallel β-sheet with the two equivalent strands from the other subunit of dimer.

At the hydrophobic interface of HIVPR dimer is an anti-parallel β-sheet formed by strands *a*, *a′*, *q* and *q′*, which consists of an extensive network of backbone hydrogen

bonds and accounts for more than 50% of intersubunit contacts (Figure 1.2). The values of equilibrium dissociation constant (K_d) of HIVPR dimer have been reported to be in the range of 10^{-7} to 10^{-10} M depending on the conditions under which measurements were made. Thermodynamic analyses of HIVPR revealed that interactions at the dimer interface are major stabilizing force of dimeric structure and thus native monomers have low conformational stability (Todd et al., 1998). These conclusions are consistent with the experimental observation that no monomeric intermediates are detectable during thermal unfolding or urea denaturation experiments (Grant et al., 1992).

Because dimerization is a prerequisite for the enzymatic activity of HIVPR, a novel approach for inhibiting protease activity is to interfere with dimer formation (Weber, 1990; Schramm et al., 1991; Zhang et al., 1991; Schramm et al., 1992). In dissociative inhibition, the inhibitor binds to the protease monomers at the interface and prevents their correct assembly into active enzyme. Detailed kinetic analyses indicate that the C-terminal tetrapeptide from HIVPR (Ac-Thr-Leu-Asn-Phe) is a true dissociative inhibitor of the enzyme (Zhang et al., 1991). Other peptides from both β-sheet forming terminal segments also inhibit protease activity (Babe et al., 1992; Franciskovich et al., 1993; Schramm et al., 1993; Schramm et al., 1996). The dissociative inhibition of enzymatic activity by interfering with subunit interactions has also been successfully applied to ribonucleotide reductase from herpes simplex virus (Dutia et al., 1986) and HIV-1 reverse transcriptase (Divita et al., 1994).

There are reasons for focusing on the dissociative inhibition of HIVPR for the development of anti-AIDS agents. First, the hydrophobic interface created by N- and C-

termini may be less prone to mutational escape than the solvated active site or substrate binding regions. Second, a comparison of the three-dimensional structures and amino acid compositions of HIVPR and other retroviral proteases reveal that most amino acid residues in the interface are highly conserved and that overall folds are nearly identical (Miller et al., 1989). Third, dissociative inhibitors may act on polyprotein precursors and prevent formation of active viral proteins.

As many of protein–protein interactions play critical roles in signal transduction and disease development, it is desirable to develop a general strategy to disrupt a protein–protein interaction of interest. Directed interruption of specific interactions or multisubunit enzymes would be an invaluable tool for the development of a novel class of inhibitors as well as for the control of cellular processes. In Chapter 2, we describe a novel genetic selection from an encoded combinatorial peptide library of dissociative inhibitors of protein–protein interactions. HIV-1 protease was chosen as a model because it is of great therapeutic interest and also provides the simplest mode of protein–protein interaction, homodimerization. Positive isolates from the selection were examined by a high-throughput screening method, which complements the *in vivo* screening, for an independent assessment of inhibitory activity. New dissociative inhibitors of HIVPR were successfully isolated and identified using these approaches.

1.5 RNASE A•RI COMPLEX

Bovine pancreatic ribonuclease A (RNase A; EC 3.1.27.5) catalyzes the hydrolysis of single-strand RNA. Exceptional chemical stability and availability in large quantity have made this enzyme one of the most extensively studied proteins for the last several decades. RNase A has been used as a model system in numerous studies of protein structure-function relationships, protein folding, conformational stability, and molecular evolution (Raines, 1998). RNase A also served as the example in the landmark work of Anfinsen that the primary sequence of a protein determines its ternary structure, which led to his Nobel Prize in Chemistry in 1972 (Anfinsen, 1973). This prize was shared with Stein and Moore, who determined the amino acid sequence of RNase A (Moore & Stein, 1973). RNase A was one of the first proteins whose three-dimensional structure was determined to the atomic level by either X-ray crystallography or nuclear magnetic resonance (NMR) techniques (Kartha et al., 1967; Santoro et al., 1993).

Although the biochemical and biophysical properties of RNase A are well understood, its biological functions inside a cell are still ambiguous. In an earlier study, it was proposed that the enzyme could have a digestive role in ruminants (Barnard, 1969). Still, a ribonuclease could be cytotoxic due to its ability to hydrolyze cellular RNA. Even though RNase A is not cytotoxic, some if its homologs appear to have interesting biological roles including anti-tumor activity and angiogenic activity (Matousek, 1973; Fett et al., 1985). Bovine seminal RNase (BS-RNase), a homolog of RNase A isolated from bull semen, is cytotoxic to certain tumor cell types (Matousek, 1973). Other cytotoxic homologs of RNase A were isolated from embryos of various frogs such as bullfrog *Rana catesbeiana* (Liao, 1992), rice paddy frog *Rana japonica* (Kamiya et al.,

1990), and leopard frog *Rana pipiens* (Ardelt et al., 1991). All of these amphibian ribonucleases are cytotoxic to certain tumor cells *in vitro* and *in vivo*. The mechanism of cytotoxicity of these ribonucleases could involve binding to the cell surface, internalization into cytosol and degradation of cellular RNA (Kim et al., 1995; Wu et al., 1995). A key to the RNA-degrading step is evasion of ribonuclease inhibitor (RI) (Leland et al., 1998).

RI is a 50-kDa protein present in the cytosol of mammalian cells. Mammalian RI's are highly conserved. For example, porcine RI (pRI) and human RI (hRI) share 77% amino acid sequence identity (D'Alessio & Riordan, 1998). Both RI's are acidic and contain 15 leucine-rich βα repeats, which assemble into a horseshoe-like shape. It forms 1:1 noncovalent complex with target ribonucleases, including RNase A. The RI•RNase A complex is one of the tightest protein–protein interactions in nature with a value of K_d in the fM range (Vicentini et al., 1990). The three-dimensional structure of the RI•RNase A complex (Figure 1.3) revealed that the tight interaction is due largely to hydrogen bonds and Coulombic interactions (Kobe & Deisenhofer, 1995). According to the structure, one-third of RNase A is buried within the RI horseshoe including the active site of the enzyme, which docks with the C-terminal end of RI.

The biological role of RI is yet to be fully understood, but several possibilities have been suggested. First, RI may be involved in the regulation of amounts of cellular RNA's by inhibiting the endogeneous ribonucleases in the cytosol (Roth, 1962). Second, RI could be a safeguard of cellular RNA's against secretory ribonucleases inadvertently appearing in the cytosol (Beintema et al., 1988). Finally, RI regulates formation of blood

vessels by inhibiting the activity of angiogenin (Lee & Vallee, 1989). The ability to evade RI appears to be a key attribute of the cytotoxicity of RNase A and its homologs (Leland et al., 1998). The lack of cytotoxicity of RNase A is due to the formation of an unusually tight complex with RI in the cytosol. Likewise, the cytotoxicity of BS-RNase and frog ribonucleases seems to be a consequence of their ability to escape trapping by RI. BS-RNase forms a dimer that is not inhibited by RI. Onconase, a cytotoxic RNase from leopard frog, still evades RI as a monomer. Onconase escapes RI with truncation in surface loops whose counterparts in RNase A are critical to the complex formation.

Even though the crystalline structure of RI•RNase A complex provides with great details of intermolecular interactions, it is still unclear which residues or segments of RNase A are most important in complex formation. To address this question, we developed a novel epitope screening method and tested the method to dissect RI–RNase A interaction, as described in Chapter 3. We expect that the information obtained by the epitope screen could help to generate small-molecule antagonists of RNase A as well as contribute to the understanding of ribonuclease cytotoxicity.

1.6 S-PEPTIDE•S-PROTEIN COMPLEX OF RIBONUCLEASE S

Treatment of RNase A with subtilisin results in the cleavage of a peptide bond between residue 20 and 21 (Richards & Vithayathil, 1957). The cleavage product, ribonuclease S (RNase S, Figure 1.4), consists of two tightly associated fragments: S-

peptide (residue 1 - 20) and S-protein (residue 21 - 124). Neither fragment alone is catalytically active because two critical active site residues, His12 and His119, are located in separate fragments. Nonetheless, a noncovalent complex formed by two fragments, RNase S, is as active as intact RNase A. The values of K_d of RNase S have been estimated to be in the range of μM to nM, depending on the solution condition. Conditions such as high pH (Schreier & Baldwin, 1976) and low ionic strength (Schreier & Baldwin, 1977) favor complex formation and stabilize the resulting complex. Numerous hydrophobic interactions and hydrogen bonds between S-protein and S-peptide are responsible for the stability of the noncovalent complex. The S-peptide–S-protein interaction has served as a model system in many studies in protein chemistry, including chemical amplification of enzyme activity (Cecchini et al., 1986), development of sequence-specific ribonucleases (Zukermann & Schultz, 1988) and a fusion protein system (Kim & Raines, 1993), and studies of protein ubiquitination (Gosink & Vierstra, 1995).

Green fluorescent protein (GFP) is a spontaneously fluorescent protein isolated from jellyfish *Aequorea victoria* (Morin & Hastings, 1971). Its biological role is to transduce blue luminescence by another protein, aequorin, into green fluorescent light. The GFP chromophore consists of a cyclic tripeptide derived from Ser-Tyr-Gly and is only fluorescent when embedded within the complete GFP protein (Cody et al., 1993). The fluorophore is formed by post-translational modifications, including cyclization and oxidation by molecular oxygen (Heim et al., 1994). These steps are autocatalytic and do not require cofactors.

Although GFP was first crystallized in 1974 (Morise et al., 1974) and diffraction patterns were reported in 1988 (Perozzo et al., 1988), the structure was first solved in 1996 independently by Ormö and coworkers (Ormö et al., 1996) and by Yang and coworkers (Yang et al., 1996). The atomic structures revealed that the protein is composed of an 11-stranded β-barrel threaded by an α-helix running up the axis of the cylinder (Figure 1.5). The chromophore is attached to the α-helix and is buried almost perfectly in the center of the cylinder, which has been called a β-can. The rigid shell in GFP surrounding the chromophore enables it to be fluorescent and protects it from photobleaching but also hinders environmental sensitivity.

Physical and chemical properties of wild type GFP have been known since the early 1970's and reveal several important characteristics. It is exceptionally stable to heat (T_m = 70 °C), alkaline pH, detergents, chaotrophic salts, organic solvents, and most common proteases (Prendergast & Mann, 1978; Ward & Bokman, 1982). The molecular cloning of its cDNA (Prasher et al., 1992) and demonstration that GFP can be expressed as a functional marker in heterologous cell types (Chalfie et al., 1994; Inouye & Tsuji, 1994) have opened a broad array of applications in cell, developmental, and molecular biology.

A first proposed application of GFP was as a reporter to detect gene expression *in vivo* (Prasher et al., 1992). The usefulness of GFP was successfully demonstrated as a marker of gene expression in intact transgenic embryos and animals (Fleischmann et al., 1998; van den Pol & Ghosh, 1998) and as a indicator of effective gene transfer (Muldoon et al., 1997). Still, the most successful and numerous class of GFP applications has been as a genetic fusion partner to host proteins to monitor their subcellular localization and

fate. The gene encoding a GFP is fused in frame with the gene encoding the endogenous protein, and the resulting chimera is expressed in the cell or organism of interest. The ideal result is a fusion protein that maintains the normal functions and localizations of the host protein but is now fluorescent. GFP has been targeted successfully to practically every major organelle of the cell, including the plasma membrane (Barak et al., 1997), nucleus (Zhu et al., 1998), endoplasmic reticulum (Pouli et al., 1998), Golgi apparatus (Presley et al., 1997), secretory vesicles (Lang et al., 1997), and mitochondria (Hedtke et al., 1999). GFP's independence from enzymatic substrates or cofactors makes it particularly promising for these applications. Besides its applications in cell biology, GFP has proven to be a useful indicator for pH (Robey et al., 1998), Ca^{++} (Miyawaki et al., 1997), protease activity (Mitra et al., 1996) and intermolecular interactions using fluorescence resonance energy transfer (FRET) (Mahajan et al., 1998).

Chapter 4 describes new applications of GFP to reveal and characterize protein–protein interactions *in vitro*. The interaction between the S-peptide and S-protein fragments of ribonuclease A was chosen as a model system. GFP-tagged S-peptide was produced, and the interaction of this fusion protein with S-protein was analyzed by two distinct methods: fluorescence gel retardation and fluorescence polarization. The fluorescence gel retardation assay is a rapid method to demonstrate the existence of a protein–protein interaction and to estimate the equilibrium dissociation constant (K_d) of the resulting complex. The fluorescence polarization assay is an accurate method to evaluate K_d in a specified homogeneous solution and can be adapted for the high

throughput screening of protein or peptide libraries. These two methods are powerful new tools to probe protein–protein interactions.

Table 1.1. Secondary structural elements of HIV-1 protease.

Name	Residues
β-strand *a*	1–4
β-strand *b*	9–15
β-strand *c*	18–27
β-strand *d*	30–35
β-strand *a′*	43–49
β-strand *b′*	52–66
β-strand *c′*	69–78
β-strand *d′*	83–85
α-helix *h*	86–94
β-strand *q*	95–99

Figure 1.1 Schematic diagram of HIV-1 protease dimer prepared with the program MOLSCRIPT (Kraulis, 1991). Elements of secondary structure were marked as described in the text and Table 1.1.

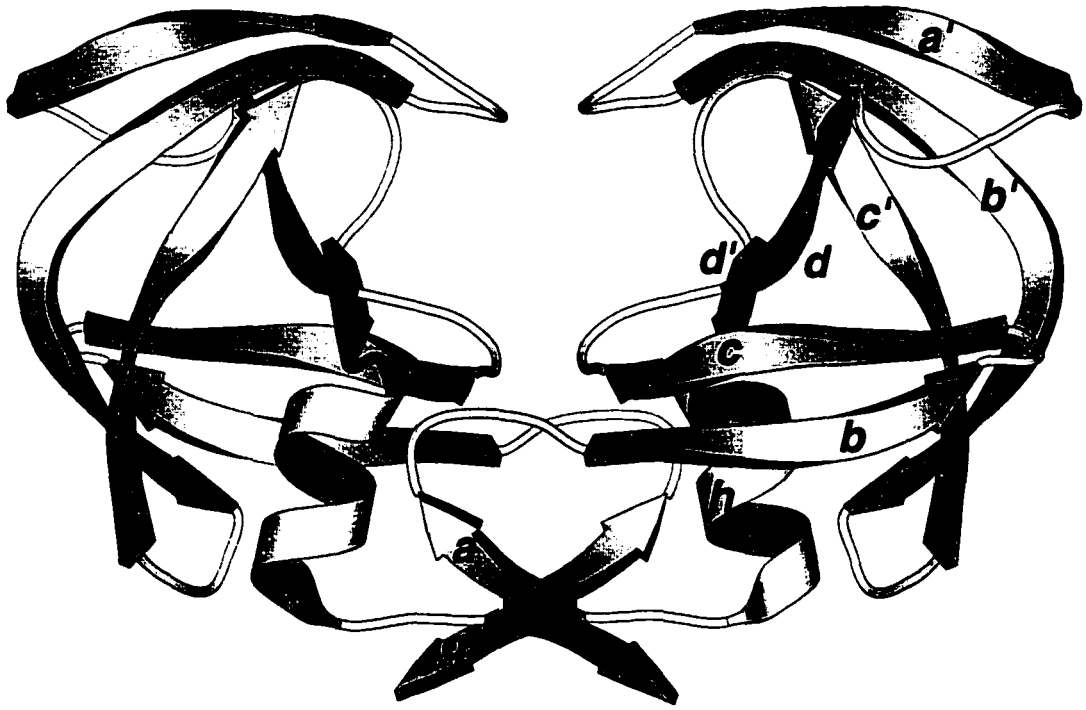
a'
b'
c'
d'
d
c
b
h
a

Figure 1.2 Diagram of a four-stranded antiparallel β-sheet at the interface of the HIVPR dimer. Residues from one subunit are indicated in blue. Marked in red are amide – amide hydrogen bonds.

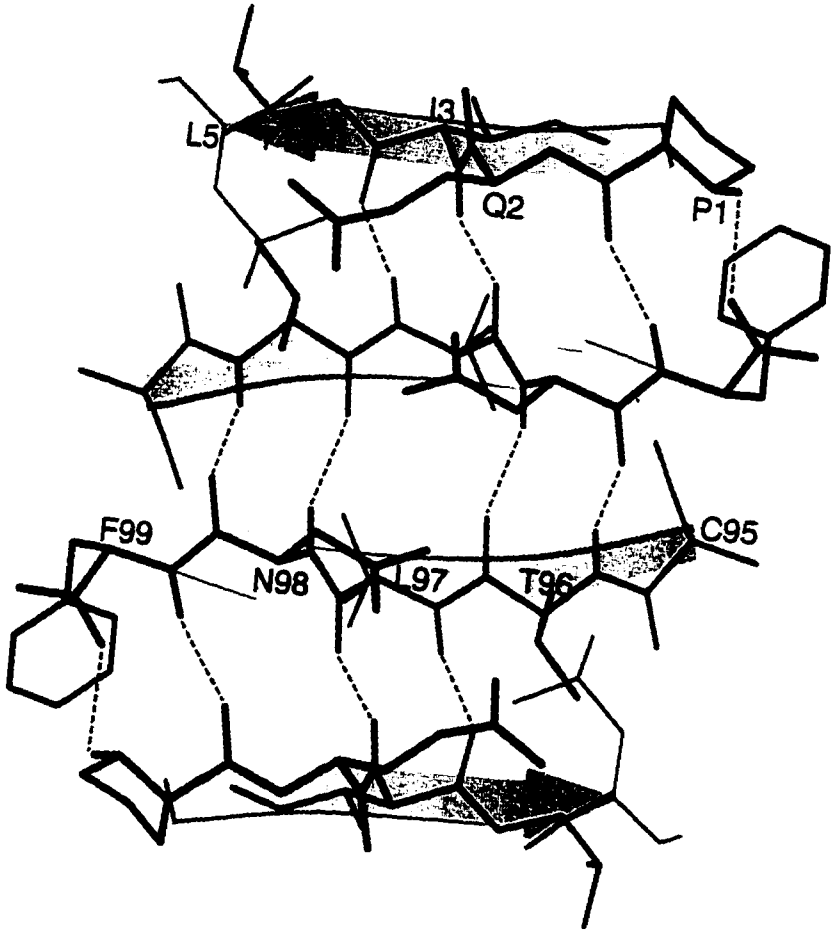
L5
I3
Q2
P1
F99
N98
L97
T96
C95

Figure 1.3 Structure of the complex of porcine ribonuclease inhibitor (dark) and RNase A (light). The diagram was prepared from Protein Data Bank (PDB) entry 1DFJ (Kobe & Deisenhofer, 1995) using MOLSCRIPT.

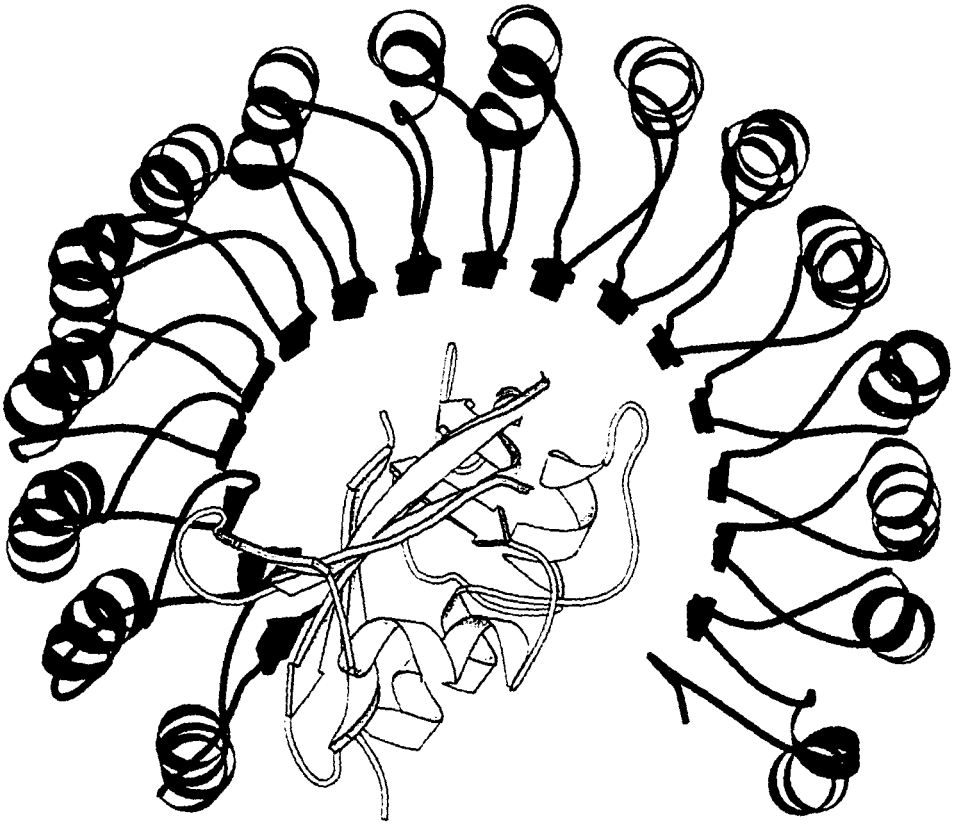

Figure 1.4 Schematic diagram of RNase S, which consists of S-peptide (residue 1 - 15, light) and S-protein (residue 24 - 124, dark).

Figure 1.5 Three-dimensional structure of the GFP S65T variant (Ormö et al., 1996). The diagram shows 11 β-strands forming a β-can through which is threaded a helix bearing the chromophore, which is shown in ball-and-stick representation. The drawing was prepared by MOLSCRIPT from the PDB entry 1EMA.

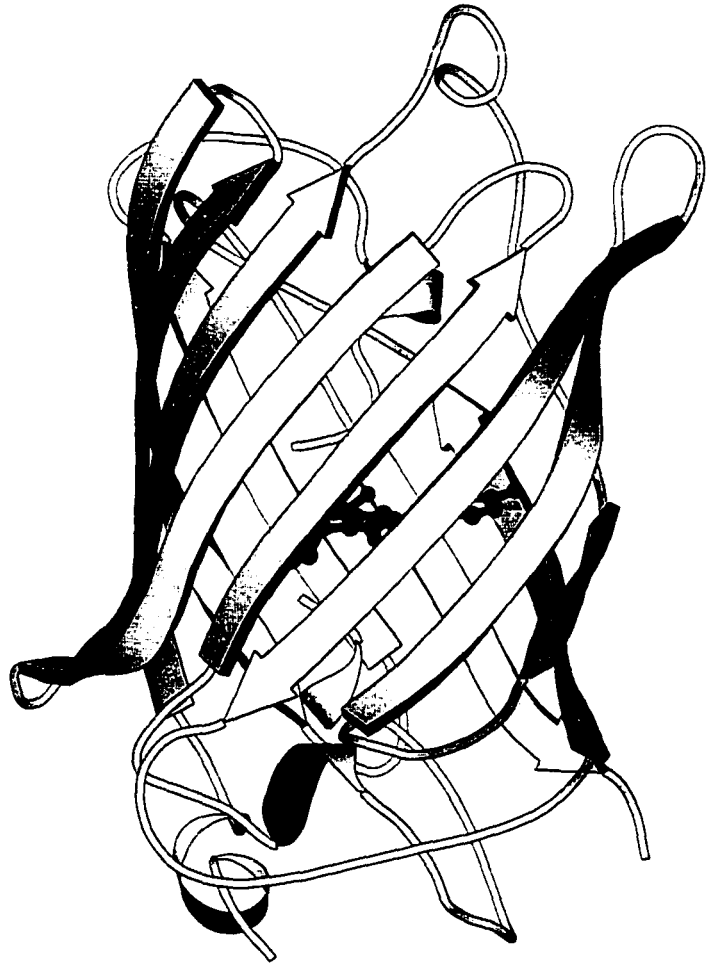

Chapter 2

Disrupting Protein–Protein Interactions: Genetic Selection of Dissociative Inhibitors of HIV-1 Protease

A portion of this work was submitted for publication as:

Sang-Hyun Park and Ronald T. Raines (1999) Genetic Selection for Dissociative Inhibitors of Designated Protein–Protein Interactions. Submitted.

2.1 INTRODUCTION

Many biological processes, such as signal transduction, cell cycle regulation, gene regulation, and viral assembly and replication, rely on protein–protein interactions. Flow of inter- and intracellular information is largely governed by the combination of protein–protein interactions, and the identification of the network of those interactions among proteins is the key to understanding the cellular mechanism of interest. During the last decade, because of the availability of methodologies like the yeast two-hybrid system (Fields & Song, 1989; Chien et al., 1991) and the phage display system (Smith, 1985), many important protein–protein and protein–peptide interactions have been identified from many different organisms. Revealing the biological function of a gene and its encoded protein can often be achieved by identification of its interacting partner and its place in the cascade of protein–protein interactions. The identification of a critical protein–protein interaction is, however, only the first step. Modulation of the interaction is necessary to produce true insight into its biological purpose (Souroujon & Mochly-Rosen, 1998).

Many of the proteins and enzymes inside a cell exert their function as oligomers formed by the heterologous or homologous association of subunits. Blocking of specific protein–protein interactions would allow development of a novel class of inhibitors (Zutshi et al., 1998), which would be a valuable tool for the control of cellular processes as well as the development of therapeutic agents. Here, we describe a general means that

uses an encoded combinatorial peptide library to identify a peptide that disrupts a specific protein–protein interaction *in vivo*.

HIV-1 protease has been studied extensively due to its critical role in viral maturation and infectivity (Peng et al., 1989) and its importance as a therapeutic target in AIDS therapy. To treat AIDS, attempts have been made to inactivate the protease using active site-directed inhibitors (Wlodawer & Vondrasek, 1998). Use of active site-directed drugs has, however, led to the appearance of the HIV variants with drug-resistant proteases (Flexner, 1998; Klabe et al., 1998). Viral mutations as well as the high toxicity of these drugs beg for an alternative approach. The active site of HIV-1 protease is composed of two identical 99-residue subunits. Dissociation of the active, dimeric form of the enzyme results in complete loss of catalytic activity. Thus, disruption of the dimeric interface has been suggested to be a novel means of inhibiting protease activity (Zhang et al., 1991; Babe et al., 1992; Babe et al., 1995; Schramm et al., 1996). To test the validity of our approach, we sought to select for a peptide that can disrupt the dimerization event of HIV-1 protease

To develop a genetic selection of dissociative inhibitor of HIVPR, we chose a repressor protein (cI) from bacteriophage λ as a sensor for dimerization. cI protein consists of two distinctive domains: N-terminal DNA-binding domain (NcI, residue 1 - 92) and C-terminal dimerization domain (residue 132 - 236) (Pabo et al., 1979). The repressor binds to its operator DNA only as a dimer and DNA-binding domain alone has little affinity for the operator. It has been shown that the C-terminal dimerization domain of cI protein can be replaced by another protein domain, which can dimerize and yield a

functional repressor inside a cell (Hu et al., 1990). A fusion of N-terminal DNA-binding domain of cI and a protease variant was created and used as a target for screening of a peptide library.

2.2 Materials and Methods

Materials. E. coli strain MC1061 was from the American Type Culture Collection (Manassas, VA). *E. coli* strain BL21(DE3) and BL21(DE3)pLysS were from Novagen (Madison, WI). *E. coli* strain XL-1 Blue was from Stratagene (La Jolla, CA). *E. coli* strain BMH71-18 (*mutS*) was from Clontech (Palo Alto, CA). *E. coli* strain AG1668 and plasmids pFG157, pJH370, and pJH391 were generous gifts from James C. Hu (Texas A&M University). pET-HIVPR was a generous gift from Jordan Tang (University of Oklahoma). pRZ4737 was a generous gift from William S. Reznikoff (University of Wisconsin – Madison). pBluescript II SK(-) and *Pfu* DNA polymerase were from Stratagene (La Jolla, CA). pMC1871, pKK223-3, dATP, dTTP, Nick columns and Superdex-75 resin were from Pharmacia Biotech (Piscataway, NJ). Ready-Lyse lysozyme was from Epicentre (Madison, WI). All other enzymes for the manipulation of recombinant DNA were from either Promega (Madison, WI) or New England Biolabs (Beverly, MA). Phosphoramidites were from Glen Research (Sterling, VA). Poly(dI-dC), salmon sperm DNA, anti-Trx antibody, and anti-rabbit IgG-alkaline phosphatase conjugate were from Sigma (St. Louis, MO). Anti-HIVPR antibody was a generous gift

from Stephen Oroszlan (National Cancer Institute). Fluorescein diphosphate and fluorogenic protease substrate were from Molecular Probes (Eugene, OR). HBVS and maleimide activated 96-well plates were from Pierce (Rockford, IL). Ultrafiltration membranes were from Amicon (Beverly, MA). Bacto yeast extract, Bacto trypton, and Bacto agar were from Difco (Detroit, MI). All other chemicals were from Sigma (St. Louis, MO), Aldrich (Milwaukee, WI), or Fisher Chemical (Fair Lawn, NJ).

General methods and instruments. Oligonucleotides were synthesized with β-cyanoethyl phosphoramidite chemistry (Sinha et al., 1984) on an ABI 392 DNA/RNA synthesizer from Applied Biosystems (Foster City, CA). PCR reactions described in this chapter were carried out using *Pfu* DNA polymerase. All the DNA fragments prepared by PCR were sequenced and their identities were confirmed before subsequent subcloning steps. DNA sequencing was performed either manually using Sequenase 2.0 kit with [α-^{35}S]dATP or automatically on ABI 377XL automated DNA sequencer from Applied Biosystems (Foster City, CA). Media for bacterial culture were prepared as described by Sambrook et al. (Sambrook et al., 1989). Fluorescence measurements were carried out on a QuantaMaster1 photon-counting fluorometer from Photon Technology International (South Brunswick, NJ). Fluorescence polarization measurements were made with a Beacon Fluorescence Polarization System from Pan Vera (Madison, WI). Fluorescence gel scanning was carried out with a fluorimager SI System from Molecular Dynamics (Sunnyvale, CA). Ultraviolet and visible absorbance measurements were made with a Cary 3 or Cary 50

spectrophotometer from Varian (Sugarland, TX). Concentrations of synthetic DNA oligonucleotides in solution were determined by assuming that a 33 μg/mL solution has $A = 1.0$ at 260 nm.

Construction of a fusion of λ repressor and protease. A gene encoding the wild type HIV-1 protease was amplified from pET-HIVPR using two oligonucleotides, OES1: GGGTACTGTGTCGACCAACTTACCGCAGATCACTCTG and A1: TAGCAGCCGGATCCGCTTAGAAGT, which contain *Sal*I and *Bam*HI (underlined), respectively. The amplified DNA was inserted into *Sal*I/*Bam*HI sites of pJH391 (Hu et al., 1990) to create a fusion of λ repressor DNA-binding domain (NcI) and wild type HIV protease. The active-site aspartate residue (Asp25) of HIV protease was changed to asparagine (Asn25) using the single-site elimination site-directed mutagenesis (Deng & Nickoloff, 1992). Mutagenesis was carried out on double-stranded plasmid DNA using a selection and a mutagenic primer with an *E. coli* strain BMH71-18 (*mutS*). Selection primer, M1: GTGACTGGTGAGGCCTCAACCAAGTC, binds to an ampicillin resistance gene and changes the unique *Sca*I site to *Stu*I site (underlined) without affecting the activity of β-lactamase. A mutagenic primer, M2: AAGCTCTGCTGAACACTGGCGCTGA, changes Asp25 of the protease to Asn25 (underlined). The resulting plasmid encoding a fusion, NcI-PR, of NcI and a protease variant (D25N) was labeled as pJH-PR. Protease referred as PR in this chapter is the D25N variant, unless otherwise noticed. A DNA encoding the N- and C-terminal segments connected by a linker ($P^1Q^2I^3T^4L^5$-GGSSG-$S^{95}T^{96}L^{97}N^{98}F^{99}$, dPR2) was created

by annealing two oligonucleotides, SH3:

TCGACCCCACAAATTACACTGGGTGGTTCCTCAGGTTCAACGTTGAACTT and

SH4:

CTAGAAGTTCAACGTTGAACCTGAGGAACCACCCAGTGTAATTTGTGGGG.

The annealed duplex results in cohesive ends compatible to *Sal*I and *Spe*I and carries an internal *Bsu*36I site (underlined). The annealed DNA was inserted into *Sal*I/*Spe*I sites of pJH391 to construct a fusion of NcI-dPR2 resulting in pJH-dPR2.

Construction of reporter plasmids. A transcription terminator (rrnB T_2) of the *E. coli* rrnB ribosomal RNA operon (Brosius et al., 1981) was amplified from pKK223-3 (Amann et al., 1984) using two primers, P20:

CGGTCTAGAAAAACAGAATTTGCCTGG and P21:

AAAGCGGCCGCAGAAACGCAAAAAGGCCATCCG, which contain *Xba*I and *Not*I sites, respectively. The PCR fragment was subcloned into *Xba*I /*Not*I sites of a phagemid pBluescript II SK(-) and the resulting plasmid was labeled as pSH13. A DNA containing λ right promoter (λP_R) and a single copy of λ operator (λO_{R1}) was amplified from pRZ4737 (Weinreich et al., 1994) using primers, P32:

CTAAGCTTGTGCGTGTTGACTATTTTACCT and P33:

AGAGAATTC*CATGG*ACACCTCCTTAGTACATGCAACC, which carry *Hind*III and *Eco*RI sites (underlined), respectively. The DNA provides for an unique *Nco*I site (italicized) with a start codon that is under control of λP_R. The amplified DNA was subcloned into *Hind*III/*Eco*RI sites of pSH13 and the resulting plasmid was labeled as

pSH14. DNA encoding an open reading frame of β-galactosidase (*lacZ*) from *E. coli* was amplified from pMC1871 (Shapira et al., 1983) using primers, P22: TTCCCATGGATCCCGTCGTTTTACAAC and P23: CGTCTAGAGTGACACCACGATGCCTGCA, which carry *Nco*I and *Xba*I sites, respectively. The amplified *lacZ* gene was subcloned into *Nco*I/*Xba*I sites of pSH14 and the resulting plasmid was labeled as pSH15. A DNA containing a tetracycline resistance gene (*tet*) was amplified from pBR322 (Bolivar et al., 1977) using primers, P24: TAACGCCTGCAGGCACCGTCCATGGAATCTAACAATGCGCTCATC and P25: TATCTAGATCTCGCCGGCTTCCATTCAGGTC, which contain *Pst*I and *Xba*I/*Bgl*II sites, respectively. Amplified *tet* gene was inserted into *Pst*I/*Xba*I sites of pBluescript II SK(-) to create pSH16. The *tet* gene from pSH16 was inserted into *Xba*I/*Pst*I sites of pSH15 resulting in a plasmid pSH18. pSH18 carries the reporter cassette of λP_R-*lacZ*-*tet*-rrnB and is based on a high-copy number phagemid with ColE1 origin. The *Hind*III/*Not*I fragment of pSH18 was transferred into the *Hind*III/*Eag*I sites of pACYC184, a low-copy number plasmid with a p15A origin (Chang & Cohen, 1978), to create pSH20. To construct reporter plasmids that drive the expression of various NcI fusions, expression modules of NcI fusions were transferred into pSH20 as follows. *Eco*RI/*Nhe*I fragments containing *lacUV5*-NcI fusions were cut out from pJH-PR, pJH-dPR2, pFG157 and pJH370, which drive expression of NcI-PR, NcI-dPR2, wild-type cI and cI-zip, respectively. The *Eco*RI overhang of the fragments were filled in to blunt end by using Klenow fragment of DNA polymerase I with dATP and dTTP (Ausubel et al., 1994). The resulting blunt end/*Nhe*I fragments from pJH-PR, pJH-dPR2, pFG157 and pJH370 were

inserted into *XmnI/NheI* sites of pJH20 to create pSH26, pSH27, pSH28 and pSH29, respectively. Due to an additional *XmnI* site in pSH20, the TIES method was used for ligation (Zeng et al., 1996).

Assay of β-galactosidase activities. E. coli strain MC1061 was transformed with plasmids pSH20, pSH26, pSH27, pSH28, and pSH29 using $CaCl_2$ method (Ausubel et al., 1994). β-galactosidase activity from lysates of transformants was measured as described (Miller, 1972). Five individual colonies were picked up from each transformation, and the measured activities were averaged.

Gel retardation assay for λO_{R1} binding of cI and NcI-PR. A fluorescein-labeled, double-stranded DNA corresponding to the λO_{R1} sequence was made by annealing oligonucleotides, OR11: TTTACCTCTGGCGGTGATAG and OR13: FCTATCACCGCCAGAGGTAAAF, where F is fluorescein. OR11 (5.0 μM) and OR13 (5.0 μM) were dissolved in 35 mM Tris-HCl buffer (pH 7.6) containing $MgCl_2$ (5.0 mM) and the resulting solution was boiled for 5 min and then left to cool to room temperature. Purified cI protein (30 μg/mL) or NcI-PR protein (50 μg/mL) was incubated in 10 μL of 10 mM Tris-HCl buffer (pH 8.0) containing $MgCl_2$ (5.0 mM), $CaCl_2$ (2.0 mM), BSA (50 μg/mL), sheared salmon sperm DNA (0.20 mg/mL), poly(dI-dC) (50 μg/mL), DTT (1 mM), glycerol (5% v/v), and fluorescein labeled λO_{R1} DNA (0.5 μM) at 25 °C for 20 min. After incubation, mixtures were loaded onto a polyacrylamide (8% w/v) gel prepared in 0.5 × TBE buffer containing $MgCl_2$ (2.0 mM) and electrophoresed at 4 °C at

10 V/cm. After electrophoresis, the gel was scanned with a fluorimager SI System using a built-in filter set (490 nm for excitation and ≥515 nm for emission).

Construction of a plasmid for peptide library expression. An *Nde*I site was incorporated at the start codon of glutathione S-transferase (GST) gene in pGEX-4T3 by a single-site elimination site-directed mutagenesis (Deng & Nickoloff, 1992) to create pSH11. A primer, M4: CTAGTATAGCGGACATATGTACTGTTTCCTGTGTGAAA, served as both mutagenic and selection primer by replacing an unique *Eco*NI site with *Nde*I site (underlined). DNA containing an open reading frame of wild-type thioredoxin (Trx) from *E. coli* was amplified from pTRX (Chivers et al., 1997) using primers, PC26: AAGAAGGAGTTATACATACATATGAGCGATAAAATTATT and P30: ATTCGAATTCGCCAGGTTAGCGTCGAGGAACTCTTT, which contain *Nde*I and *Eco*RI sites (underlined), respectively. The GST fragment in pSH11 was replaced with thioredoxin gene at *NdeI/EcoRI* sites to create pSH12, which directs expression of Trx under control of a strong *tac* promoter.

Construction of 9-mer peptide library in pSH12. A degenerate oligonucleotide, PL9: AATTTAGGTGGTGGT$(XYZ)_9$TAACCCGGCG, where X = A(32%)/G(39%)/C(21%)/T(8%), Y = A(27%)/G(23%)/C(25%)/T(24%), and Z = G(40%)/T(60%), was synthesized to encode random 9-mer peptides. Phosphoramidites of four bases were manually mixed by the given ratio and a separate bottle of the mixed phosphoramidites was used for each position of X, Y, and Z during synthesis. The base

composition of the randomized codon was according to the previous report (LaBean & Kauffman, 1993). Two anchor primers, P42: ACCACCACCTA and P43: TCGACGCCGGGTTA, were synthesized and purified along with PL9 from a denaturing acrylamide gel (15% or 8% w/v) in 0.5 × TBE containing urea (7.0 M) (Ausubel et al., 1994). The purified primers were phosphorylated at their 5′-ends using T4 polynucleotide kinase with ATP. A gapped duplex DNA (Cwirla et al., 1990) was prepared by annealing PL9 with P42 and P43, in which the 5′ and 3′ ends of resulting duplex are compatible with *Eco*RI and *XhoI*, respectively. The annealed insert (100 pmol) was ligated to *Eco*RI/*XhoI* digested pSH12 (10 pmol) using T4 DNA ligase and ATP. After incubation at 14 °C for 18 h, ligase was inactivated by heating at 75 °C for 15 min, and the reaction mixture was desalted on a Nick column. MC1061 cells were grown to log phase in LB (2.0 L) and subjected to preparation of electrocompetent cells (Ausubel et al., 1994). One tenth of the desalted ligation mixture was mixed with fresh electrocompetent cells (75 μL) in an electroporation cuvette (0.1 cm gap). DNA was electroporated into cells with a GenePulser System (Bio-Rad; Hercules, CA) at 20 KV/cm, 25 μF, and 400 Ω. Transformants from 10 electroporations were combined and grown in LB (0.70 L) containing ampicillin (0.10 mg/mL) for 4 h at 37 °C before preparation of library plasmids.

Determination of optimal tetracycline concentrations. To determine the highest tetracycline concentration usable for the screening, MC1061 cells cotransformed with pSH20 and pSH12 were spread on LB-agar plates containing chloramphenicol (0.10

mg/mL), ampicillin (0.10 mg/mL), IPTG (20 μM), and varying amounts of tetracycline (1 – 100 μg/mL). The viability of cells was monitored after incubation for 24 h at 37 °C. For the determination of the lowest effective concentration tetracycline for screening, MC1061 cells cotransformed with pSH15 and pSH12 were treated as described above.

Screening of library. DNA of library plasmids (1 μg) was transformed into MC1061 cells using electroporation. Transformants were resuspended in SOC (2.0 mL) and incubated at 37 °C for 45 min. Transformants were inoculated in LB (0.35 L) containing ampicillin (0.10 mg/mL) and grown for 4 h at 37 °C and subjected to the preparation of electrocompetent cells. The reporter plasmid, pSH26 (1 μg), was subsequently transformed into fresh competent cells of library/MC1061 transformants by electroporation. Cotransformants were resuspended in SOC (1.0 mL) and incubated at 37 °C for 1 h. Cells were plated on six large petri dishes of LB-agar containing ampicillin (0.10 mg/mL), chloramphenicol (50 μg/mL), X-Gal (75 μg/mL), tetracycline (20 μg/mL), and IPTG (20 μM) and grown for 24 h at 37 °C until $lacZ^{+}tet^{R}$ colonies appear. The library plasmids were rescued from $lacZ^{+}tet^{R}$ colonies and retransformed into *E. coli* strain XL-1 Blue.

Elimination of false positives in vivo. The rescued library plasmids from $lacZ^{+}tet^{R}$ colonies were retransformed into pSH28/MC1061. Transformants were plated under the same condition as described above, and clones showing a $lacZ^{+}tet^{R}$ phenotype were discarded.

Preparation of lysates for gel retardation assays. The rescued library plasmids from *lacZ*$^+$*tet*^{R} clones were retransformed into MC1061. Each transformant was grown in LB (2.0 mL) containing ampicillin (0.10 mg/mL) until the log phase and IPTG (to 0.5 mM) was added. IPTG-induced cells were grown further for 2.5 h at 37 °C and harvested by centrifugation. Cells were resuspended in 30 μL of 20 mM Tris-HCl buffer (pH 8.0) containing PMSF (1 mM), DTT (0.5 mM), EDTA (1 mM), and glycerol (10 % v/v). Ready-Lyse lysozyme (2500 units) was added to resuspended cells with brief vortexing, and the mixture was incubated at 25 °C for 15 min for lysis to occur. After centrifugatation at 18,000 × *g* for 15 min at 4 °C, the cleared lysate was recovered and kept on ice or frozen at -80 °C for future use.

Elimination of false positives in vitro. Lysates were mixed with purified cI protein (30 μg/mL) and incubated in 9 μL of 10 mM Tris-HCl buffer (pH 8.0) containing $MgCl_2$ (5 mM), $CaCl_2$ (2 mM), BSA (50 μg/mL), sheared salmon sperm DNA (0.2 mg/mL), poly(dI-dC) (50 μg/mL), DTT (1 mM), and glycerol (5% v/v) at 25 °C. After 20 min of incubation, 1 μL of λO_{R1} DNA (5 μM) was added, and the reaction was incubated for another 15 min at 25 °C before electrophoresis in a polyacrylamide (8% w/v) gel as described above. Library isolates that caused the disappearance of a shifted band were discarded.

Immobilization of proteins on maleimide activated plates. Purified HIV-1 protease (20 μg/mL) was incubated in 0.10 mL of 0.10 M HEPES-NaOH buffer (pH 7.0) or in 0.10 M MES-NaOH buffer (pH 6.6) containing urea (6.0 M) in maleimide-activated plates at 25 °C for 3h. Plate wells were washed with PBS (5 × 0.20 mL) to remove unbound protein. Unreacted maleimide groups were blocked by incubating with cysteine (10 μg/mL) at 25 °C for 3h. Unless otherwise noted, the plate was washed with PBS (5 × 0.20 mL) by mild vortexing at 25 °C for 3 min between each of following steps. Trx was also immobilized on the maleimide-activated plates using the same protocol.

ELISA. The lysates of expressed Trx–peptide fusions were prepared as described above, except for the use of PBS buffer instead of Tris-HCl buffer. For the binding of peptides to the immobilized protease, lysate (20 μL) was mixed with PBS buffer (80 μL) and incubated at 4 °C overnight in each well of the plates. Anti-Trx antibody (0.10 mL) in 1:5000 dilution in PBS buffer containing BSA (1 mg/mL) was incubated in each well at 25 °C for 1 h. Subsequently, anti-rabbit IgG-alkaline phosphatase conjugate (0.20 mL) in 1:5000 dilution in PBS buffer was incubated at 25 °C for 1 h. Fluorescein diphosphate (FDP) was used as a fluorescent substrate of phosphatase (Huang et al., 1992). FDP (0.20 mM) in 75 μL of 0.10 M CAPS-NaOH buffer (pH 10.3) containing NaCl (50 mM) and $MgCl_2$ (10 mM) was added to each well, and the resulting solution was incubated at 25 °C for 10 min. The plates were either scanned by a fluorimager SI System or photographed on an UV transilluminator.

Sequence alignments of positive isolates. A sequence similarity was identified among 9 representative clones that a strong signal in the ELISA assay. The sequences were grouped into 3 subgroups according to the similarity. The alignment was obtained by using the Multialign interface with the Blosom62 algorithm (Corpet, 1988).

Synthesis and purification of peptides. Peptides described in this chapter were synthesized with an ABI 432A peptide synthesizer (Applied Biosystems; Foster City, CA) using F-moc chemistry (Carpiro & Han, 1972). Synthetic peptides were purified with a C-18 reverse-phase column (Vydac; Hesperia, CA) on an HPLC System (Waters; Milford, MA) using acetonitrile containing TFA (0.1% v/v) as a mobile phase. The peptide was identified by an electrospray ionization mass spectrometry on an API 365 LC/MS/MS System (PE Biosystems; Foster City, CA) and quantified by an amino acid analysis on an ABI model 421 amino acid analyzer (Applied Biosystems; Foster City, CA).

Analytical gel filtration chromatography. A column (22 cm × 20 mm^2) was packed with Superdex 75 gel filtration resin and equilibrated in 50 mM sodium acetate buffer (pH 4.7) on an FPLC system. Pep52 (5.0 mM or 0 mM) was incubated for 30 min at 25 °C in 50 mM sodium acetate buffer (pH 4.7) containing wild-type protease (2.8 μM). The mixture (0.10 mL) was loaded onto the column. The absorbance at 280 nm was monitored by using FPLC Manager software (Pharmacia; Piscataway, NJ).

Crosslinking of peptides. A peptide (NH_2-IVQVDAEGGC-CO_2H) (10 mg/mL) was mixed with HBVS (4 mM) in 0.50 mL of 0.20 M sodium borate buffer (pH 8.5) containing TCEP (2 mM) and incubated at 25 °C for 4 h. Unreacted HBVS was blocked by incubating with cysteine (20 mM). Crosslinked peptide was purified and identified as described above.

Purification of proteins. Trx was purified from *E. coli* strain pTRX/BL21(DE3) (Chivers et al., 1997). Fresh overnight culture of the strain in LB (3.0 mL) containing ampicillin (0.10 mg/mL) was inoculated to the same medium (0.30 L) and grown at 37 °C to early log phase ($A_{600\,nm}$ = 0.5). IPTG was added to 1 mM to and cells were further grown at 37 °C for 6 h. Induced cells were harvested by centrifugation at 3000 × *g* for 10 min and resuspended 10 mL of 20 mM Tris-HCl (pH 8.0) containing EDTA (1 mM). Ready-Use Lysozyme (5×10^5 units) and DNase I (2500 units) were added to the resuspended cells and incubated at 25 °C for 20 min. Partially lysed cells were boiled three times using a microwave oven, and then kept on ice. Lysate was cleared by centrifugation at 17000 × *g* for 25 min at 4 °C and the supernatant containing mostly Trx was collected and concentrated to 3 mL using a microconcentrator (Amicon; Beverly, MA) with YM3 ultrafiltration membrane. The concentrate was loaded onto a Superdex 75 gel filtration column (Pharmacia; Piscataway, NJ), which had been equilibrated with 20 mM Tris-HCl buffer (pH 8.5) containing EDTA (0.4 mM), and proteins were eluted in the same buffer. Fractions containing Trx were pooled and concentrated by ultrafiltration

as described above. Purified TRX was quantified by using the extinction coefficient (ε = 13700 $M^{-1}cm^{-1}$ at 280 nm (Krause et al., 1991)).

Wild-type HIV-1 protease was produced in *E. coli* strain pET-HIVPR/BL21(DE3)pLysS and purified as described earlier (Ido et al., 1991). The same protocol was used for the production and purification of NcI-PR from *E. coli* strain pJH-PR/BL21(DE3)pLysS.

cI protein was produced and purified from *E. coli* strain pFG157/MC1061. LB (0.75 L) containing ampicillin (0.10 mg/mL) was inoculated with a fresh overnight culture (7.5 mL) of pFG157/MC1061 and cells were grown at 37 °C. IPTG (to 1 mM) was added at early log phase ($A_{600\,nm}$ = 0.5), and the cells were grown at 30 °C for an additional 4 h before harvesting by centrifugation at 3000 × *g* for 10 min. The cell pellet was resuspended in 25 mL of 20 mM Tris-HCl buffer (pH 8.0) containing DTT (1 mM), EDTA (0.5 mM), PMSF (1 mM), and glycerol (5% v/v) and quickly frozen in an ethanol/dry ice bath. Thawed cells were lysed by passing through a French pressure cell twice, and the lysate was cleared by centrifugation at 18000 × *g* for 30 min at 4 °C. The supernatant containing cI protein was fractionated by ammonium sulfate precipitation (25% – 50% w/v) (Scopes, 1994). The precipitate was dissolved in 5 mL of 20 mM Tris-HCl buffer (pH 8.0) containing EDTA (0.5 mM) and glycerol (5% v/v), and this solution was desalted by exhaustive dialysis against the same buffer. Protein solution was loaded onto a Blue-Sepharose CL-6B column (20 cm × 2.4 cm^2) that had been equilibrated with 20 mM Tris-HCl buffer (pH 8.0) containing EDTA (0.5 mM) and glycerol (5% v/v). Proteins were eluted with a linear gradient of KCl (0.1 – 0.6 M) in the same buffer.

Fractions containing cI protein were pooled and dialyzed against with 20 mM Tris-HCl buffer (pH 8.0) containing EDTA (0.5 mM) and PMSF (0.5 mM). cI protein was further purified by loading onto a Mono-S column (Pharmacia; Piscataway, NJ) that had been pre-equilibrated with 20 mM Tris-HCl buffer (pH 8.0) containing EDTA (0.5 mM). The protein was eluted with a linear gradient of KCl (0.05 – 0.5 M) in the same buffer. Pooled fractions were desalted and concentrated by ultrafiltration in 20 mM Tris-HCl buffer (pH 8.0) containing EDTA (0.5 mM) and DTT (0.5 mM).

Assay of HIV-1 protease activity. A fluorogenic substrate, Arg-Glu(EDANS)-Ser-Gln-Asn- Tyr-Pro-Ile-Val-Gln-Lys(DABCYL)-Arg (Matayoshi et al., 1990), was used to monitor proteolytic activity, which was measured using a QuantaMaster1 fluorometer as described before (Wondrak et al., 1996) with modifications. In the modifications, the protease was preincubated with or without inhibitor for 30 min at 25 °C in 97 μL of 0.10 M sodium acetate buffer (pH 4.7) containing glycerol (5% v/v), PEG8000 (0.1% v/v), DTT (5 mM), EDTA (1 mM), and NaCl (0 or 1.0 M). The substrate (3 μL) was added to a final concentration of 3.75 μM to start the reaction. Data were collected for the first 3 – 5 min to obtain the initial velocity.

Kinetic analysis of dissociative inhibition. Dissociative inhibition of HIVPR was characterized by a kinetic analysis described by Zhang and Poorman (Zhang et al., 1991). In the method, kinetic and thermodynamic parameters of the inhibition can be expressed in terms to enzyme and inhibitor concentrations and initial velocity of catalysis as:

$$\frac{E_t}{\sqrt{k}} = \frac{K_m}{k_{cat}}\sqrt{k} + \frac{\sqrt{K_d K_m}}{2\sqrt{k_{cat}}}\left(1 + \frac{I}{K_{id}}\right) \tag{2.1}$$

where E_t is the total enzyme concentration, k is the initial rate constant, I is the concentration of inhibitor, K_d is the equilibrium dissociation constant of the protease dimer, K_{id} is the inhibition constant of dissociative inhibition. Equation 2.1 is valid under conditions where competitive, uncompetitive, and noncompetitive inhibitions are negligible. Plotting $E_t/\sqrt{k}$ as a function of $\sqrt{k}$ at different inhibitor concentrations will generate a series of parallel lines if inhibition is purely dissociative. In the absence of inhibitor, Equation 2.1 is simplified as:

$$\frac{E_t}{\sqrt{k}} = \frac{K_m}{k_{cat}}\sqrt{k} + \frac{\sqrt{K_d K_m}}{2\sqrt{k_{cat}}} \tag{2.2}$$

Initial velocity of hydrolysis of the fluorogenic substrate by HIV-1 protease was determined at various concentrations of enzyme. $E_t/\sqrt{k}$ was plotted versus $\sqrt{k}$ according to Equation 2.2 to get a straight line. Values of K_d and k_{cat}/K_m were obtained from the slope and y-intercept.

Initial velocity was also measured in the presence of inhibitors at different E_t. The data were plotted according to Equation 2.1 to determine the mode of inhibition. The value of K_{id} can be obtained from the y-intercept of a straight line. For a more accurate determination of the K_{id} value, inhibitor concentration was varied in a series of

experiments with constant substrate concentration and varying E_t. In order to plot all the series of data in a single linear form, Equation 2.2 was transformed into following form:

$$\frac{\frac{E_t}{\sqrt{k}} - \frac{\sqrt{K_d K_m}}{2\sqrt{k_{cat}}}}{\sqrt{k}} = \frac{K_m}{k_{cat}} + \frac{\sqrt{K_d K_m}}{2K_{id}\sqrt{k_{cat}}}\frac{I}{\sqrt{k}} \qquad (2.2)$$

By plotting the left member of the equation versus $I/\sqrt{k}$, a straight line should be obtained for all inhibitor concentrations. The value K_{id} was obtained from the slope of this line.

2.3 RESULTS

Construction of a functional hybrid repressor, NcI-PR. Our approach takes advantage of an unique property of the repressor protein (cI) from bacteriophage λ, which binds to its operator DNA in a dimerization-dependent manner at physiological concentration. A variant of HIVPR (D25N) was fused to the C-terminus of the DNA-binding domain of cI (NcI, residues 1 - 132) to create a hybrid repressor (NcI-PR). To maintain a stable fusion protein, the D25N replacement was introduced into the active site of HIVPR, eliminating its autoprocessing activity. The D25N variant is known to dimerize as native subunit does and is identical to native subunit except for the lack of catalytic activity (Darke et al.,

1994). Because the NcI domain alone is not capable of binding to DNA, the function of NcI-PR as a repressor is dependent on dimerization mediated by the protease domain. The hybrid NcI-PR was tested for its ability to bind to operator DNA by gel retardation experiments (Figure 2.1). Purified NcI-PR was incubated with fluorescein-labeled synthetic DNA oligonucleotides containing the sequence of λ operator (λO_{R1}). According to the Figure 2.1, the NcI-PR fusion is predominantly dimeric *in vitro* and able to bind to λO_{R1} as the wild-type cI does.

To test whether NcI-PR acts as a functional repressor inside a cell, *E. coli* cells were transformed with a series of reporter plasmids (pSH26 – 29), which drive expression of NcI-PR and other cI fusions and also carry a reporter cassette (λP_R-*lacZ*-*tet*-rrnB). The β-galactosidase activity and susceptibility to tetracycline of the transformed cells were measured to monitor the capability of NcI-PR to repress transcription from λP_R. Bacterial cells that contained wild-type cI were sensitive to tetracycline and showed tight repression (98%) of *lacZ* transcription. Cells with a cI-zip fusion, a known hybrid repressor of NcI and leucine zipper dimerization domain from the yeast transcription factor GCN4 (Hu et al., 1990), showed sensitivity to tetracycline and 84% of repression. Cells containing NcI-PR were also sensitive to tetracycline and transcription of *lacZ* was repressed to 82%, comparable to that by cI-zip. Thus, the protease domain efficiently mediates the dimerization of NcI-PR, and NcI-PR acts as a functional repressor *in vivo*.

Construction of a peptide library. A peptide library of random 9 residues (PL9) was constructed as a fusion to the C-terminus of thioredoxin (Trx) from *E. coli*. We took advantage of the genetic encoding of randomized sequences because it allows for the

creation, maintenance, and reproduction of a large library (Houghten, 1993). As small peptides are highly susceptible to proteolysis *in vivo*, it is desirable to express the peptide library as a fusion to a stable carrier protein. Trx was chosen as a carrier protein because it has exceptional stability and solubility inside a cell and it is not cytotoxic even when overexpressed. The library was constructed in a plasmid (pSH12) in which the transcription of Trx is driven by a strong *tac* promoter. A short, flexible linker (Ser-Gly-Gly-Gly) was put between Trx and each 9-mer peptide for the efficient presentation of the peptide (Figure 2.2). The resulting library contained 5×10^8 clones, and 95% of them carried inserts. Representative clones from an unamplified library were isolated and the randomness of sequences was confirmed by sequencing.

Genetic selection. For the selection of library, a reporter plasmid (pSH26) was created that contains a selection cassette of λP_R-*lacZ*-*tet*-rrnB and an expression cassette of *lacUV5*-NcI-PR (Figure 2.3). An $rrnBT_2$ transcription terminator was inserted to increase the stability of the plasmid (Brosius et al., 1981). The *tet* and *lacZ* genes were chosen to enable the growth selection and easy color detection of phenotypes, and put under control of λP_R. Expression of NcI-PR was driven by a weak promoter (*lacUV5*) to prevent non-specific DNA binding of NcI-PR because the NcI domain alone can bind to λO_{R1} at high concentration. When a bacterium is transformed with pSH26, NcI-PR represses the transcription of the reporter genes and the transformant shows a $lacZ^- tet^S$ phenotype. Upon cotransformation with library plasmids, cells that carry dissociative peptides would fail to maintain a functional repressor and therefore show a reversed phenotype ($lacZ^+ tet^R$). Only $lacZ^+ tet^R$ cells should be able to survive and form blue colonies on a

medium containing appropriate concentration of tetracycline, which enables a genetic selection and screening of the peptide library (Figure 2.4).

To determine the optimal concentration of tetracycline for the selection, cells transformed with the reporter plasmid were tested for a *tet*^{S} phenotype under various concentration of tetracycline. It was determined that between 10 and 40 μg/mL of tetracycline, the stringency of selection is dependent on the tetracycline concentration. To screen the library, bacteria were transformed sequentially with the library plasmids and the reporter plasmid, and then selected for the *tet*^{R} phenotype at 20 μg/mL of tetracycline. Approximately 300 clones showed *lacZ*$^+$*tet*^{R} phenotype out of 3×10^8 cotransformants, resulting in a selection of 1 in 10^6. Library plasmids were rescued from *lacZ*$^+$*tet*^{R} cotransformants.

Elimination of false positives. False positives are common to *in vivo* screenings that rely on the transcriptional control of reporter genes. The most abundant false positives in our method are likely to be ones that can interfere with the interaction between λO_{R1} and NcI, and therefore result in a *lacZ*$^+$*tet*^{R} phenotype regardless of the dissociation of the protease dimer. The ability of the library peptides to interfere with this DNA–protein interaction was tested by using a gel retardation assay (Figure 2.5). In this method, cellular extracts expressing the Trx-peptide fusions were mixed with the wild-type cI protein and a fluorescein labeled λO_{R1} DNA. False positives would interfere with the binding of cI to λO_{R1} and therefore result in the disappearance of the shifted band.

Library plasmids from *lacZ*$^+$*tet*^{R} clones were also retransformed into bacterial cells with pSH28, which is identical to pSH26 except for the expression of wild-type cI instead

of NcI-PR. Likewise in the gel retardation assay, false positives would interfere with the interaction of λO_{R1} and cI and therefore confer the cells *lacZ*$^+$*tet*^{R} phenotype. False positive clones identified by both the *in vitro* and *in vivo* methods were discarded.

ELISA for identification of true positives. Clones that passed the false positive elimination are not necessarily true positives. An independent biochemical test is required to verify the true positives. A dissociative inhibitor would likely bind to the interface region of HIVPR to prevent the formation of the dimer. We developed a high-throughput ELISA screening to test the ability of positives clones to bind to monomeric protease (Figure 2.6A). Either urea-denatured or native protease was immobilized covalently on the surface of a maleimide-activated 96-well plate through the two reactive cysteine residues (Cys67 and Cys95). Free monomers were washed away from immobilized monomers by extensive washing following the immobilization reaction. Positive isolates that survived the false positive elimination were tested for their ability to bind to the protease monomer. After cellular extracts of positive clones were applied to the surface, plates were subsequently probed with anti-Trx antibody and secondary antibody conjugates. Bound Trx–peptides fusions were identified using fluorescein diphosphate (FDP) as a substrate for the alkaline phosphatase conjugate (Figure 2.6B). The affinity of a peptide toward the protease should be proportional to the intensity of the ELISA signal given that each isolate is treated equally through the detection process. Clones that showed bright signals were identified and sequenced.

Sequence alignment. Alignments of sequences from positive clones reveal that they fall into three different groups (Figure 2.7). A common feature in all three groups of the alignment is that aliphatic and hydrophobic residues (A, G, V, and W) are highly represented and at least one charged residues (E, D, and K) occurs in most positive isolates.

Kinetic analysis of dissociative inhibition by peptides from genetic selection. Representative peptides from the sequence alignment were synthesized chemically to test for the ability to interfere with the dimerization of HIVPR. Dissociative inhibitors of multisubunit enzymes (Zutshi et al., 1998) differ in their mechanism of action from that of traditional enzyme inhibitors (competitive, noncompetitive, and uncompetitive). The determination of the mode of inhibition and inhibition constants followed the kinetic analysis developed by Zhang and Poorman, in which one can distinguish between true competitive, uncompetitive, and dissociative inhibition of a homodimeric enzyme (Zhang et al., 1991). Zhang-Poorman analysis also enables the determination of K_d for the protease dimer and k_{cat}/K_m for catalysis by the enzyme in the absence of inhibitor. The initial velocity for hydrolysis of the fluorogenic substrate was measured without inhibitor. Plotting of the data according to Equation 2.2 yielded a straight line (Fig. 2.8A, no inhibitor) The K_d and k_{cat}/K_m values obtained from the y-intercept and slope were 14 nM and 4.4×10^3 $M^{-1}s^{-1}$, respectively.

One (pep52; IVQVDAEGG) of the peptides from the genetic selection showed inhibitory activity against HIVPR. The initial velocity was measured at different

concentrations of pep52 at low ionic strength (0.10 M added NaCl). Plotting the data according to Equation 2.1 resulted in a series of straight lines (Fig. 2.8A), which indicates pep52 is a purely dissociative inhibitor. Dissociative inhibitors affect the value of *y*-intercept by a factor of $[I]/K_{id}$, but have no effects on the slope, which results in parallel straight lines. For a more accurate determination of K_{id} value of pep52, data were plotted according to Equation 2.3. As shown in the Figure 2.8B, initial velocity data obtained in the absence of pep52 and at three different concentrations of pep52 did yield a single straight line. From the slope and *y*-intercept of this line, the value of K_{id} was determined to be 32 μM.

Interestingly, the peptide showed a mixed mode of inhibition (competitive and dissociative) at high ionic strength (1.0 M of added NaCl), which generated non-parallel lines (Fig. 2.9). The high ionic strength also affected the stability of the protease dimer. The value of K_d measured at high ionic strength was 60 pM.

Gel filtration of HIVPR with pep52. Even though the kinetic analysis of inhibition by pep52 indicates dissociative inhibition, this finding merited verification by an independent biochemical approach. To test the ability of pep52 to disassemble HVIPR dimer, wild-type protease was incubated with or without pep52 and then subjected to analytical gel filtration chromatography. A dissociative inhibitor should result in a shift of protein from a dimer peak to a monomer peak. The chromatogram in the Figure 2.10 shows that pep52 does indeed induce the dissociation of protease dimer.

Crosslinking of pep52. To attempt to increase the potency of inhibitor, a tethered peptide was made by crosslinking pep52 at its C-terminus (Figure 2.11). For the crosslinking reaction, we chose a sulfydryl-reactive homobifunctional crosslinker, HBVS, which contains vinylsulfone functionality at both ends. A derivative of pep52, which carries an additional cysteine residue at its C-terminus, was synthesized and reacted with HBVS. The resulting tethered peptide (dim52) was purified using HPLC and its identity was confirmed by an electrospray ionization mass spectrometry.

Kinetic analysis of dim52. The Zhang-Poorman analysis revealed that dim52 is still a dissociative inhibitor but now has a K_{id} value of 780 nM (Figure 2.12). Thus, a 40-fold decrease in the K_{id} value was achieved simply by crosslinking two monomeric inhibitors.

2.4 DISCUSSION

Protein–protein interactions play a pivotal role in biological events including signal transduction and in regulating activity of multisubunit enzymes in both normal and disease states. The ability to block such protein–protein interactions provides a means to elucidate the role of specific proteins and to slow or stop the process of disease development. To this end, several attempts have been made to identify small biopolymers that have ability to interfere with certain protein–protein interactions. A semi-rational but inefficient way to achieve this goal is to derive short sequences from the interface regions

of interacting proteins and test their ability to inhibit complex formation. A peptide inhibitor of the interaction between a G-protein–coupled receptor kinase (GRK) and the $\beta\gamma$ subunit of G-protein ($G_{\beta\gamma}$) was identified using this approach (Koch et al., 1993).

Combinatorial approaches take advantage of the *in vitro* screening of random sequences to identify molecules with affinity toward either interacting protein. Then, the positives isolates, which have affinity for the whole molecule not the interface, are tested individually for the ability to disrupt the interaction. Aptameric RNA molecules were selected *in vitro* from a random RNA library for their ability to interfere with the interaction between NF-κB and Tax protein from human T-cell leukemia virus (Tian et al., 1995). Another example of this approach is the identification of short peptides that can inhibit binding of calmodulin to camlodulin-dependent kinase (Nevalainen et al., 1997). This method is a time-consuming, multi-step approach that is not yet systematic.

Here, a degenerate oligonucleotide containing randomized sequences was synthesized to encode 9-mer peptides as a fusion to Trx. The base composition of the randomized codon was designed to minimize the occurrence of stop codons and to code for a natural distribution of amino acid residues (LaBean & Kauffman, 1993). Efficient cloning of oligonucleotides with a long sequence presents a special problem. The complexity of as few as six degenerate codons exceeds that of the entire human genome and thus, it is not practical to create double-stranded degenerate inserts simply by annealing complementary degenerate oligonucleotides. To overcome this problem, we used the gapped-duplex method (Cwirla et al., 1990), in which a long degenerate oligonucleotide is annealed to two short nucleotides ("anchors") complementary to nondegenerate regions

3′ ends. Annealing of anchor primers generates cohesive ends that are compatible to certain restriction enzymes. The repair machinery inside an *E. coli* cell fills in the gap in the duplex DNA. Thus, this method allows the skipping of *in vitro* steps of restriction digestion and DNA synthesis, which is beneficiary in creating a large library. A library of 5×10^8 members was created using this method.

The selection cassette (λP_R-*LacZ*-*tet*-rrnB) includes dual reporter genes, whose transcription is driven by a λP_R promoter. The λP_R promoter was designed to contain only a single copy of the λO_{R1} operator to avoid complexity arising from cooperative binding of repressor to multiple copies of operator. The *lacZ* and *tet* genes are transcribed in a polycistronic manner resulting in a single mRNA molecule containing both genes. The *tet* gene was designed to contain an endogeneous ribosomal binding site. Thus, two separate polypeptides are translated from the same mRNA molecule. The polycistronic transcription ensures that expression of the two reporter genes is equal and under control of λP_R. Use of the *tet* gene allows for a growth selection, which is essential to screen a large library. Screening of more than 10^8 transformants is possible due to the high-density plating enabled by *tet* selection. The use of dual reporter genes has advantages. The two gene products share little in their mode of action and expression of one gene does not affect that of the other. The simultaneous observation of the expression of both genes eliminates false positives resulting from erroneous expression of either gene due to spontaneous mutations *in vivo*.

Conformational constrains are often used to enhance the activity biologically relevant peptides. Previously, random sequences were inserted into the active-site loop of Trx to

identify peptides with affinity for an immobilized antibody (Lu et al., 1995). Peptides screened from this approach appear to be in their "active conformations" and achieve tight binding to the target molecules at the expense of conformational entropy. This approach may take advantage of the target region or cleft being displayed and held on a surface, where all possible peptide aptamers have access to the target regardless of structural constraints. Yet, in screening for dissociative inhibitors, where peptides must intervene and bind to the interface of a protein complex, conformationally constrained peptides may not be effective because many members of the library would be denied access to the interface due to their rigid, pre-organized structures. Therefore, we decided to construct a library of unconstrained linear peptides as a fusion to the C-terminus of Trx.

Sequences of positive clones show some interesting features (Figure 2.7). That there is not a strong similarity among the sequences is not surprising because the clones are from a single round of an *in vivo* selection rather than from multiple rounds of an *in vitro* selection (as are usually employed in a phage display screen, where positive clones are enriched at each round). A common feature in all three groups of clones is a high representation of aliphatic and hydrophobic residues (A, G, V, and W) and the presence of a charged residues (E, D, and K). This content is consistent with the characteristics of the dimer interface of the HIV protease. The interface of the protease forms an anti-parallel β-sheet composed of four N- and C-terminal segments of dimer (NH_2-$P^1Q^2I^3T^4$ and $T^{96}L^{97}N^{98}F^{99}$-COOH, respectively) of mostly hydrophobic residues. Therefore, a dissociative peptide is likely to be hydrophobic. In addition, Trx–peptide fusions need to

be stably exposed in the cytosol of a bacterial cell during the selection process for access to the transcription machinery of the reporter genes. A charged residue in the peptides enhances the solvation and hence accessibility of the peptide during the *in vivo* screening. Thus, the sequence content of the positives demonstrates the imperatives of the selection process: hydrophobicity and solubility. Furthermore, the sequences of positive isolates (including pep52) share little similarity with those of known dissociative inhibitors, which are derived from N- or C-terminal segments of HIVPR. This indicates that a non-biased, combinatorial screen may identify novel sequences that differ in their primary sequences from the authentic target region but nevertheless are more potent.

Both pep52 and dim52 show true dissociative inhibition of HIVPR at low ionic strength (0.10 M added NaCl) but a mixed mode of inhibition at high ionic strength (1.0 M added NaCl). The influence of ionic strength on the inhibition mechanism may be due to the salt stabilization of protease dimers (Szeltner & Polgar, 1996). The salt stabilization of protease dimer is evident from the large change in the values of K_d of protease dimer measured under different conditions (12 nM at low salt and 60 pM at high salt). Another reason for the salt influence may be the larger contribution of hydrophobic contacts for peptides bound to the hydrophobic subsites of HIVPR than the interface (Schramm et al., 1996). Still, the condition of low ionic strength under which the peptides show dissociative inhibition is far closer to the intracellular condition ($I = 0.15$ M (Cayley et al., 1991)) than the non-natural high salt condition ($I > 1.0$ M).

The global two-fold symmetry in the homodimeric structure of the protease allows for a simple approach to increase the potency of a dissociative inhibitor. Tethering a peptide

in a head-to-head or tail-to-tail fashion would present the peptide with symmetry and increased valency, and could lead to higher affinity. It has been reported that crosslinked peptides from N- or C-terminus of HIVPR enhanced dissociative inhibition as compared to the monomeric form of the peptides (Babe et al., 1992; Zutshi et al., 1997; Bouras et al., 1999). The fact that a crosslinked peptide (dim52) is 40-fold more potent than the monomeric peptide (pep52) suggests that this can be a simple and general approach to improve the ability of dissociative inhibitors of homodimeric enzymes. It is also known that the length (Zutshi et al., 1997) as well as the rigidity and chemical nature (Bouras et al., 1999) of crosslinkers are important for the efficacy of tethered peptides as dissociative inhibitors. Optimization of these factors could further decrease K_{id} of dim52.

According to analytical gel filtration chromatography, pep52 promotes the dissociation of the protease dimer (Figure 2.10). In the chromatogram, the monomer peak is broader than the dimer peak, which can be explained by heterogeneity or the lack of a compact structure in the monomer–pep52 complex, or both. Monomer–inhibitor complex is a single species only from kinetic data. At the molecular level, binding of the inhibitor could involve more than one site, provided that binding at the sites preclude dimerization (Zhang et al., 1991). Therefore, multiple species of monomer–pep52 complex can exist. The monomeric form of protease is known to be energetically unfavorable and its structure has never been experimentally determined (Grant et al., 1992; Todd et al., 1998).

High rates of viral turnover and the low fidelity of HIV reverse transcriptase have resulted in the emergence of HIV variants with resistance against drugs including

protease inhibitors (Condra et al., 1995; Condra, 1998). To overcome resistance to individual drugs, combination therapy has been practiced in which multiple inhibitors with different antiviral mechanisms are used simultaneously to treat AIDS (Li et al., 1998; Palella et al., 1998). But recent evidence suggests that the conventional triple-drug therapy has failed because of the emergence of HIV isolates with cross-resistance against different drugs (Fatkenheuer et al., 1997; Piketty et al., 1998). Furthermore, some of these cross-resistant HIV variants show resistance to many new compounds in clinical trials including protease and reverse transcriptase inhibitors (Palmer et al., 1999). All of the clinically approved inhibitors of HIVPR are peptide mimetics that binds in the active site and adjacent binding pocket.

Mutations that result in drug resistance have arisen mostly from single amino acid changes in substrate binding pocket of the enzyme during treatment of AIDS with small molecule inhibitors (Flexner, 1998; Klabe et al., 1998). Active site-directed inhibitors rely on a few high-affinity interactions with the protease. In contrast, interactions between a dissociative inhibitor and protease monomer would involve many residues spreading over a larger surface area. Moreover, the residues in the interface are highly conserved even among the protease variants resistant to active site-directed drugs (Schinazi et al., 1997). The interface region may be less tolerant to mutations than the substrate-binding pocket in terms of enzyme activity. Thus, point mutations that preserve protease activity but evade dissociative inhibitors are unlikely to occur, which may make dissociative inhibitors less prone to drug resistance. The other advantage of dissociative

inhibitors over active site-directed inhibitors is that dissociative inhibitors can act on the polyprotein precursor before the active site of the enzyme is formed.

It is also possible that dissociated HIVPR monomers are good substrates for the active dimers, considering that there are several autoproteolysis sites in HIVPR (Rose et al., 1993). The extent of hydrolysis would be governed by the degree of dissociation, which is triggered by the binding of inhibitory peptides. Autoproteolysis would shift the dimer-monomer equilibrium toward monomer, eventually reducing the population of active dimers. This novel mechanism could be effective in inhibiting protease activity *in vivo* with the use of dissociative inhibitor.

A high-throughput ELISA screen was developed for the verification of true positives selected from the genetic selection. These two methods nicely complement each other in that genetic selection enables the screening of a huge library and ELISA provides a tool for the rapid biochemical examination of positives generated by the selection. Combined, these approaches make a complete package to control protein–protein interaction. A stable hybrid repressor can be formed through the heterodimerization of two interacting proteins (Marchetti et al., 1995; Jappelli & Brenner, 1996). Therefore, our approach is expandable to the disruption of heterologous protein–protein interactions, which would provide a useful means for the regulation of biological processes and drug discovery. Although a peptide library was used in our screening, libraries of other biopolymers including RNA and DNA, and cell-permeable small molecules can be screened using this approach. Another interesting application of our method is the disruption of protein–DNA interactions. High occurrence of false positives (~ 25%) that can interfere with the

interaction of NcI and λO_{R1} DNA indicates that this system can be an effective tool to identify inhibitors of specific protein–DNA interactions of interest from a combinatorial library. No other screening methods have described.

The advent of combinatorial and recombinant DNA technologies has opened a way to rapid generation of large libraries of biopolymers. The idea here is that it should be possible, from a library of small peptides, to select individual molecules *in vivo* that recognize and block a specific protein–protein interaction. A genetic selection of an encoded peptide library provides a powerful tool to identify lead compounds for a new class of inhibitors that disrupt the assembly of the multisubunit enzymes. In this chapter, I described a genetic selection of dissociative inhibitors of protein–protein interaction. The HIV-1 protease was tested as a model target because it has great therapeutic interest and also uses the simplest mode of protein–protein interaction, homodimerzation. A potent dissociative inhibitor was identified from a combinatorial peptide library and potency of the peptide was further increased simply by covalent crosslinking of two peptides.

Table 2.1 Regulatory properties of wild-type and hybrid repressors on transcription from λP_R-*lacZ*-*tet*-rrnB. Plasmids were transformed into strain MC1061 to test for *in vivo* binding of hybrid repressors to λO_{R1}. The low copy number plasmid pSH20 contains the reporter cassette alone. pSH26 – 29 are derivatives of pSH20 with the expression modules for various repressor hybrids driven by the *lacUV5* promoter. cI-dPR2 is a hybrid protein of NcI and the C- and N-terminal segments of HIV-1 protease tethered by a linker ($P^1Q^2I^3T^4L^5$-GGSSG-$S^{95}T^{96}L^{97}N^{98}F^{99}$). cI-zip is a hybrid of NcI and GCN4. Susceptibility to tetracycline and β-galactosidase activity were measured as indicative of binding to λO_{R1}.

Plasmid	Repressor	Susceptibility to tetracycline[a]	β-gal units	% Repression[b]
pSH20	none	resistant	$(1.1\pm0.1)\times10^4$	0
pSH26	NcI-PR	sensitive	$(2.0\pm0.2)\times10^3$	82
pSH27	NcI-dPR2	sensitive	$(2.8\pm0.4)\times10^2$	98
pSH28	cI	sensitive	$(2.0\pm0.1)\times10^2$	98
pSH29	NcI-zip	sensitive	$(1.7\pm0.1)\times10^3$	84

[a] Determined in 10 μg/mL tetracycline.

[b] % Repression is calculated as: 1 – (β-galactosidase activity with repressor / β-galactosidase activity without repressor).

Figure 2.1 Gel retardation assay of NcI-PR and cI with fluorescein-labeled λO_{R1}. Purified cI protein (30 μg/mL) or NcI-PR protein (50 μg/mL) was incubated in 10 mM Tris-HCl buffer (pH 8.0) containing $MgCl_2$ (5.0 mM), $CaCl_2$ (2.0 mM), BSA (50 μg/mL), sheared salmon sperm DNA (0.20 mg/mL), poly(dI-dC) (50 μg/mL), DTT (1 mM), glycerol (5% v/v), and fluorescein-labeled λO_{R1} DNA (0.5 μM) at 25 °C for 20 min. After incubation, mixtures were electrophoresed in a polyacrylamide (8% w/v) gel prepared in 0.5 × TBE buffer containing $MgCl_2$ (2.0 mM). After electrophoresis, the gel was scanned with a fluorimager SI.

NcI–PR
cI
no repressor
Free
DNA

Figure 2.2 Design of a 9-mer peptide library as a fusion to *Escherichia coli* thioredoxin (Trx). The library was constructed in a plasmid using a gapped duplex method. Random 9-mer peptides are produced as a fusion to the C-terminus of *E. coli* Trx. A flexible linker (Ser-Gly-Gly-Gly) was put between Trx and each 9-mer peptide.

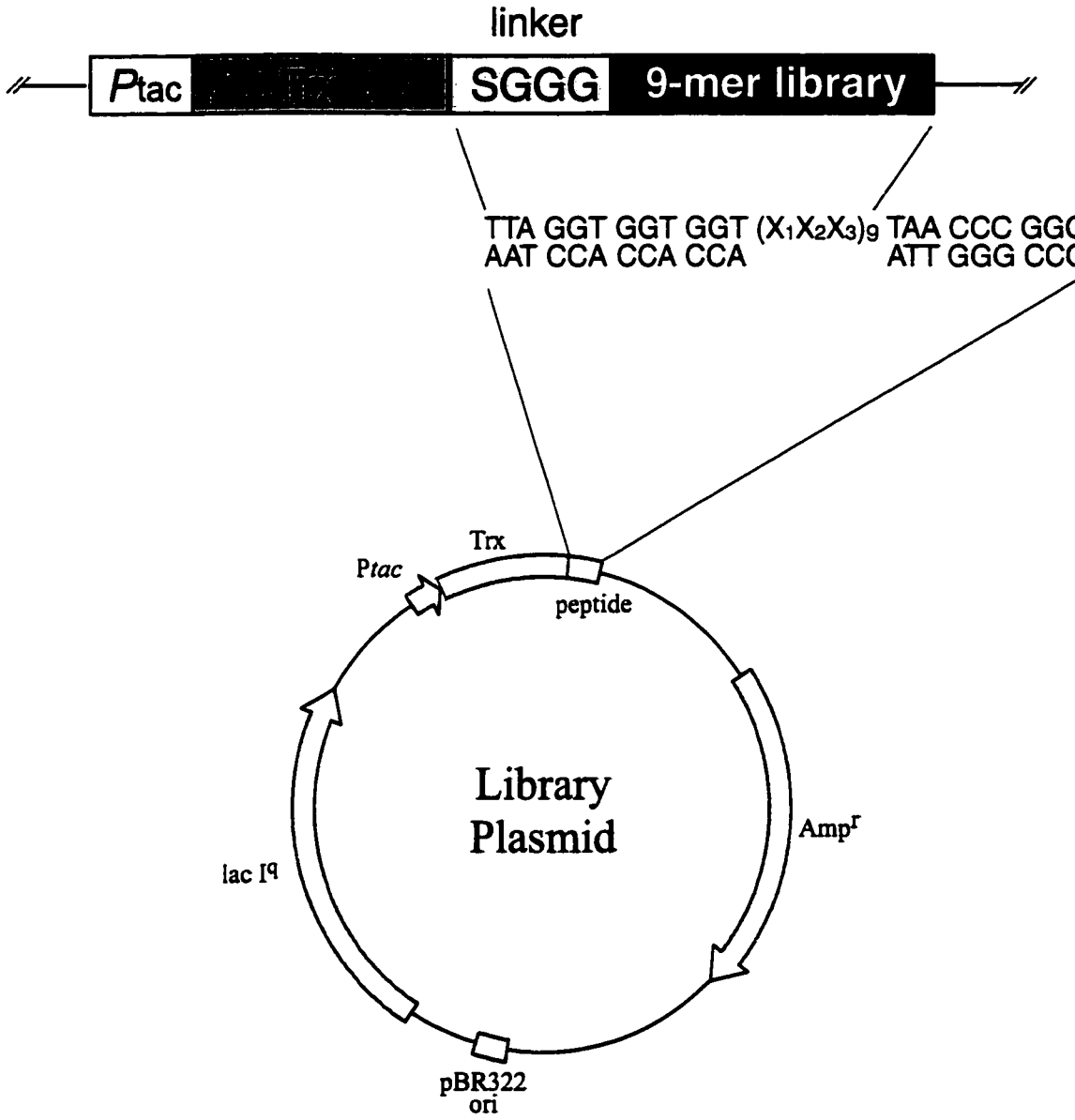
linker
Ptac
SGGG
9-mer library
TTA GGT GGT GGT (X1X2X3)9 TAA CCC GGC
AAT CCA CCA CCA ATT GGG CCG
Trx
Ptac
peptide
Library
Plasmid
Amp^r
lac I^q
pBR322
ori

Figure 2.3 Map of the reporter plasmid pSH26.

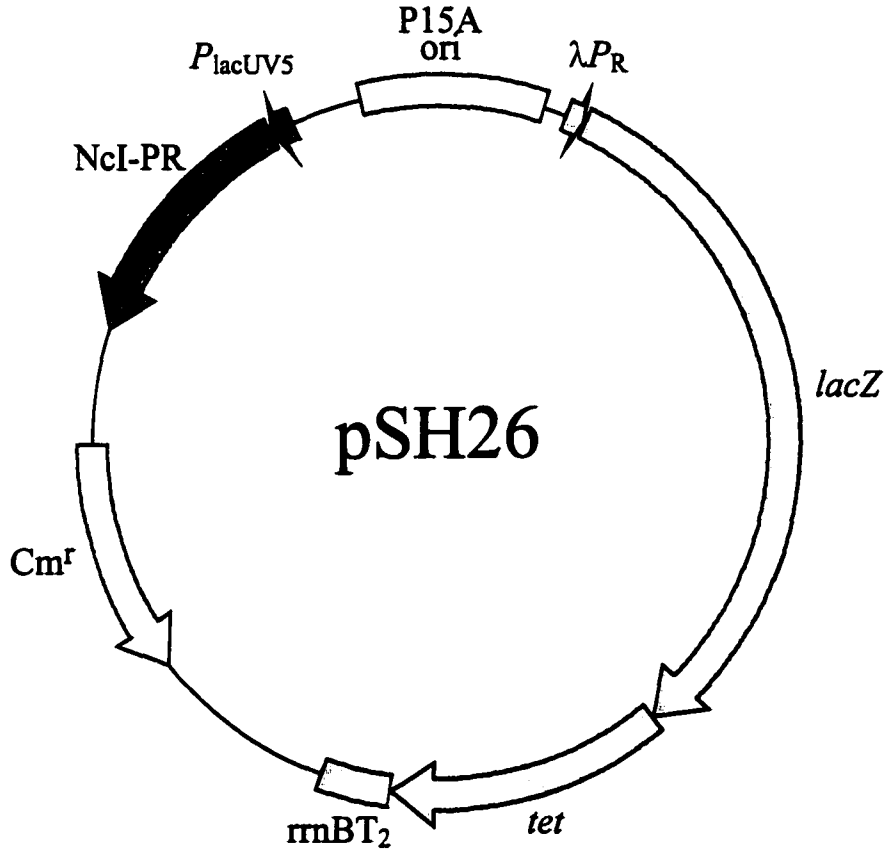
P15A
ori
P_{lacUV5}
λP_R
NcI-PR
pSH26
lacZ
Cm^r
rrnBT$_2$
tet

Figure 2.4 Genetic selection for dissociative inhibitors of a protein–protein interaction. Upon dissociation of the dimeric protein triggered by a peptide from a combinatorial library, transcription of the reporter genes is turned on. Only *lacZ*$^{+}$*tet*^{R} cells survive in a selective condition.

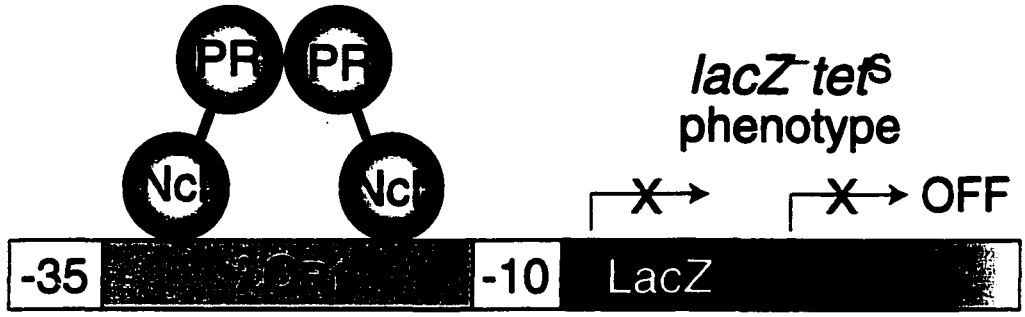
PR
PR
Nc
Nc
lacZ⁻ tetˢ
phenotype
OFF
-35
-10
LacZ


Trx
combinatorial
peptide library

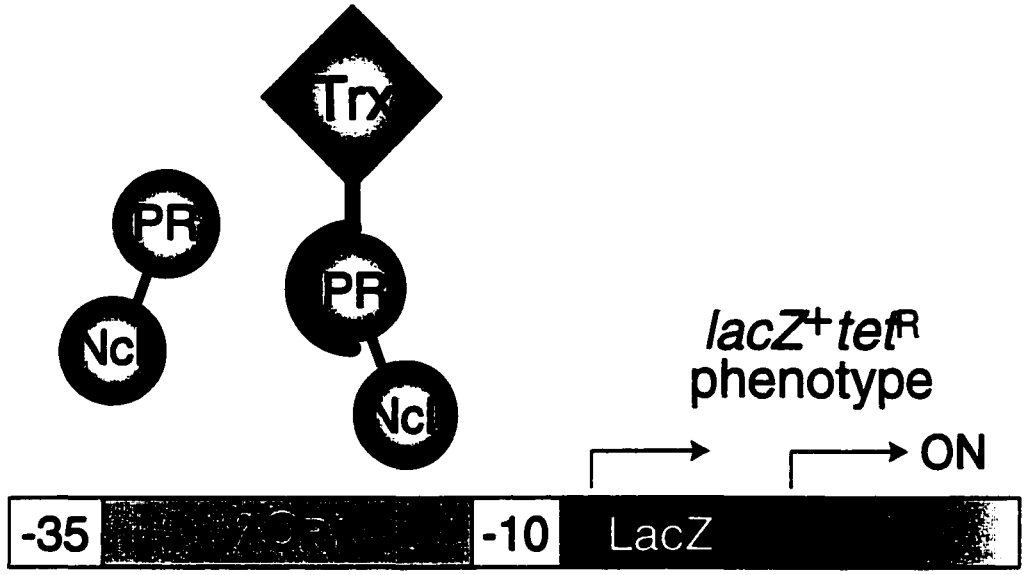
Trx
PR
PR
Nc
Nc
lacZ⁺ tetᴿ
phenotype
ON
-35
-10
LacZ

Figure 2.5 Gel retardation assay to eliminate false positives that interfere with the protein–DNA interaction. Lysates of the *lacZ*$^+$*tet*^{R} clones were mixed with purified cI protein (30 μg/ml) and incubated in 9 μL of 10 mM Tris-HCl buffer (pH 8.0) containing $MgCl_2$ (5 mM), $CaCl_2$ (2 mM), BSA (50 μg/ml), sheared salmon sperm DNA (0.2 mg/ml), poly(dI-dC) (50 μg/ml), DTT (1 mM), and glycerol (5% v/v) at 25 °C. After 20 min of incubation, 1 μL of λO_{R1} DNA (5 μM) was added, and the reaction was incubated for another 15 min at 25 °C before electrophoresis in a polyacrylamide (8% w/v) gel as described in Figure 2.1.

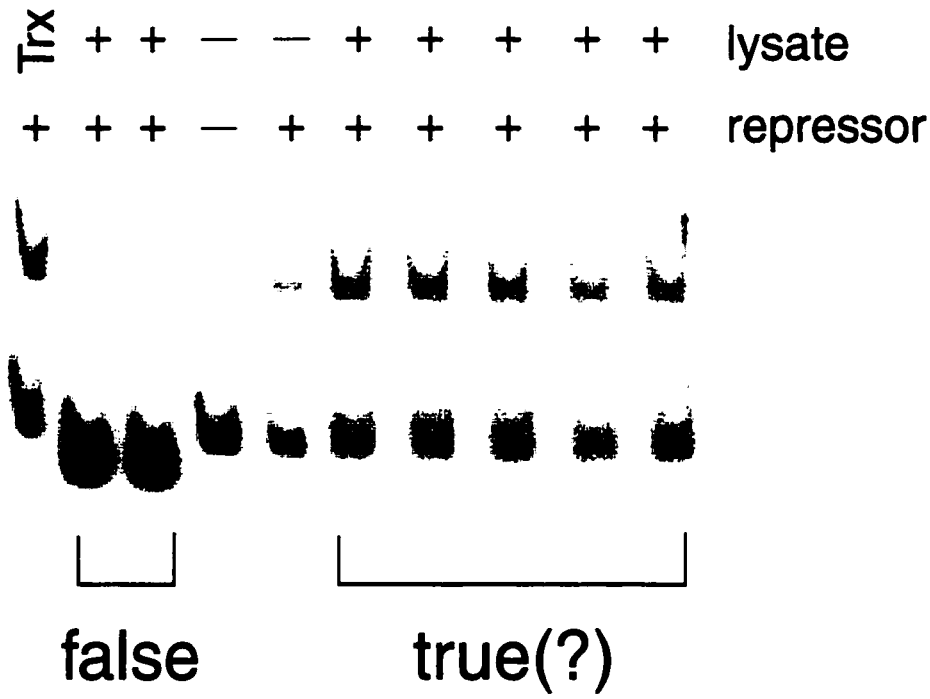
Trx + + — — + + + + +
lysate
+ + + — + + + + + +
repressor
false
true(?)

Figure 2.6 **A.** Scheme for a high-throughput ELISA.

B. Results of typical high-throughput ELISA. Isolates not identified as false positives were tested for *in vitro* binding to immobilized monomeric protease. Lysate containing Trx–peptide fusion was mixed with PBS buffer and incubated at 4 °C overnight in each well of the plates. Anti-Trx antibody (100 μL) in 1:5000 dilution in PBS buffer containing BSA (1 mg/ml) was incubated in each well at 25 °C for 1 h. Subsequently, anti-rabbit IgG-alkaline phosphatase conjugate (200 μL) in 1:5000 dilution in PBS buffer was incubated at 25 °C for 1 h. A substrate solution (75 μL) of 0.10 M CAPS-NaOH buffer (pH 10.3) containing NaCl (50 mM), FDP (0.20 mM), and $MgCl_2$ (10 mM) was added to each well, and the resulting solution was incubated at 25 °C for 10 min. The plates were either scanned by a fluorimager SI System or photographed on an UV transilluminator. A1 through E8 represent protease-coated surfaces to which lysates from 40 clones were applied. F1 represents the surface coated with free cysteine and no lysate was applied during the process. F2 is a protease-coated surface in which lysate of cells producing Trx with no peptide fusion was used. F3 is the protease-coated surface with no lysate applied and anti-protease antibody used instead of anti-Trx antibody. F4 is a surface on which purified Trx was immobilized and no lysate was applied.

A

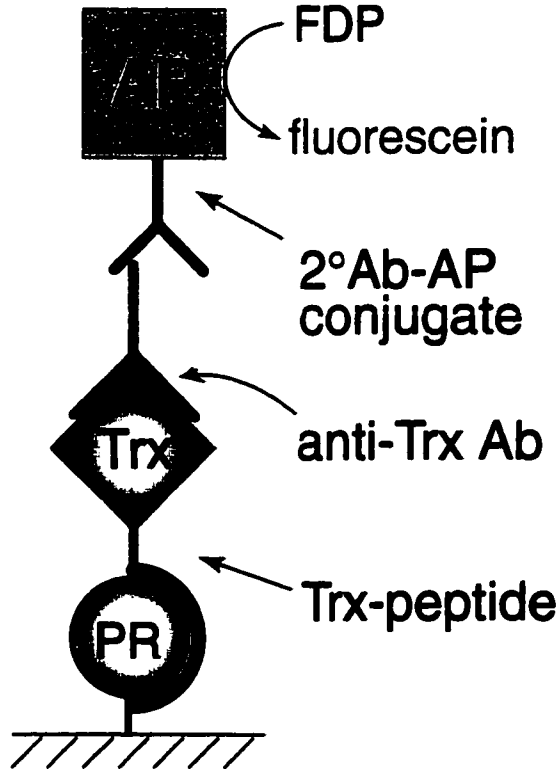
FDP
fluorescein
2°Ab-AP
conjugate
anti-Trx Ab
Trx
Trx-peptide
PR

B

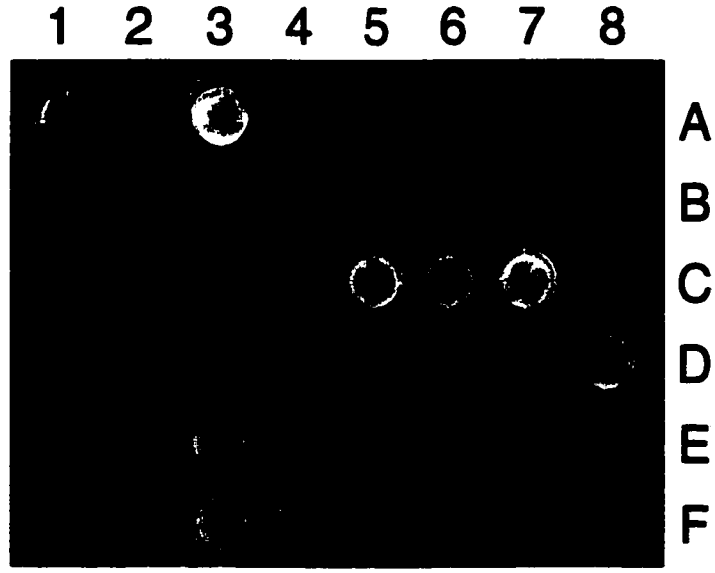
1 2 3 4 5 6 7 8
A
B
C
D
E
F

Figure 2.7 Sequence alignments of positive isolates from the genetic selection for dissociative inhibitors of HIV-1 protease. Residues that are conserved to >67% are in the gray boxes, and those conserved 100% are in the black boxes. The pep52 is boxed.

12				M	G	V	G	S	E	G	V	A
87	Y	C	I	G	V	G	-	Q	G	V	
20				V	R	V	G	E	K	E	V	D
52	I	V	Q	V	D	A	E	G	G		
55	S	V	D	W	-	A	K	G	V	H	
83	L	A	C	W	D	A	T	G	V		
15	E	V	A	D	D	I	A	D	N		
82		I	A	G	D	R	A	V	L	R	
58			D	G	A	S	A	V	Y	A	H

Figure 2.8 **A.** Zhang-Poorman plot for inhibition of HIV-1 protease by pep52 at low ionic strength. A fluorogenic substrate, Arg-Glu(EDANS)-Ser-Gln-Asn-Tyr-Pro-Ile-Val-Gln-Lys(DABCYL)-Arg, was used to monitor the proteolytic activity. The protease (10 – 100 nM) was preincubated for 30 min at 25 °C in 97 μL of 0.10 M sodium acetate buffer (pH 4.7) containing glycerol (5% v/v), PEG8000 (0.1% v/v), DTT (5 mM), EDTA (1 mM), NaCl (0.10 M), and varying amounts of pep52: 232 μM (triangles), 116 μM (squares), 58 μM (closed circles), and 0 μM (open circles).. The substrate (3 μL) was added to a final concentration of 3.75 μM to start the reaction and the initial velocity was measured. A plot was constructed by plotting $Ev/\sqrt{k}$ as a function of $\sqrt{k}$ as shown in Equation 2.1.

B. Zhang-Poorman plot for pep52 at low ionic strength. The data were plotted according to Equation 2.3 for accurate measurement of the K_{id} value.

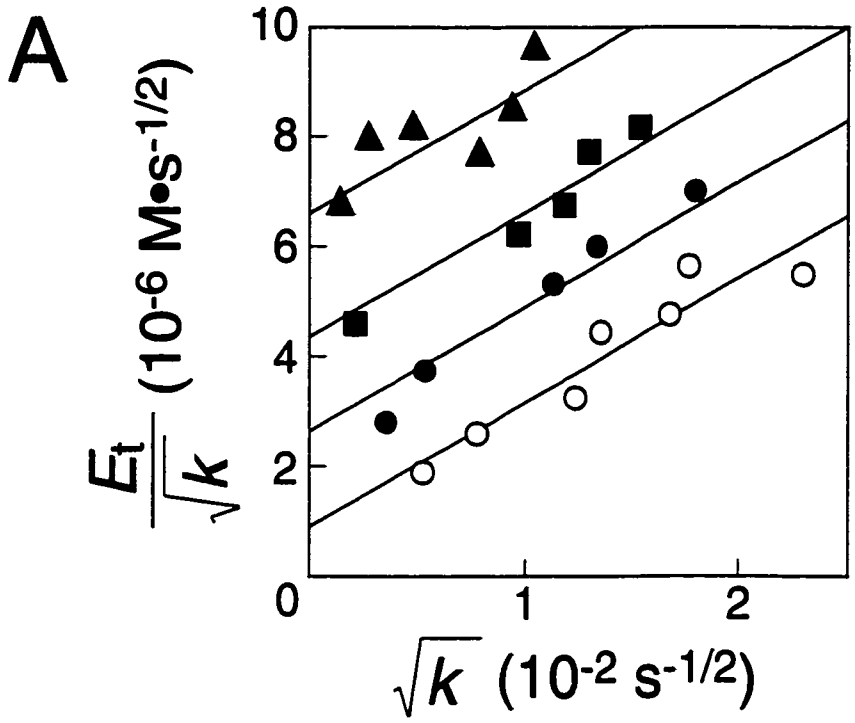
A
10
8
6
4
2
0
1
2
$\frac{E_t}{\sqrt{k}}$ (10^{-6} M•s$^{-1/2}$)
$\sqrt{k}$ (10^{-2} s$^{-1/2}$)

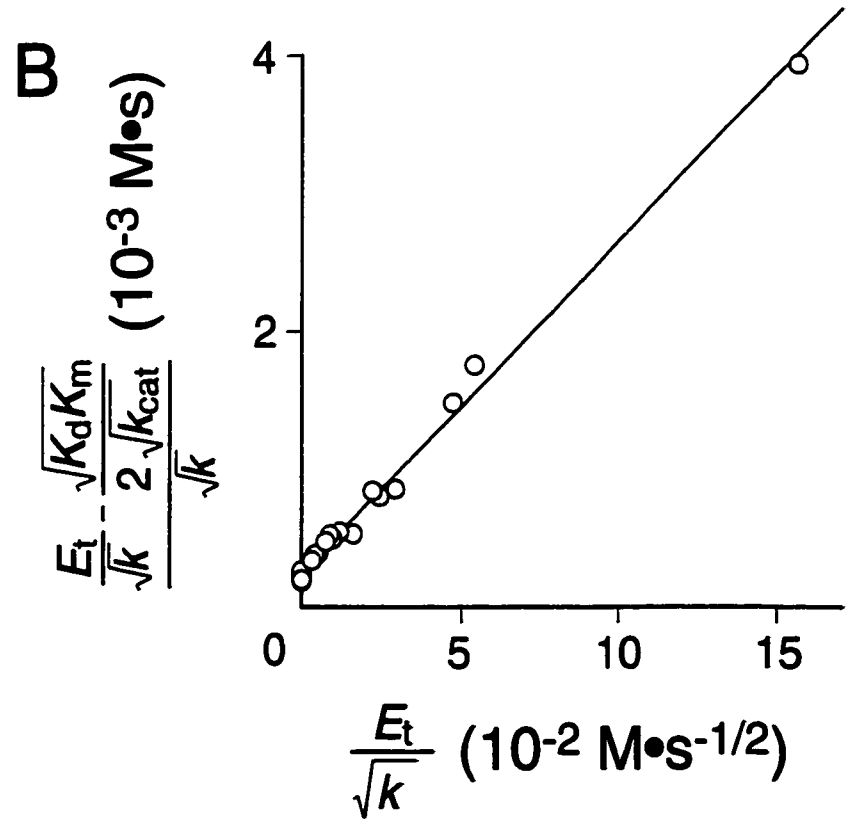
B
4
2
0
5
10
15
$\frac{E_t}{\sqrt{k}} - \frac{\sqrt{K_d K_m}}{2\sqrt{k_{cat}}}\frac{1}{\sqrt{k}}$ (10^{-3} M•s)
$\frac{E_t}{\sqrt{k}}$ (10^{-2} M•s$^{-1/2}$)

Figure 2.9 Zhang-Poorman plot for inhibition of HIV-1 protease by pep52 at high ionic strength. The initial velocity of protease activity was measured at different concentrations of pep52: 232 μM (triangles), 116 μM (squares), 58 μM (closed circles), and 0 μM (open circles). The measurements were made as described in Figure 2.8, except for NaCl (1.0 M). A plot was constructed by plotting $Ei/\sqrt{k}$ as a function of $\sqrt{k}$ as shown in Equation 2.1

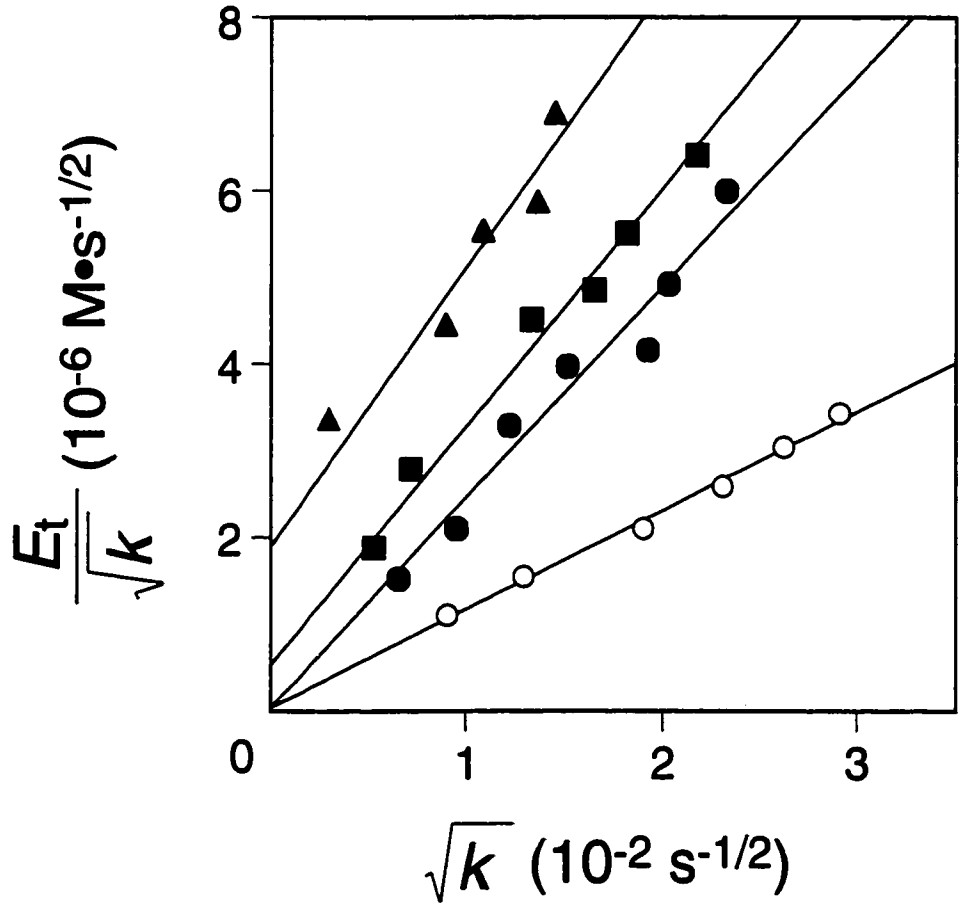
8
6
4
2
0
1
2
3
$\frac{E_t}{\sqrt{k}}$ (10^{-6} M•s$^{-1/2}$)
$\sqrt{k}$ (10^{-2} s$^{-1/2}$)

Figure 2.10 A chromatogram from analytical gel filtration chromatography of wild-type HIV-1 protease in the presence (5 mM, black) or absence (0 mM, gray) of pep52. Pep52 (0 or 5 mM) was incubated for 30 min at 25 °C in 50 mM sodium acetate buffer (pH 4.7) containing wild-type protease (2.8 μM). The mixture (100 μL) was loaded onto a Superdex 75 gel filtration column (22 cm × 20 mm^2) that had been equilibrated in 50 mM sodium acetate buffer (pH 4.7). The absorbance at 280 nm was monitored.

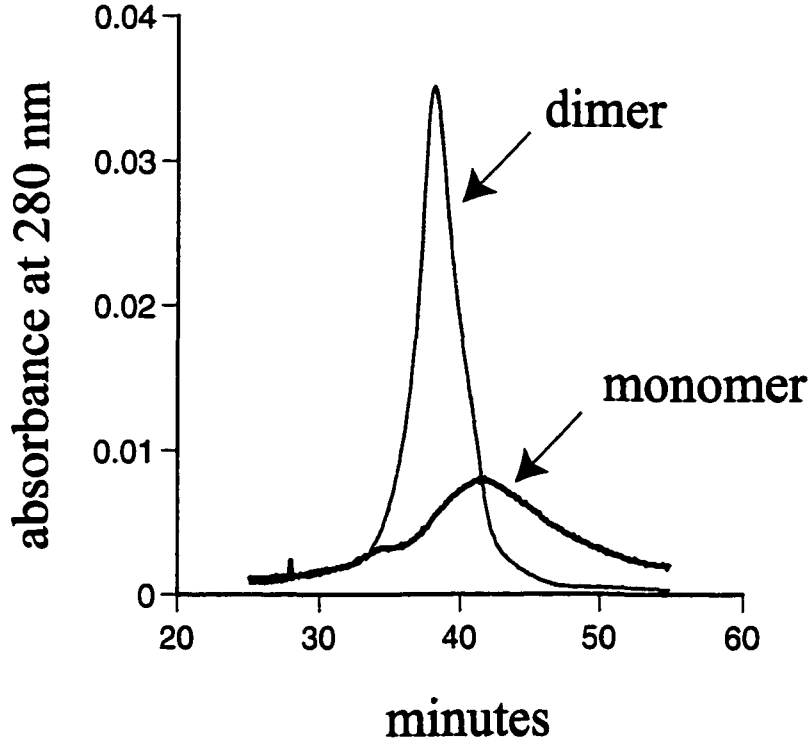
0.04
0.03
0.02
0.01
0
absorbance at 280 nm
dimer
monomer
20
30
40
50
60
minutes

Figure 2.11 Primary structure of dim52, a crosslinked dimer of pep52.

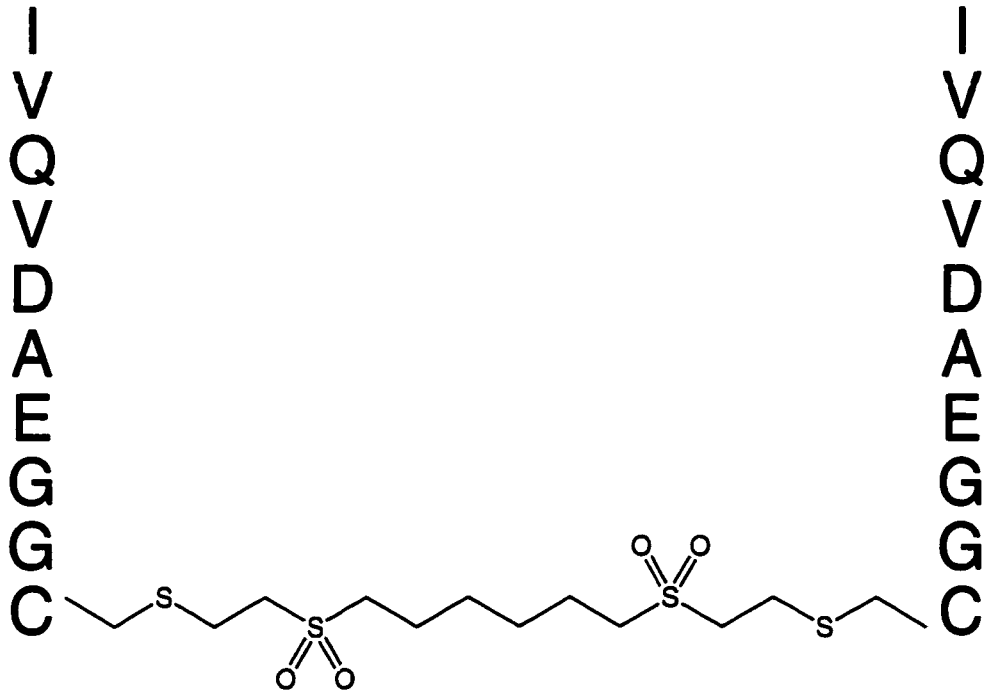

dim52

Figure 2.12 **A.** Zhang-Poorman plot for dim52. For the measurement of initial velocity, protease (10 – 100 nM) was preincubated for 30 min at 25 °C in 97 μL of 0.10 M sodium acetate buffer (pH 4.7) containing glycerol (5% v/v), PEG8000 (0.1% v/v), DTT (5 mM), EDTA (1 mM), NaCl (0.10 M), and varying amounts of dim52: 2.96 μM (squares), 1.48 μM (closed circles), and 0 μM (open circles). The substrate (3 μL) was added to a final concentration of 3.75 μM to start the reaction. A plot was constructed by plotting $Et/\sqrt{k}$ as a function of $\sqrt{k}$ as shown in Equation 2.1

B. Zhang-Poorman plot for dim52. The data were plotted according to Equation 2.3 for accurate measurement of the K_{id} value.

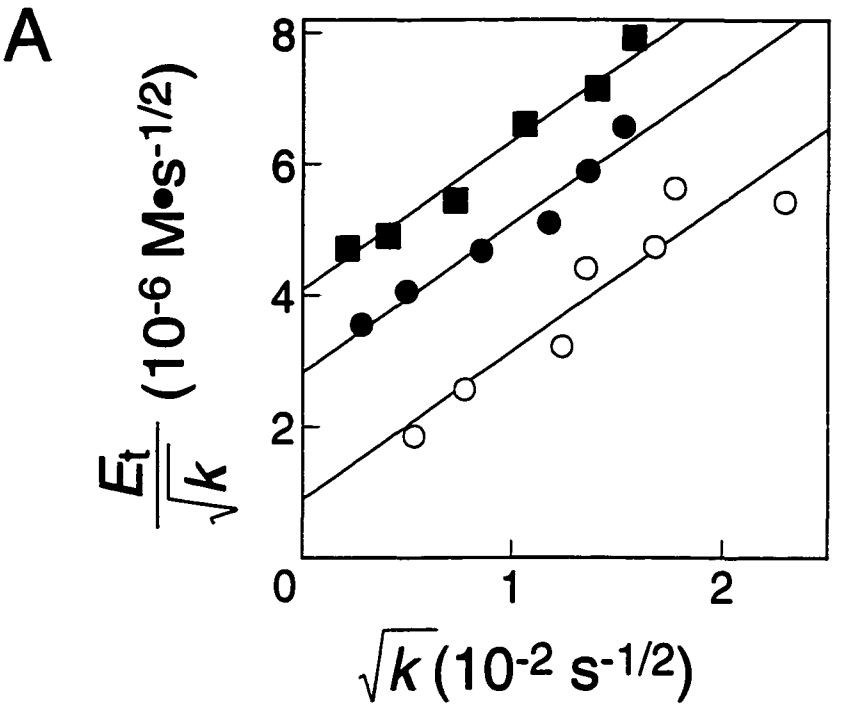
A
8
6
4
2
0
1
2
$\frac{E_t}{\sqrt{k}}$ (10^{-6} M•s$^{-1/2}$)
$\sqrt{k}$ (10^{-2} s$^{-1/2}$)

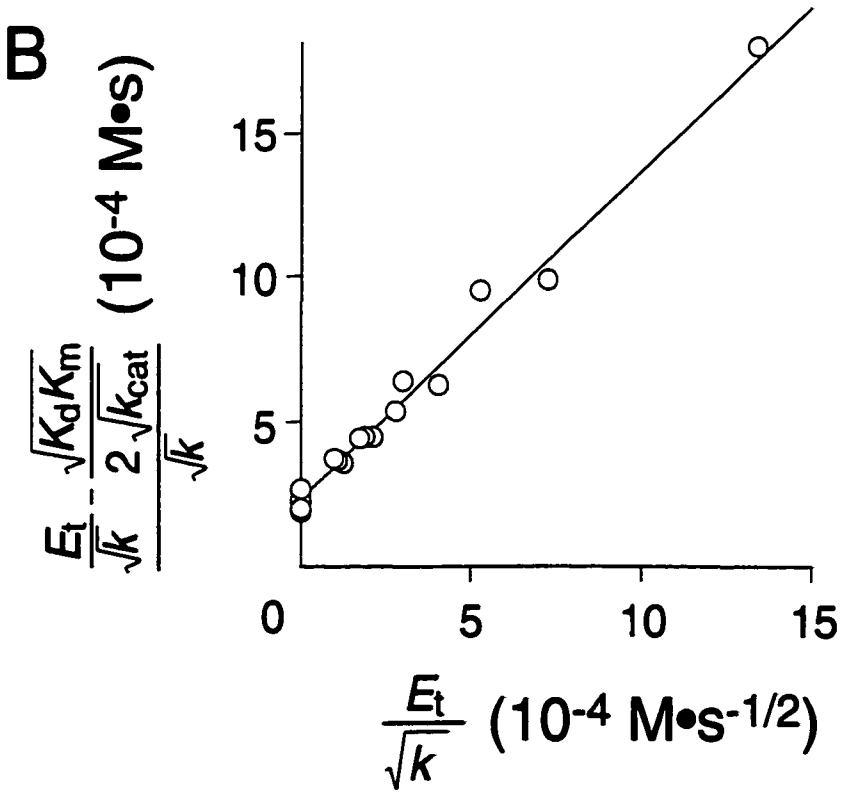
B
15
10
5
0
5
10
15
$\frac{E_t}{\sqrt{k}} - \frac{\sqrt{K_d K_m}}{2\sqrt{k_{cat}}}$ (10^{-4} M•s)
$\frac{E_t}{\sqrt{k}}$ (10^{-4} M•s$^{-1/2}$)

Chapter 3

A Genetic Screen to Dissect Protein–Protein Interactions

A portion of this work is to be submitted for publication:

Sang-Hyun Park and Ronald T. Raines (2000). A Genetic Screen to Identify Important Residues in Protein–Protein Interactions, in preparation.

3.1 INTRODUCTION

Bovine pancreatic ribonuclease A (RNase A; EC 3.1.27.5) catalyzes the hydrolysis of single-stranded RNA. It is a small enzyme consisting of 124 amino acid residues and secreted by exocrine cells of the bovine pancreas. The enzymatical and biophysical properties of RNase A are well characterized (Raines, 1998). RNase A has been an object of many important studies in protein chemistry due to its exceptional chemical stability and availability in its large quantity. Its biological function, however, has yet to be determined.

The biological function typically ascribed to ribonucleases is to process and turnover cellular RNA. Some homologs of RNase A appear to have unusual biological activities. These homologous ribonucleases include angiogenin (Fett et al., 1985), bovine seminal ribonuclease (BS-RNase) (Matousek, 1973), onconase (Ardelt et al., 1991), and the eosinophilic ribonucleases (Rosenberg et al., 1995). Human angiogenin plays a critical role in the establishment of wide range of human tumors through its ability to induce neovascularization (Fett et al., 1985; Olson et al., 1995) and to serve as an adhesion molecule for tumor cells (Soncin et al., 1994). BS-RNase has antitumor and immunosuppressive activity (Matousek, 1973; Soucek et al., 1983; Soucek et al., 1986). Onconase inhibits tumor growth (Mikulski et al., 1990; Ardelt et al., 1991). Eosinophilic ribonucleases are neurotoxic and possess antiviral activity (Gleich et al., 1986; Domachowske et al., 1998).

All RNase A homologs catalyze the cleavage of RNA. Their ribonucleolytic activities differ significantly in magnitude and in specificity due to differences in the structures of their active sites. Nonetheless, the majority of the biological activities of these homologs appears to depend on ribonucleolytic activity. These biological functions are lost when residues essential for the catalysis are mutated or chemically modified, as had been shown for the angiogenic activity of angiogenin (Shapiro et al., 1989; Shapiro & Vallee, 1989), immunosuppressive and antitumor activity of BS-RNase (Vescia et al., 1980; Kim et al., 1995), and antitumor activity of onconase (Wu et al., 1993; Boix et al., 1996). The lack of cytotoxicity of RNase A itself (Leland et al., 1998) is the consequence of its high affinity toward a ribonuclease inhibitor (RI) protein. Likewise, a key to the biological activities of the homologous ribonucleases is their ability to evade RI in the cytosol.

RI is a 50-kDa protein that constitutes ~ 0.01% of cytosolic protein in mammalian cells (Lee & Vallee, 1993; D'Alessio & Riordan, 1998). RI contains 15 leucine rich, βα repeats arranged symmetrically in a horseshoe. The β-strands form a solvent-exposed β-sheet that defines the inner circumference of RI. RI forms a 1:1, noncovalent complex with its target ribonucleases. Binding of RI to its target is extraordinarily tight. Values of the inhibition constant (K_i) for the interaction of human RI (hRI) with human angiogenin and RNase A are in the fM range (Lee & Vallee, 1989; Vicentini et al., 1990). RI inhibits ribonucleases by blocking access of the substrate to the active site, as is apparent from the crystalline structures of complexes (Kobe & Deisenhofer, 1995; Papageorgiou et al., 1997). The resulting complexes have no detectable ribonucleolytic activity. Of

mammalian ribonucleases, only those belonging to the superfamily of RNase A are inhibited by RI. Two noticeable exceptions are BS-RNase and onconase.

The Biological function of RI inside a cell is not yet clearly understood. A few possible roles have been suggested, and they include the regulation of amounts of cellular RNA (Roth, 1962), a safeguard of cellular RNA against heterologous ribonucleases (Beintema et al., 1988), and the regulation of angiogenesis (Lee & Vallee, 1989). In spite of the ambiguity in its biological functions, the availability of purified RI has allowed for its use in many practical applications such as *in vitro* translation (Scheele & Blackburn, 1979) and cDNA synthesis (Eichler et al., 1981).

Upon the formation of the complex between RI and RNase A, a vast region of surface area (2551 $Å^2$) is buried in the interface (Kobe & Deisenhofer, 1995). This interface is 60% larger than that of typical protease–protein inhibitor or antibody–protein antigen complexes (Janin & Chothia, 1990). The crystalline structure of the RI•RNase A complex provides atomic details of this intermolecular interactions. Still, it is unclear which residues or segments of RNase A are most important in complex formation. Here, we describe a novel genetic screen to dissect a protein–protein interaction using the RI•RNase A complex as a model system.

Our approach takes advantage of the repressor protein (cI) from bacteriophage λ, which binds to its operator DNA as a dimer. A fusion protein was created where RI is fused to the C-terminus of DNA-binding domain of cI (NcI; residues 1 – 131). The resulting hybrid (NcI-PR) is not a functional repressor because RI does not dimerize. We created a library of epitopes of RNase A as a fusion to the C-terminus of NcI. Upon

coexpression of NcI-RI and the NcI-epitope hybrids, a functional repressor can be reconstructed through the interaction of RI with RNase A epitopes and can be identified by a readily detectable phenotype resulting from the transcription repression of a reporter gene (*lacZ*). We identified from the screening of an epitope library a subset of segments in RNase A that interact with hRI. One of these epitopes was synthesized chemically and tested for its ability to antagonize the formation of RI•RNase A complex. This approach could provide a general tool to dissect protein–protein interactions for the identification of important interactions and the development of antagonists against the interactions.

3.2 MATERIALS AND METHODS

Materials. E. coli strain MC1061 was from the American Type Culture Collection (Manassas, VA). pBR-RI was generous gift from Promega (Madison, WI). pJH370, pJH391, and λKH54 were generous gifts from James C. Hu (Texas A&M University). pACYC184 was from New England Biolabs (Beverly, MA). pGEX-4T3, DNase I, dNTP, G25 spin columns, and shrimp alkaline phosphatase were from Pharmacia Biotech (Piscataway, NJ). pGEM3Zf(+) and ΦX174 DNA/*Hin*fI markers were from Promega (Madison, WI). SYBR Green I was from Molecular Probes (Eugene, OR). 16S- and 23S-rRNA was from Boehringer Mannheim (Indianapolis, IN). *Pfu* DNA polymerase was from Stratagene (La Jolla, CA). All other enzymes for the manipulation of recombinant DNA were from either Promega (Madison, WI) or New England Biolabs (Beverly, MA).

General methods and instruments. PCR's described in this chapter were carried out using *Pfu* DNA polymerase. All the DNA fragments prepared by the PCR were sequenced and their identities were confirmed before subsequent subcloning steps. DNA sequencing was performed automatically on an ABI 377XL automated DNA sequencer from Applied Biosystems (Foster City, CA). Fluorescence gel scanning was carried out with a fluorimager SI System from Molecular Dynamics (Sunnyvale, CA).

Construction of plasmid for epitope library expression. A plasmid pGEX-4T3 was digested with *Bam*HI/*Bsu*36I and 5′-overhangs were filled in to blunt ends using Klenow fragment with dNTP. The DNA was purified from an agarose gel and circularized by ligation to create plasmid pSH49, which is identical to pGEX-4T3 except for the lack of an expression module for GST. pSH49 was cut with *Sal*I, the 5′-overhang was filled in to blunt ends, and the resulting DNA was digested with *Eco*RI. The *Eco*RI/*Eco*RV fragment from pJH370 was inserted into the blunt end/*Eco*RI fragment of pSH49 to create pSH52. The P_{lacUV5}-NcI fragment was amplified from pJH391 using oligonucleotides P62: TTGGATCCTAGTTAGTT*AGGCCT*CCCATCTCTCCGCATCACCTTTG, which contains *Bam*HI and *Stu*I sites, and p63: TCGCTAGCCCCTTTCGTCTTCAAGAAT. The resulting PCR fragment was inserted into the *Bam*HI/*Eco*RI sites of pSH52 to create an expression vector for the epitope library, pSH53.

Construction of λ repressor fusions. A DNA fragment containing NcI domain was amplified from pJH391 using oligonucleotides P50: GTATCTCGAGGCCCTTTCGTCTTC and P51: TTTCCTAGGTCGACACCCATCTCTCCGC, which contains a *Sty*I site. The PCR fragment was digested with *Eco*RI/*Sty*I and ligated to an *Eco*RI/*Spe*I fragment of pJH391 to create an expression vector for NcI, pSH50. A gene encoding wild-type RNase A was amplified from plasmid pBXR (delCardayre et al., 1995) using oligonucleotides P59: GCGTCGACCAAGGAAACTGCAGC and P60: CGAGATCTACACTGAAGCATCAAA, which contain *Sal*I and *Bgl*II sites, respectively. The PCR fragment was inserted into the *Sal*I/*Bam*HI sites of plasmid pJH391 to create an expression vector for NcI-RNase A fusion, pSH47. A gene encoding human ribonuclease inhibitor (Lee et al., 1988) was amplified from plasmid pBR-RI using oligonucleotides P57: ACCTCGAGCCTGGACATCCAGAGC and P58: GAAGATCTTCAGGAGATGACCCTCAG, which contain *Xho*I and *Bgl*II sites, respectively. The resulting PCR fragment was inserted into the *Sal*I/*Bam*HI sites of plasmid pJH391 to create an expression vector for NcI-RI fusion, pSH48. A DNA fragment containing an expression module for NcI-RNase A fusion was amplified from plasmid pSH47 using oligonucleotides P63: TCGCTAGCCCCTTTCGTCTTCAAGAAT and P64: TGACTCGGGATGCTGTCGGAATGGACG, which contain *Nhe*I and *Ava*I sites, respectively. The PCR fragment was digested with *Nhe*I/*Ava*I and ligated to a 5560 bp *Nhe*I/*Ava*I fragment of pSH48 to create an expression vector for both NcI-RNase A and NcI-RI fusions, pSH51.

Construction of reporter plasmids. A 653 bp *Hind*III/*Ssp*I fragment from pGEM3Zf(+) was ligated with a 2556 bp *Hind*III/*Hinc*II fragment from pACYC184, resulting in plasmid pSH46, which is a general cloning vector containing a p15A replication origin, a chloramphenicol resistance marker, and multi-cloning sites from pGEM3Z vector. C*la*I/*Bgl*II fragments from plasmids pSH48 and pSH50 were ligated to a *Cla*I/*Bam*HI fragment of plasmid pSH46 to create pSH54 and pSH55, respectively. A DNA fragment containing the reporter cassette of λP_R-*lacZ*-rrnB was prepared by digesting plasmid pSH15 (Chapter 2) with *Not*I and *Hind*III. The 5′-overhangs were filled in to blunt ends using Klenow fragment with dNTP's. The resulting DNA fragment was inserted into the *Sma*I site of pSH54 and pSH55 to create pSH58 and pSH59, respectively.

Generation of blunt-ended epitope inserts of RNase A gene. The cDNA of RNase A was amplified using oligonucleotides P59 and P60 as described above, and ten PCR reactions were combined and purified. The PCR fragments were digested partially with DNase I by incubation in 0.20 mL of 50 mM Tris-HCl buffer (pH 7.5) containing $MgCl_2$ (10 mM), BSA (50 μg/mL), $MnCl_2$ (10 mM), and DNase I (2 units) at 20 °C for 10 min. After incubation, EDTA (9 μL of a 0.5 M solution) and SDS (2 μL of a 10% w/v solution) were added to inactivate the DNase I. Resulting DNA was stained with SYBR Green I and electrophoresed along with fluorescein-labeled molecular weight markers in a polyacrylamide (10% w/v) gel in 1 × TBE buffer at 15V/cm for 1.5 h. Immediately

after electrophoresis, the gel was scanned with a fluorimager SI System and DNA bands corresponding 20 – 45 bp were cut out of the gel to fractionate the DNA into 20 – 30 bp, 28 – 35 bp, and 35 – 45 bp in size. DNA was purified from the gel pieces (Ausubel et al., 1994) and dephosphorylated using shrimp alkaline phosphatase.

Construction of an epitope library of RNase A. The epitope DNA inserts (20 – 30 bp; 0.20 μg) were ligated to *Stu*I-digested pSH53 (2 μg) using T4 DNA ligase with ATP by incubating at 37 °C for 6 h. The ligated DNA was digested with *Stu*I to linearize self-ligated pSH53 and then desalted. One third of each DNA sample was transformed into electrocompetent XL-1 Blue cells as described in the Chapter 2. Transformed cells were resuspended in SOC medium (1.0 mL) and grown at 37 °C for 1 h. One fifth of each of the cells was subjected to library amplification and the remaining cells were frozen and kept at -80 °C for future use. For amplification of the library, cells (0.20 mL) were plated on a large petri dish of LB-agar containing ampicillin (0.10 mg/mL) and grown for 37 °C for 16 h. LB medium (10 mL) was added to the plates and cells were recovered by scrubbing the surface of the medium with a glass rod. The library plasmid DNA was prepared from the collected cells.

Screening RNase A epitope library. Epitope library plasmids (0.20 μg) were simultaneously transformed with pSH58 (0.20 μg) into electrocompetent MC1061 cells. Cotransformants were plated onto a large petri dish of LB-agar containing ampicillin (0.10 mg/mL), chloramphenicol (0.10 mg/mL), X-Gal (50 μg/mL), and IPTG (30 μM),

and grown at 37 °C for 24 h until *lacZ*⁻ colonies appear. The library plasmids were rescued from *lacZ*⁻ colonies and retransformed into *E. coli* strain XL-1 Blue.

Dot plaque assay with λKH54. The rescued library plasmids from *lacZ*⁻ colonies were retransformed into pSH58/MC1061 and fresh overnight cultures were made in 2.0 mL of LB containing ampicillin (0.10 mg/mL), chloramphenicol (0.10 mg/mL), $MgSO_4$ (10 mM) and maltose (0.2% w/v). Cells (0.10 mL) were mixed with molten top LB-agar (1.0 mL) containing ampicillin (0.10 mg/mL), chloramphenicol (0.10 mg/mL), and IPTG (30 μM) and poured onto LB-agar plate with same composition. After the top agar had dried, aliquots (3 μL) of bacteriophage λKH54 (containing $10^2 - 10^6$ pfu) were spotted on the surface of the solid medium containing cells and the resulting plates were incubated at 37 °C until plaques appear.

Gel-based assay of inhibition by ribonuclease inhibitor. Wild-type RNase A (10 ng) was incubated in 9 μL of 0.10 M MES-NaOH buffer (pH 6.0) containing NaCl (0.10 M), DTT (2 mM) and RI (0 – 40 units) at 25 °C for 10 min. Substrate, 16S- and 23S-rRNA (1.0 μL of a 4 mg/mL solution), was added and the reaction mixtures were further incubated at 37 °C for 10 min. After addition of loading buffer (2 μL) (Ausubel et al., 1994), the mixtures were subjected to electrophoresis in an agarose (1.5% w/v) gel made in 1 × TAE buffer containing ethidium bromide (1 μg/mL).

3.3 RESULTS

Construction of λ repressor fusions. Fusions of NcI-RNase A and NcI-RI were made in plasmids pSH47 and pSH48, respectively, where the expression of fusion proteins was driven by a weak promoter, P_{lacUV5}. Both fusion proteins were of the expected molecular weights judged by SDS-PAGE or zymogram electrophoresis (Figure 3.1).

Design of epitope screening. A reporter cassette (λP_R-*lacZ*-rrnB) was constructed, where a *lacZ* gene is under control of a λP_R containing a single copy of λO_{R1} followed by an rrnB transcription terminator. This cassette was originally designed for the library screening described in the Chapter 2. The *tet* gene was removed from the original construct because the screening of the epitope library does not need the tetracycline selection. The reporter cassette was placed in a reporter plasmid, pSH58, from which the expression of NcI-RI is also driven (Figure 3.2). A scheme depicting the epitope screening is shown in Figure 3.3. In the scheme, a functional repressor is reconstructed through the interaction of RI and an epitope of RNase A, and thus transcription of *lacZ* gene is turned off. In contrast to the screening described in Chapter 2 where positives trigger onset of the reporter genes ($lacZ^+$), the epitope screening is looking for the opposite phenotype ($lacZ^-$).

Because epitope screening utilizes the reconstruction of a functional repressor, it is important that NcI-RI alone cannot bind to λO_{R1} nor act as a repressor. To test for the possibility, pSH58/MC1061 cells were subjected to a dot plaque assay. In the assay, cells

producing a functional repressor undergo lysogenic growth upon infection with bacteriophage λKH54 (Meyer & Ptashne, 1980), which has a deletion in cI gene. But cells without a functional repressor undergo a lytic cycle upon infection with λKH54 and form plaques. λKH54 has been used as a tool to determine the existence of a repressor inside a cell (Hu et al., 1990; Marchetti et al., 1995). As shown in Figure 3.4, pSH58/MC1061 cells are sensitive to the λKH54 infection, and therefore NcI-RI is not capable of binding to λO_{R1}.

Epitope library of ribonuclease A. The overall scheme of constructing an epitope library of RNase A as a fusion to the C-terminus of NcI is illustrated in Figure 3.5. A DNA fragment containing the open reading frame of RNase A was amplified by PCR. The PCR fragment was subjected to partial digestion with DNase I in the presence of Mn^{++} ion to generate small DNA fragments (20 – 30 bp) corresponding to 7 – 10 amino acid residues. For the purpose of cloning, the ends of the digested DNA must be blunt-ended. In the presence of Mg^{++} ion, DNase I produces nicks in duplex DNA, while in the presence of Mn^{++} ion, the enzyme produces double-stranded breaks in the DNA (Campbell & Jackson, 1980). Reaction time and temperature were varied to maximize the population of DNA in the desired size. DNA fragments with a size of 20 – 30 bases were recovered from an acrylamide gel (Figure 3.6A) and dephosphorylated and ligated to *Stu*I-digested pSH53. pSH53 was designed to carry an unique *Stu*I site between the C-terminus of NcI and three tandem repeats of stop codons (Figure 3.5). The PCR-amplified cDNA of RNase A does not carry a *Stu*I recognition sequence. The ligation mixture was digested with *Stu*I to destroy the self-ligated pSH53 and to enrich selectively

the plasmids that carry inserts. The size of library was 5×10^5, and the more than 90% of library plasmids carried an insert (Figure 3.6B). The number of possible epitopes of RNase A with a length of 8 amino acid residues is 117 (124 – 8 + 1). Considering possible frames of codon triplet (3) and the possible directions (2) during the blunt-end ligation, the maximum size of epitope library is still under 1,000 ($117 \times 2 \times 3 = 702$). The size of epitope library constructed here far exceeds this theoretical number, and thus the library should contain all possible epitopes.

Library screening. The library plasmids were cotransformed with pSH58 into MC1061 using electroporation. About 100 out of 5000 cotransformants showed a *lacZ*$^-$ phenotype (white colonies) and library plasmids were recovered from these *lacZ*$^-$ cotransformants. To test the ability of the epitopes from *lacZ*$^-$ clones to interact with RI, the library plasmids were retransformed into pSH58/MC1061 cells and the cotransformants were subjected to λKH54 infection (Figure 3.7). About 60 of the 100 *lacZ*$^-$ isolates showed immunity to λKH54 infection. The *lacZ*$^-$ and λKH54-immune clones were identified, and library plasmids from the clones were sequenced.

Analysis of positive clones. Sequence analysis of clones that showed immunity to λKH54 revealed five regions (hot spots) in the primary sequence of RNase A. These hot spots include residues 31 – 39, 68 – 74, 77 – 83, 99 – 104, and 108 – 114. The positions of these five regions in the structure of the hRI•RNase A complex are shown in Figure 3.8. Based on the proximity to the RI interface, the segment of residues 31 – 39 was chosen for further analysis and was synthesized chemically (pep3139).

Gel assay of RI binding to RNase A in the presence of the epitope. A gel-based assay was performed to determine the ability of the epitope peptide (pep3139) to interfere with the RI–RNase A interaction. As shown in Figure 3.9, most of the ribonucleolytic activity of RNase A remains inhibited by RI in the presence of pep3139, implying that pep3139 is a weak antagonist.

3.4 DISCUSSION

Protein–protein interactions often generate a large surface area buried in the interfaces. Even with the availability of the atomic structure of a complex, it is difficult to identify the residues important for the interaction. Knowing the most crucial residues in the interface of a protein–protein interaction allows for understanding of the energetic details of the interaction. Traditionally, attaining this knowledge requires extensive biochemical studies and time-consuming mutational analyses. Here, a genetic screen of an epitope library was developed to isolate and identify in a protein the segments of residues that are important in the interaction with another protein.

We chose the RI•RNase A complex as a model target. An epitope library of RNase A was created and screened for the interaction with RI to identify regions in RNase A that are responsible for the formation of a tight complex. The screen resulted in five 'hot spot' regions, which are spread throughout the primary sequence of RNase A. A segment containing residues 31 – 39 (pep3130) was selected and tested for its ability to interfere

with the complex. According to the gel-based assay of RNase A inhibition, pep3139 showed only weak inhibitory activity against the formation of RI•RNase A complex. This result indicates that residues 31 – 39 of RNase A alone do not interact strongly with the RI–RNase A interface. The stability and strength of a protein–protein interaction is collective of all the individual interactions at the interface. It is, therefore, not surprising that a single segment in the interface is an ineffective antagonist toward the interaction, as was observed in this study.

The construction of the epitope library relied on a blunt-end ligation of epitope DNA and the library plasmid. To avoid the occurrence of concatenating epitopes, the epitope DNA was dephosphorylated prior to the ligation. The library plasmid, pSH53, was digested with *Stu*I to generate blunt ends. Intramolecular ligation (self-ligation of plasmid) is favored over intermolecular ligation (plasmid + insert), especially when the inserts are dephosphorylated. For the integrity of the library, it is necessary to have a means to enrich in plasmids carrying an insert by eliminating self-ligated plasmids. Digestion with *Stu*I achieved this goal because only the self-ligated plasmid contains a *Stu*I site. Using this method, we were able to create an epitope library of RNase A with a size of 5×10^5 in which 90% of the plasmids carried an insert.

Considering the small size of RNase A (124 residues), linear epitopes longer than 10 residues would limit severely the diversity of the library and epitopes shorter than 6 residues are unlikely to have sufficient binding affinity. Therefore, the average size of epitopes was designed to be 8 amino acid residues. Because the diversity of the epitope library is limited and the sequences in the library are restricted, it is unlikely for false

positives that bind to NcI to occur. Thus, the initial *lacZ*$^-$ positives were not subjected to an extensive test for false positives. Instead, the interaction of RI and epitopes from *lacZ*$^-$ isolates was confirmed by an independent method of the λKH54 infection to library transformants followed by a dot plaque assay. Non-false but meaningless positives are likely to be those that bind to the outer surface of RI.

Identifying continuous epitopes in RNase A that interact strongly with RI would be an initial step toward creating small-molecule inhibitors of RI–RNase A. Such small-molecule inhibitors could potentiate the cytotoxicity of onconase or other homologs of RNase A. Moreover, identifying the crucial residues could be valuable in creating new cytotoxic variants of RNase A that can evade RI.

The approach described here can be expanded to the selection of a cDNA or random peptide library for ligands that have affinity to a protein of interest. Utilization of an appropriate substrate of β-galactosidase (P-Gal) and a host strain (*E. coli C*) allows the counter selection for a *lacZ*$^-$ phenotype (Gossen et al., 1992). The reconstruction of a functional repressor through the interaction between the target protein and a ligand (protein) from library can be easily scored by the growth selection. The bacterial growth selection enables the screening of a large library (> 10^9) for interacting partners *in vivo*.

Figure 3.1 **A.** SDS-PAGE analysis of the NcI-RI fusion protein. Lane M, molecular weight markers; Lane 1, cellular extracts of pSH48/MC1061 induced with IPTG (0.5 mM); Lane 2, cellular extracts of pSH48/MC1061 without induction.

B. Zymogram electrophoresis analysis of NcI-RNase A fusion protein. Lane 1, purified RNase A; Lane 2, cellular extracts of pSH47/MC1061 induced with IPTG (0.5 mM); Lane 3, duplicate of Lane 2, from another colony of pSH47/MC1061; Lane 4, cellular extracts of pSH47/MC1061 without induction.

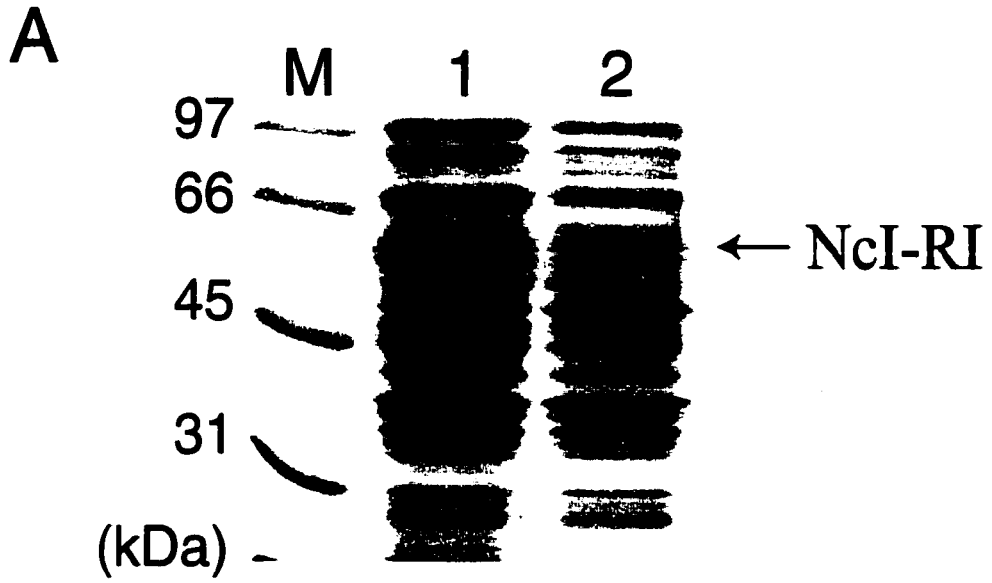
A
M
1
2
97
66
45
31
(kDa)
NcI-RI

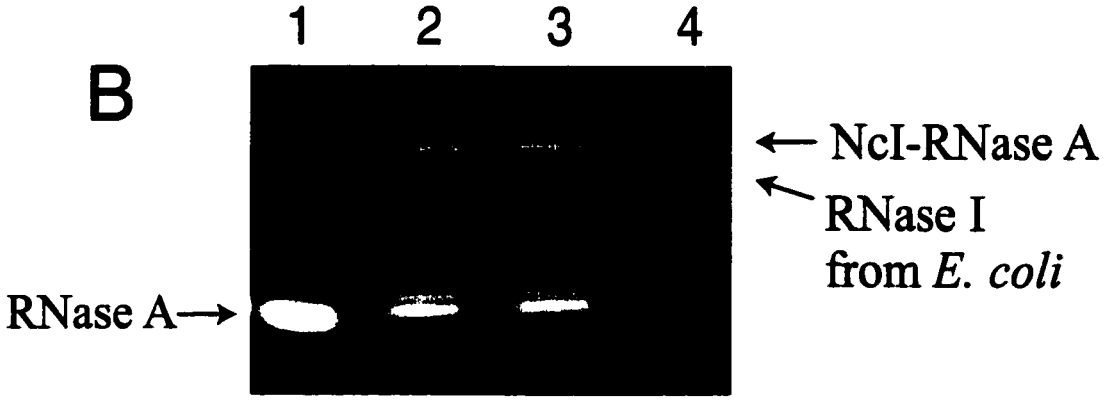
1
2
3
4
B
NcI-RNase A
RNase I
from E. coli
RNase A

Figure 3.2 Map of reporter plasmid pSH58. Plasmid pSH58 contains the reporter cassette (λP_R-*lacZ*-rrnB) and the expression cassette for the NcI-RI fusion protein (P_{lacUV5}-NcI-RI-T7Φ). rrnB and T7Φ are transcription terminators from the *E. coli* rrnB ribosomal RNA operon and bacteriophage T7, respectively. Upon transformation with pSH58, *E. coli* cells show a *lacZ*$^+$ phenotype due to the inability of NcI-RI to repress the transcription of *lacZ* gene by the λP_R promoter.

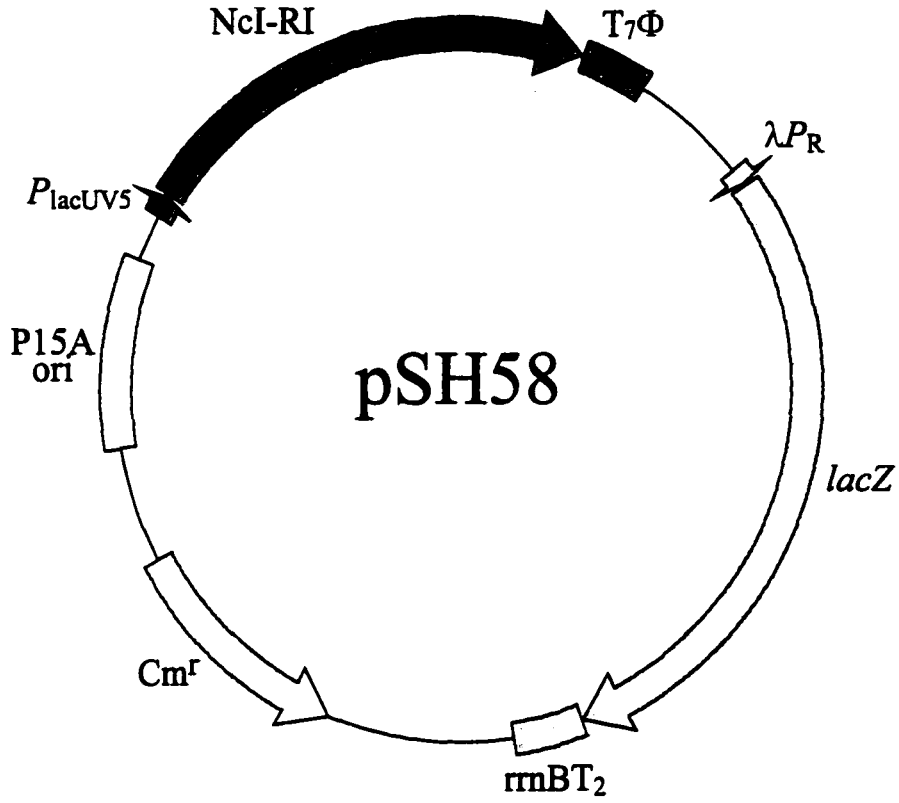
NcI-RI
T7Φ
λPR
PlacUV5
P15A
ori
pSH58
lacZ
Cmr
rrnBT2

Figure 3.3 Basis for the genetic screen of an RNase A epitope library for segments that interact with RI. The NcI-RI fusion protein alone is not a functional repressor, and transcription of *lacZ* is not repressed (*lacZ*$^+$). Epitopes of RNase A are produced as a fusion to the C-terminus of NcI. A functional repressor is reconstructed through binding of an epitope to RI and can be detected by screening for a *lacZ*$^-$ phenotype.

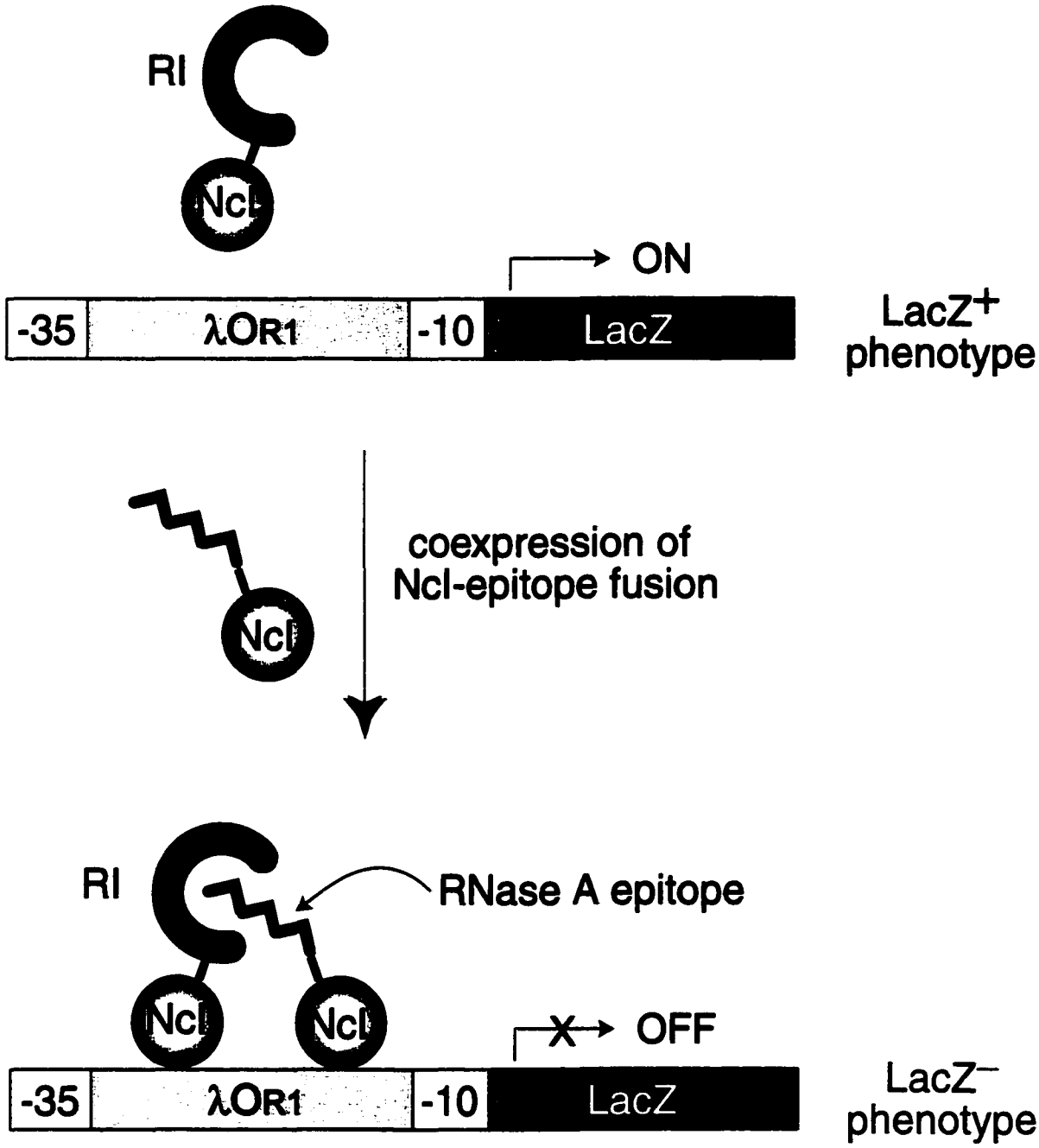
RI
NcI
ON
-35
λOR1
-10
LacZ
LacZ+
phenotype
coexpression of
NcI-epitope fusion
NcI
RI
RNase A epitope
NcI
NcI
OFF
-35
λOR1
-10
LacZ
LacZ−
phenotype

Figure 3.4 Dot plaque assay of λKH54 infection of MC1061 cells producing the NcI-PR fusion proteins. Cells producing a functional repressor are immune to λKH54 infection. Cells that lack a functional repressor are sensitive to λKH54 and thus form plaques. Different amounts of λKH54 (10^2 – 10^6 pfu) were spotted on the surface of solid medium containing;

A. MC1061 cells cotransformed with pSH52 and pSH58, where the NcI-zip and NcI-RI fusions are both produced. NcI-zip is a functional repressor.

B. MC1061 cells cotransformed with pSH53 and pSH58, where NcI and the NcI-RI fusion protein are both produced. The NcI-PR fusion protein is not a functional repressor.

C. MC1061 cells cotransformed with pSH47 and pSH58, where the NcI-RNase A and NcI-RI fusion proteins are both produced. Neither fusion protein is a functional repressor.

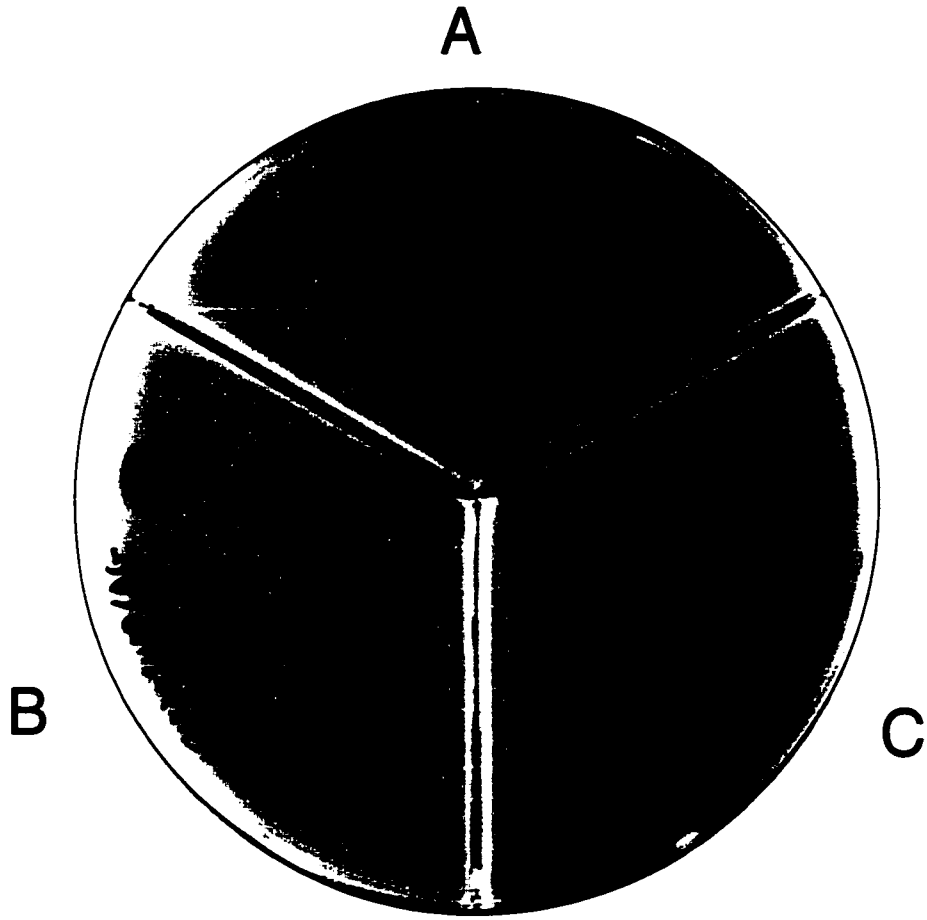
A
B
C

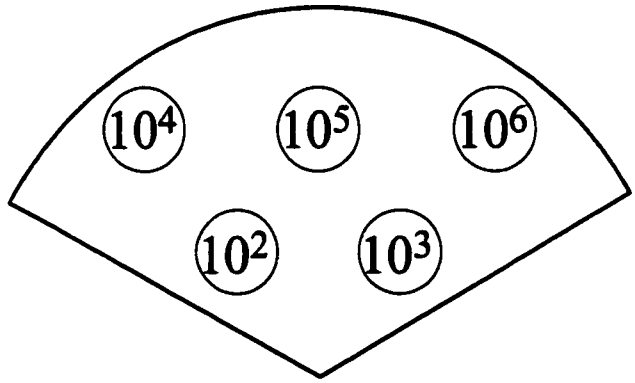
10^4
10^5
10^6
10^2
10^3

Figure 3.5 Scheme for the construction of an RNase A epitope library. A library of epitopes from RNase A was constructed as a fusion to the C-terminus of NcI. The size of the library is 5×10^5 and the average length of the epitopes is 8 amino acid residues.

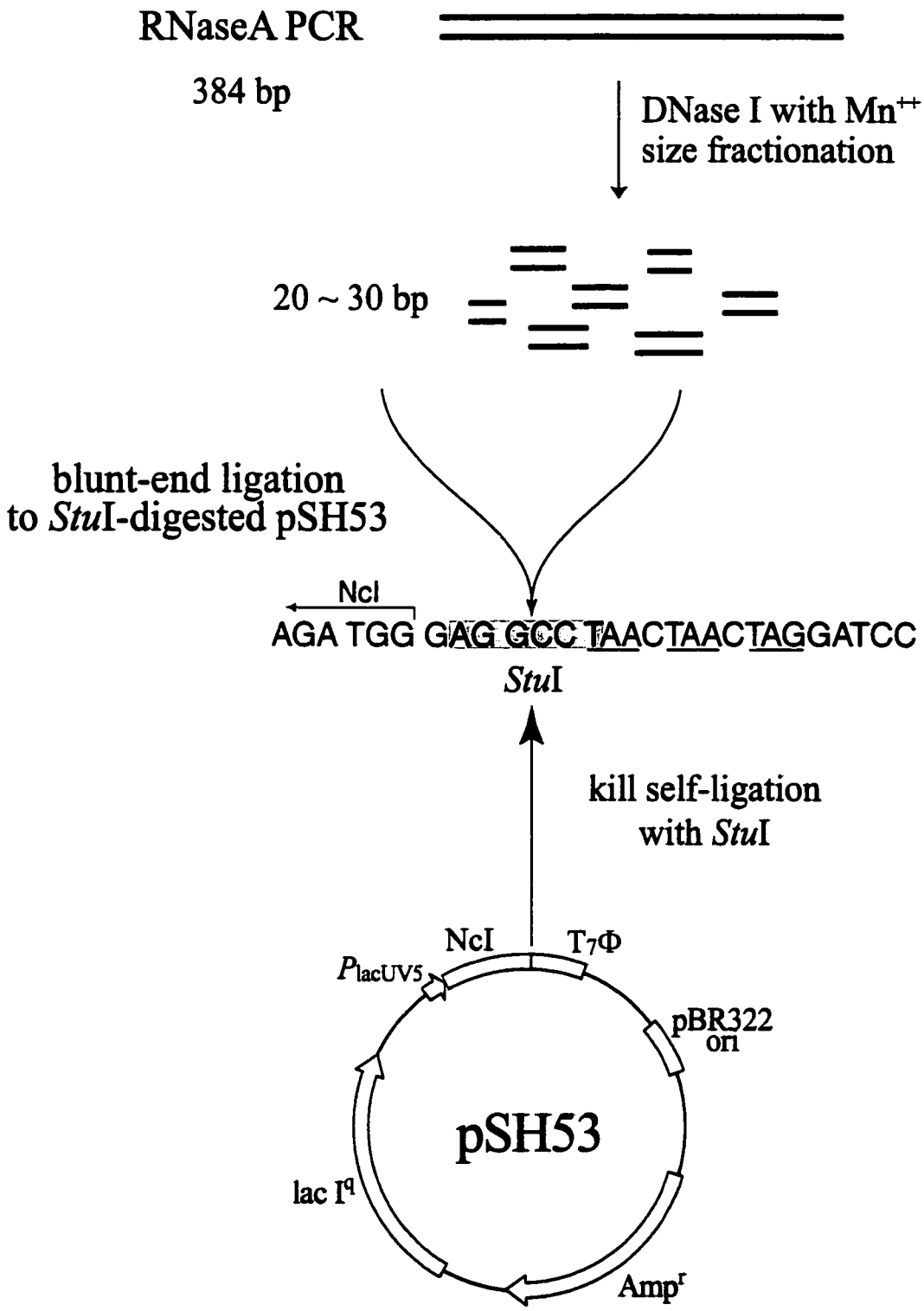
RNaseA PCR
384 bp
DNase I with Mn++
size fractionation
20 ~ 30 bp
blunt-end ligation
to StuI-digested pSH53
NcI
AGA TGG GAG GCC TAACTAACTAGGATCC
StuI
kill self-ligation
with StuI
NcI
T7Φ
PlacUV5
pBR322
ori
pSH53
lac Iq
Ampr

Figure 3.6 **A.** Analysis of DNA fragments for library construction. PCR-amplified cDNA encoding RNase A was digested partially by DNase I, and the resulting DNA was fractionated by size and purified from an acrylamide gel. DNA fragments in the size of 20 – 45 bp were fractionated further into three groups. Lane 1, DNA of 20 – 30 bp, which was used for construction of epitope library; Lane 2, DNA of 28 – 35 bp; Lane 3, DNA of 35 – 45 bp.

B. Analysis of epitope library plasmids by restriction digestion. Plasmids from 10 library clones and pSH53 were digested with *Bam*HI and *Hind*III, which at the flanks of the epitope insertion site. Digestion of the blank vector (pSH53) generates a 56-bp fragment. All 10 library plasmids carry inserts of the correct size (20 – 30 bp).

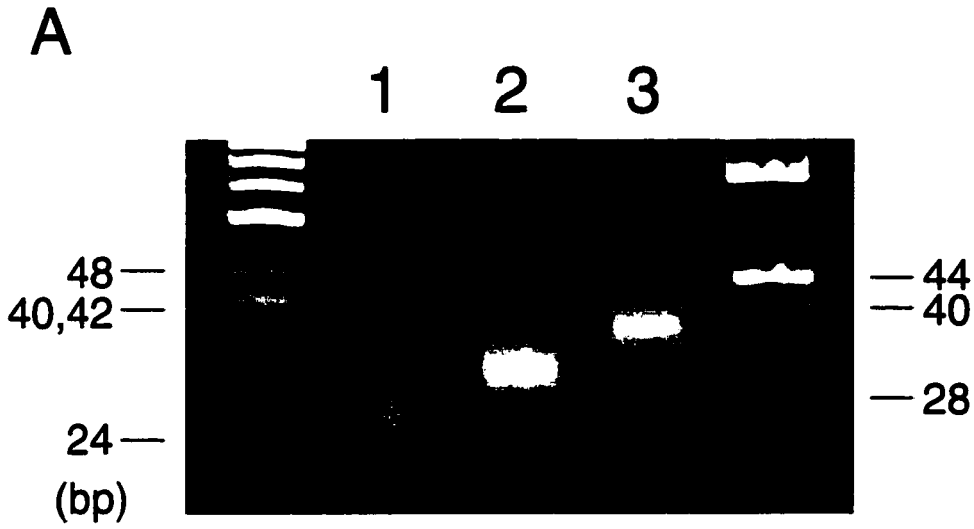
A
1
2
3
48
40,42
24
(bp)
44
40
28

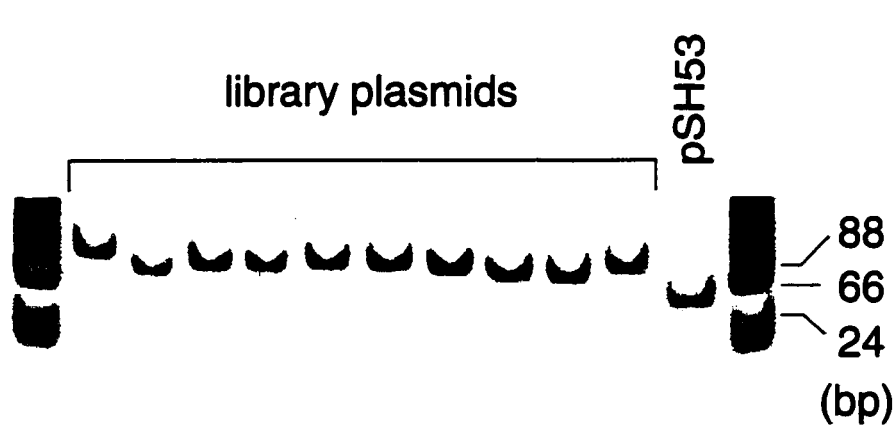
B
library plasmids
pSH53
88
66
24
(bp)

Figure 3.7 Results of typical dot plaque assay of positive (*lacZ*$^-$) isolates from the library screening. Library plasmids were rescued from *lacZ*$^-$ cotransformants and retransformed into pSH58/MC1061 for λKH54 infection. Library clones that are immune to λKH54 must carry epitopes that have an affinity for RI.

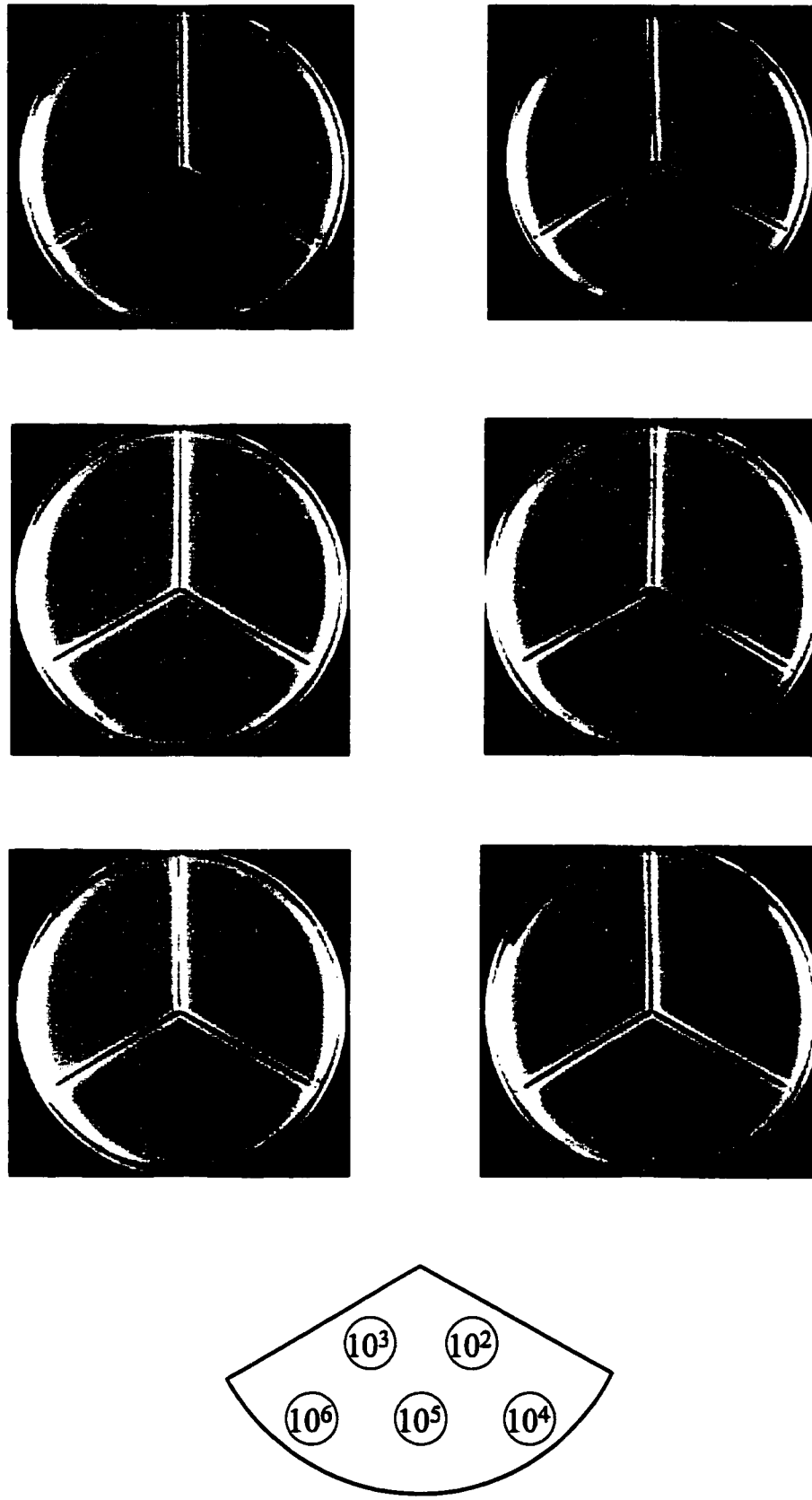
10^3
10^2
10^6
10^5
10^4

Figure 3.8 Topology of epitopes isolated from the library screening in the complex of RI and RNase A. The five hot spots are residues 31 – 39 (red), 68 – 74 (green), 77 – 83 (yellow), 99 – 104 (blue), and 108 – 114 (cyan). The solvent-accessible surface of RI was calculated by rolling of a sphere with a radius of 1.4 Å (as in a water molecule). The electrostatic potential of the surface is indicated, with blue denoting positive charge and red denoting negative charge. The image including the surface map of RI was generated with the program WebLabViewerPro 3.5 for WindowsNT (Molecular Simulations; San Diego, CA).

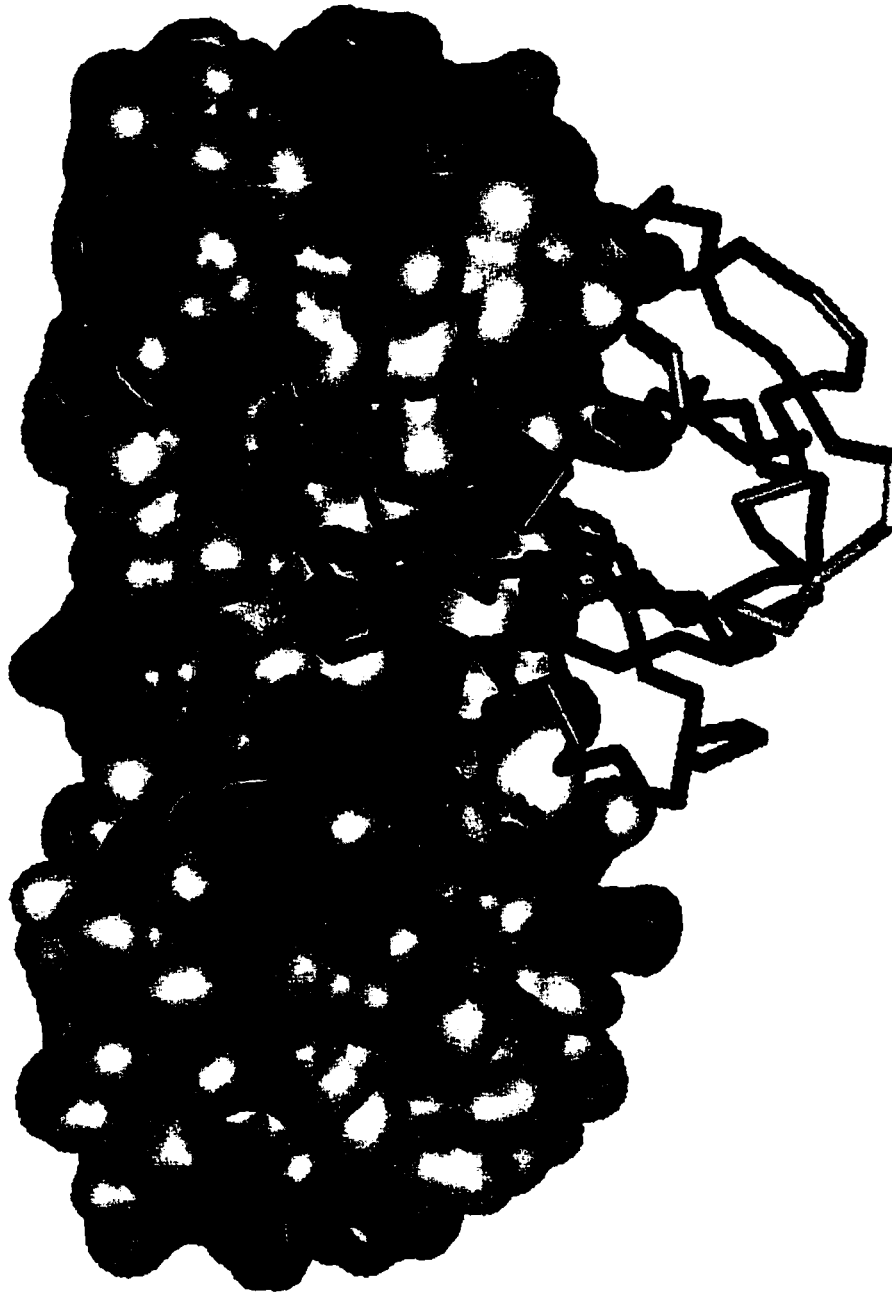

Figure 3.9 Gel assay of RNase A inhibition by hRI in the presence of pep3139. The residual ribonucleolytic activity of RNase A (0 or 10 ng) inhibited by RI (0 or 20 units) was assessed by visualizing the RNase A-catalyzed degradation of 16S- and 23-S rRNA in the presence of pep3139 (0, 50, 100, or 200 μg).

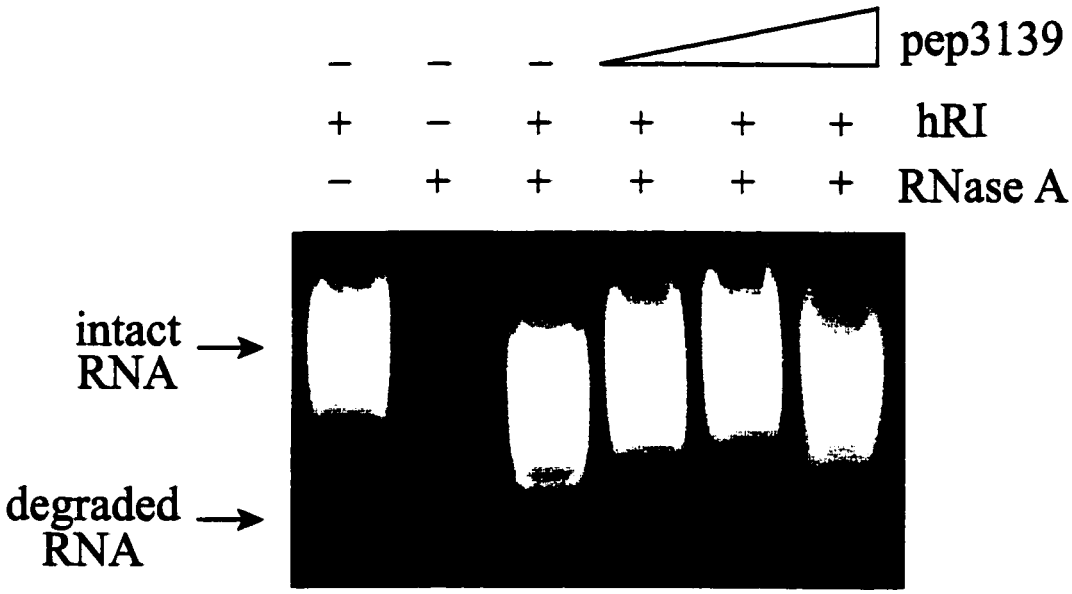
pep3139
hRI
RNase A
intact RNA
degraded RNA

Chapter 4

Green Fluorescent Protein to Detect Protein–Protein Interactions

A portion of this work was published as:

Sang-Hyun Park and Ronald T. Raines (1997) Green fluorescent protein as a signal for protein–protein interactions. *Protein Sci.* **6**, 2344-2349.

Sang-Hyun Park and Ronald T. Raines (2000) Green fluorescent protein chimeras to probe protein–protein interactions. *Methods in Enzymol.*, in press.

4.1 INTRODUCTION

Green fluorescent protein (GFP) from the jelly fish *Aequorea victoria* has exceptional physical and chemical properties such as spontaneous fluorescence, high thermal stability, and resistance to detergents, organic solvents, and proteases. These properties endow GFP with enormous potential for biotechnical applications (Bokman & Ward, 1981; Ward, 1981; Ward & Bokman, 1982). To date, GFP has been used largely *in vivo*—as a marker for gene expression and a fusion tag to monitor protein localization in living cells (Chalfie et al., 1994; Inouye & Tsuji, 1994; Ren et al., 1996; Topham et al., 1998; Maletic-Savatic et al., 1999; Perez et al., 1999).

Since the cDNA that codes for GFP was cloned (Prasher et al., 1992), a variety of GFP variants have been generated in response to the demand for improved properties that could broaden the spectrum of its application (Cubitt et al., 1995; Delagrave et al., 1995; Ehrig et al., 1995; Heim et al., 1995; Crameri et al., 1996; Ward, 1997). Among those variants, S65T GFP (Figure 4.1A) is unique in having increased fluorescence intensity, faster formation of fluorophore, and altered excitation and emission spectra than that of the wild-type protein (Heim et al., 1995). The groups of Phillips and Remington have determined the crystalline structures of wild-type (Yang et al., 1996) and S65T (Ormö et al., 1996) GFP by X-ray diffraction analysis. These studies indicate that the fluorophore is held rigidly within the protein. The wavelengths of the excitation and emission maxima of S65T GFP (490 nm and 510 nm, respectively) resemble closely those of fluorescein. The fluorescein-like spectral characteristics of S65T GFP enable its use with

use with instrumentation, such as fluorescence-activated cell sorting (FACS) devices or fluorescence microscopes that had been designed specifically for use with fluorescein.

Here, we describe the use of S65T GFP to probe protein–protein interactions *in vitro* (Park & Raines, 1997). This method requires fusing GFP to one of the target proteins to create a GFP chimera. The interaction of this fusion protein with another protein can be analyzed by two distinct methods.

The first method is a fluorescence gel retardation assay. The gel retardation assay has been used widely to study protein–DNA interactions (Carey, 1991). This assay is based on the electrophoretic mobility of a protein–DNA complex being less than that of either molecule alone. In a fluorescence gel retardation assay, electrophoretic mobility is detected by the fluorescent properties of S65T GFP. The fluorescence gel retardation assay is a rapid method to demonstrate the existence of a protein–protein interaction and to estimate the equilibrium dissociation constant (K_d) of the resulting complex.

The second method is a fluorescence polarization assay. The fluorescence polarization assay is an accurate method to evaluate K_d in a specified homogeneous solution. Fluoresence polarization assays usually rely on fluorescein as an exogenous fluorophore. S65T GFP can likewise serve in this role. Further, the fluorescence polarization assay can be adapted for the high-throughput screening of protein or peptide libraries.

4.2 MATERIALS AND METHODS

Materials. E. coli strain BL21(DE3) and plasmid pET-29b were from Novagen (Madison, WI). cDNA for wild type GFP (TU#58) was a generous gift from Martin Chalfie (Columbia University). *Pfu* DNA polymerase was from Stratagene (La Jolla, CA). All other enzymes for the manipulation of recombinant DNA were from either Promega (Madison, WI) or New England Biolabs (Beverly, MA). Ni^{++}~NTA agarose column was from Qiagen (Chatsworth, CA). HEPES, PMSF, DTT, poly(C) and S-protein were from Sigma (St. Louis, MO). PCR reactions described in this chapter were carried out using *Pfu* DNA polymerase. All the DNA fragments prepared by PCR were sequenced and their identities were confirmed before subsequent subcloning steps. Fluorescence polarization measurements were made with a Beacon Fluorescence Polarization System from Pan Vera (Madison, WI). Fluorescence imaging was carried out with a fluorimager SI System (Molecular Dynamics; Sunnyvale, CA).

His_6~GFP(S65T)~S15 construction. The His_6 tag and S65T mutation were introduced simultaneously into the cDNA that codes for wild-type GFP (TU#58) (Chalfie et al., 1994) by PCR mutagenesis (Picard et al., 1994) using three oligonucleotides, P39: GGCATATGCACCACCACCACCACCACGGCGGTAGCAAAGGAG AAGAAC (for the His_6 tag and an *NdeI* site), M5: CCATGGCCAACACTGGTCACCACTTTCA CCTATGGTGTTCAATGCTT (for the S65T change), and P36: GTGAATTCTTGT ATAGTTCA TCCATGCCA (for an *Eco*RI site). The resulting PCR fragment was

digested with *Eco*RI and *Nde*I and inserted into an *Eco*RI/*Nde*I site of pET-29a (Novagen; Madison, WI) by the TIES method (Zeng et al., 1996) (which was used because of an internal *Nde*I site in GFP gene). The DNA fragment encoding S15 was generated from pET-29b by PCR using P37: GGGAATTCCGGCGG CAAAGAAACCGCTGCT GCTAAA (with an *Eco*RI site) and P38: TGGTCGACTTAGCTGTCC ATGTGCTGGCGTTCGA (with a *Sal*I site) and inserted into *Eco*RI/*Sal*I site of the above plasmid to give pSH24.

S15~GFP(S65T)~His$_6$ construction. The coding region of GFP(S65T) was amplified from pSH24 with P53: TCAAGATCTTAGCAAAGGAGAAGAACTT (with a *Bgl*II site) and P54: GCCCTCGAGCTTGTATAGTTCATCCATGC (with an *Xho*I site) The PCR fragment was digested with *Bgl*II and *Xho*I and inserted into *Bgl*II/*Xho*I site of pET-29b to give pSH41.

Expression and purification of the fusion proteins. His$_6$~GFP(S65T)~S15 and S15~GFP(S65T)~His$_6$ were produced from *E. coli* strain BL21(DE3)/pSH24 and BL21(DE3)/pSH41, respectively. Cells were grown at 37 °C in LB (0.50 L) until the absorbance at 600 nm was 0.5. IPTG was then added to a final concentration of 0.5 mM, and the cells were grown at 30 °C for an additional 4 h. The culture was harvested and resuspended in 25 mL of 50 mM HEPES-NaOH buffer (pH 7.9) containing NaCl (0.30 M), DTT (0.50 mM), and PMSF (0.20 mM), and the cells were lysed by using a French pressure cell. The lysed cells were subjected to centrifugation at 18,000 × *g*. The

supernatant was collected and loaded onto a Ni^{++}~NTA agarose column. The column was washed with 50 mM HEPES-NaOH buffer (pH 7.9) containing imidazole (8.0 mM), NaCl (0.30 M), and PMSF (0.50 mM). GFP(S65T) fusion proteins were eluted in the same buffer containing imidazole (0.10 M). The green fractions were pooled and further purified by FPLC on a Superdex 75 gel filtration column (Pharmacia; Piscataway, NJ) with elution by 50 mM HEPES-NaOH buffer (pH 7.9).

Fluorescent gel retardation assay. Purified fusion proteins were quantified by using the extinction coefficient (ε = 39.2 $mM^{-1}cm^{-1}$ at 490 nm (Heim et al., 1995)) of S65T GFP. S-protein was quantified by using its extinction coefficient (ε = 9.56 $mM^{-1}cm^{-1}$ at 280 nm (Connelly et al., 1990)). To begin the gel retardation assay, purified S15~GFP(S65T)~His_6 (1.0 μM) was incubated at 20 °C with varying amounts of S-protein in 10 μL of 10 mM Tris-HCl buffer (pH 7.5) containing glycerol (5% v/v). After 20 min, the mixtures were loaded onto a native continuous polyacrylamide (6% w/v) gel (Laemmli, 1970), and the loaded gel was subjected to electrophoresis at 4 °C at 10 V/cm. Immediately after electrophoresis, the gel was scanned by a Fluorimager SI System using a built-in filter set (490 nm for excitation and ≥515 nm for emission).

Calculation of equilibrium dissociation constants. The fluorescence intensities of bound and free S15~GFP(S65T)~His_6 were quantified by using the program Image QuaNT 4.1 (Molecular Dynamics; Sunnyvale, CA). The values of **R** (= fluorescence

intensity of bound S15~GFP(S65T)~His_6 / total fluorescence intensity) were determined from the fluorescence intensities, and values of K_d were calculated from the equation:

$$K_d = \frac{1-\mathbf{R}}{\mathbf{R}} \times \left([\text{S} - \text{protein}]_{total} - \mathbf{R} \times [\text{S15} \sim \text{GFP(S65T)} \sim \text{His}_6]_{total}\right) \tag{4.1}$$

Fluorescence polarization assay. Fluorescence polarization (P) is defined as:

$$P = \frac{I_{\parallel} - I_{\perp}}{I_{\parallel} + I_{\perp}} \tag{4.2}$$

where $I_{\parallel}$ is the intensity of the emission light parallel to the excitation light plane and $I_{\perp}$ is the intensity of the emission light perpendicular to the excitation light plane. P, being a ratio of light intensities, is a dimensionless number and has a maximum value of 0.5. Fluorescence polarization can be measured with a Beacon Fluorescence Polarization System (Wittmayer & Raines, 1996). Purified S15~GFP(S65T)~His_6 (0.50 n*M*) is incubated at (20 ± 2) °C with various concentrations of S-protein (20 μM – 1.0 nM) in 1.0 mL of 20 mM Tris-HCl buffer (pH 8.0) containing NaCl (0 or 0.10 *M*). Five to seven polarization measurements are made at each S-protein concentration.

Calculation of equilibrium dissociation constants. Values of K_d were determined by using the program DeltaGraph 4.0 (DeltaPoint; Monterey, CA) to fit the data to the equation:

$$P = \frac{\Delta P \bullet F}{K_d + F} + P_{min} \qquad (4.3)$$

In Equation 4.3, P is the measured polarization, ΔP (= $P_{max} - P_{min}$) is the total change in polarization, and F is the concentration of free S-protein. The fraction of bound S-protein (f_B) is obtained by using the equation:

$$f_B = \frac{P - P_{min}}{\Delta P} = \frac{F}{K_d + F} \qquad (4.4)$$

The binding isotherms (Figure 4.5) were obtained by plotting f_B versus F.

4.3 RESULTS

Production, purification and detection of S65T GFP chimeras. To demonstrate the potential of S65T GFP in exploring protein–protein interactions, we have chosen as a model system the well-characterized interaction of the S-peptide and S-protein fragments of bovine pancreatic ribonuclease A (RNase A). Subtilisin treatment of RNase A yields two tightly associated polypeptide chains: S-peptide (residues 1 – 20) and S-protein (residues 21 – 124)(Richards, 1955). Although the two individual polypeptide chains are inactive, full enzymatic activity is restored upon complex formation (Richards &

Vithayathil, 1959). Because a truncated form of S-peptide (S15, residues 1 – 15) is necessary and sufficient to form an enzymatically active complex with S-protein (Potts et al., 1963), we used S15 in our studies. Specifically, we generated fusion proteins in which S15 is fused to the N- or C-terminus of S65T GFP.

DNA encoding S15 and six histidine residues (His_6) (Hochuli et al., 1988) was added to the 5′ and 3′ ends of the cDNA encoding S65T GFP. The two resulting proteins, His_6~GFP(S65T)~S15 and S15~GFP(S65T)~His_6 (Figure 4.1B), were produced in *Escherichia coli* strain BL21(DE3) and purified by affinity chromatography using a Ni^{++}~NTA column (Figure 4.2A). The presence of an intact and functional S15 sequence on the fusion proteins was confirmed by zymogram electrophoresis in a poly(C)-containing gel, which was then incubated with S-protein (Figure 4.2B) (Kim & Raines, 1993; Kim & Raines, 1994). Both His_6~GFP(S65T)~S15 and S15~GFP(S65T)~His_6 remain fluorescent after electrophoresis in a native polyacrylamide gel (Figure 4.3A). Further, the altered excitation and emission spectra of S65T GFP are well suited for detection by a fluorimager. The sensitivity of S65T GFP detection in a native polyacrylamide gel is $\geq$0.1 ng (Figure 4.2C), which is comparable to that of an immunoblot using an anti-GFP antibody (Colby et al., 1995).

Purified His_6~GFP(S65T)~S15 migrates as two distinct species during SDS-PAGE (Figure 4.2A), zymogram electrophoresis (Figure 4.2B), and native PAGE (Figure 4.3A). No unexpected mutations are present in the gene encoding His_6~GFP(S65T)~S15. The results of Ni^{++}~NTA affinity chromatography and zymogram electrophoresis indicate that both the N- and the C-termini of His_6~GFP(S65T)~S15 are intact (Kim & Raines,

1994). Apparently, two isoforms of His_6~GFP(S65T)~S15 exist that migrate differently during electrophoresis, even in the presence of SDS (Figure 4.2B).

Fluorescence gel retardation assay. Gel mobility retardation is a popular tool for both qualitative and quantitative analyses of protein–nucleic acid interactions (Carey, 1991). The fluorescence gel retardation assay shown in Figure 4.3B is the first to apply gel retardation to the study of a protein–protein interaction. In this assay, free and bound S15-tagged S65T GFP were resolved and visualized in a native polyacrylamide gel. As shown in Figure 4.3B, only the slower migrating isoform of His_6~GFP(S65T)~S15 was shifted upon binding to S-protein during native PAGE, indicating that only this species has an accessible S15. The S15 portion of the faster migrating species is inaccessible to S-protein, perhaps because it becomes buried inside the GFP moiety during the folding process. We therefore believe it to be prudent to construct GFP fusions in which the target protein is fused to the N-terminus of GFP, rather than to the C-terminus. All subsequent experiments were performed with S15~GFP(S65T)~His_6.

The fluorescence gel retardation assay was used to quantify the interaction between S-protein and S15~GFP(S65T)~His_6. A fixed quantity of S15~GFP(S65T)~His_6 was incubated with a varying quantity of S-protein prior to electrophoresis in a native polyacrylamide gel. After electrophoresis, the gel was scanned with a fluorimager and the fluorescence intensities of bound and free S15~GFP(S65T)~His_6 were quantified (Figure 4.4A). From the relative fluorescence intensities of the bound and free S15~GFP(S65T)~His_6, the binding ratio (**R** = fluorescence intensity of bound

S15~GFP(S65T)~His_6 / total fluorescence intensity) at each concentration was obtained. The dissociation constant (K_d) of the complex formed in the presence of different S-protein concentrations was calculated from the values of **R** and the total concentrations of S-protein and S15~GFP(S65T)~His_6. The average (± SD) value of K_d is $(6 \pm 3) \times 10^{-8}$ M.

A competition assay was used to probe the specificity of the interaction between S15~GFP(S65T)~His_6 and S-protein. S15~GFP(S65T)~His_6 and S-protein were incubated to allow for complex formation. Varying amounts of S-peptide were added and the resulting mixture was incubated further, and then subjected to native gel electrophoresis. As shown in the Figure 4.4B, the addition of S-peptide converts bound S15~GFP(S65T)~His_6 to the free state. We conclude that S15~GFP(S65T)~His_6 and S-peptide bind to the same region of S-protein.

Fluorescence polarization assay. The fluorescence gel retardation assay is a convenient method to visualize a protein–protein interaction as well as to estimate the K_d of the resulting complex. Still, gel retardation assays have an intrinsic limitation in measuring accurate dissociation constants. In a gel retardation assay, it is assumed that a receptor–ligand interaction remains at equilibrium during sample loading and electrophoresis. Yet, as samples are loaded and migrate through a gel, complex dissociation is unavoidable and results in an underestimation of the value of K_d. Furthermore, if the conditions (*e.g.*, pH, or salt type or concentration) encountered during

electrophoresis differ from those in the incubation, then the measured value of K_d could be inaccurate.

Fluorescence polarization was used to quantify the interaction between S-protein and S15-tagged S65T GFP. In this assay, the formation of a complex is deduced from an increase in fluorescence polarization, and the dissociation constants are determined in a homogeneous aqueous environment. Most applications of fluorescence polarization assay have used fluorescein as a fluorophore (LeTilly & Royer, 1993; Radek et al., 1993; Wittmayer & Raines, 1996). We reasoned that the complex between S15~GFP(S65T)~His_6 and S-protein is likely to rotate more slowly and therefore to have a higher rotational correlation time than does free S15~GFP(S65T)~His_6. Such an increase in rotational correlation time results in an increase in fluorescence polarization, which can be used to assess complex formation (Jameson & Sawyer, 1995). In contrast to a gel retardation assay, the fluorescence polarization assay is performed in a homogeneous solution in which the conditions can be dictated precisely.

Fluorescence polarization was used to determine the effect of pH on the complex formation. As shown in Figure 4.5A, the K_d values obtained were 1.4×10^{-8} M, 1.1×10^{-8} M and 1.0×10^{-8} M at pH 7.5, 8.0, and 8.5, respectively. The interaction between S-protein and S15~GFP(S65T)~His_6 was not affected significantly by changing the pH by 1.0 unit. The insensitivity of K_d values to the pH change (pH 7.5 to pH 8.5) was not unexpected, as none of the amino acid sidechains involved in the interaction is known to change its protonation state in this pH range. The K_d (= 1.4×10^{-8} M) at pH 7.5

is approximately 4-fold lower than the K_d (= 6×10^{-8} M) obtained by the fluorescence gel retardation assay performed at the same pH. The difference in the K_d values is consistent with an increase in complex dissociation during the course of the gel retardation assay.

Fluorescence polarization was used to determine the effect of salt concentration on complex formation. The value of K_d increased by 3.8-fold when NaCl was added to a final concentration of 0.10 M (Figure 4.5B). A similar salt-dependence for the dissociation of RNase S had been observed previously (Schreier & Baldwin, 1977). The added salt is likely to disturb the water molecules hydrating the hydrophobic patch in the complex between S-peptide and S-protein, resulting in a decrease in the binding affinity (Baldwin, 1996). Finally, the value of $K_d = 4.2 \times 10^{-8}$ M that we observed in 20 mM Tris-HCl buffer (pH 8.0) containing NaCl (0.10 M) was similar (*i.e.*, 2.6-fold lower) than that obtained by titration calorimetry in 50 mM sodium acetate buffer (pH 6.0) containing NaCl (0.10 mM) (Connelly et al., 1990).

4.4 DISCUSSION

Methods to reveal and characterize the noncovalent interaction of one molecule with another are necessary to understand and control such interactions (Attie & Raines, 1995; Winzor & Sawyer, 1995; Klotz, 1997). We describe two new methods for probing protein–protein interactions. The first method is a fluorescence gel retardation assay in which one protein is fused to GFP. The GFP fusion protein is incubated with the other

protein, and the mixture is separated by native PAGE. The interaction between the two proteins is evident by a decrease in the mobility of the fluorescent fusion protein that results from complex formation.

The fluorescence gel retardation assay is a fast and convenient way to demonstrate interactions between two proteins, and in addition allows for an estimation of the value of K_d for the resulting complex. Conventional methods to demonstrate an interaction between two proteins (*e.g.*, protein **A** and protein **B**) are more laborious or less informative (or both) (Carr & Scott, 1992; Lu et al., 1993; Rajagopal et al., 1997; Cooper, 1998; Kameshita et al., 1998; Lakey & Raggett, 1998). In a typical method, protein **A** is fused to an affinity tag (such as glutathione S-transferase), which is then used to immobilize protein **A** on a resin. Protein **B** is applied to the resin to allow for complex formation. The complex is eluted and detected by an immunoblot using an antibody to protein **B**. In contrast, the fluorescence gel retardation assay requires simply mixing a protein **A**~GFP chimera with protein **B**, separating the mixture by native PAGE, and scanning the gel with a fluorimager. The interaction between protein **A** and protein **B** is apparent from the shift of the protein **A**~GFP band that results from complex formation. The sensitivity of S65T GFP detection (≥0.1 ng; Figure 4.2C) approaches that of an immunoblot using an anti-GFP antibody (Colby et al., 1995). Recently brighter GFP variants became available. These variants show similar excitation and emission spectra but two- to eight-fold stronger fluorescence intensity than the S65T variant (Patterson et al., 1997; Tsien, 1998; Cubitt et al., 1999). Using these brighter variants in the gel

retardation assay will improve further the sensitivity of the fluorescence gel retardation assay.

The second new method for probing protein–protein interactions, a fluorescence polarization assay, provides a more accurate assessment of the value of K_d. Most applications of fluorescence polarization have focused on analyzing protein–DNA interactions, with fluorescein (linked to DNA) serving as the fluorophore. Here, a GFP fusion protein is titrated with another protein, and the equilibrium dissociation constant is obtained from the increase in fluorescence polarization that accompanies binding. The interaction between the two proteins is detected in a homogeneous solution rather than a gel matrix. The fluorescence polarization assay thereby allows for the determination of accurate values of K_d in a wide range of solution conditions. GFP is particularly well-suited to this application because its fluorophore (Figure 4.1A) is held rigidly within the protein, as revealed by the three-dimensional structures of wild-type GFP and the S65T variant (Ormö et al., 1996; Yang et al., 1996). Such a rigid fluorophore minimizes local rotational motion, thereby ensuring that changes in polarization report on changes to the *global* rotational motion of GFP, as effected by a protein–protein interaction. Finally, it is worth noting that this assay is amenable to the high-throughput screening of protein or peptide libraries for effective ligands (Jolley, 1996).

Another advantage of both of these new methods is the ease with which a protein can be fused to GFP using recombinant DNA techniques and the high integrity of the resulting chimera. Traditionally, fluorophores have been attached to proteins by chemical modification with reagents such as fluorescein isothiocyanate (FITC) (Radek et al., 1993;

Heyduk et al., 1996; Lundblad et al., 1996). In this approach, additional purification steps are necessary to separate labeled protein from the reagent and unlabeled protein. Further, labeling the protein at a single site can be difficult or impossible. In contrast, labeling a protein with GFP is complete and generates a single species. Purification of that species can be facilitated by the incorporation of an affinity tag such as His_6 (Hochuli et al., 1988) or S-Tag (Raines et al., 2000). The success of S65T GFP as the fluorophore in fluorescence gel retardation assays and fluorescence polarization assays arises largely from the altered spectral characteristics and increased fluorescence intensity of S65T GFP (Heim et al., 1995). The availability of brighter S65T variants makes these assays more promising tools to investigate and analyze protein–protein interactions *in vitro*. We suggest that the role of fluorescein as a fluorescent label can be replaced by S65T GFP or its variants in many biochemical analyses.

Figure 4.1 Green fluorescent protein chimeras.

A. Chemical structure of the fluorophore in the core of the S65T variant of green fluorescent protein (Ormö et al., 1996). This fluorophore forms spontaneously from residues Thr65, Gly66, and Tyr67. The quinone methide resonance form shown here is likely to be responsible for the characteristic fluorescence of S65T GFP.

B. GFP fusion proteins used in this study. In His_6~GFP(S65T)~S15 (top), six histidine residues are fused to the N-terminus and S15 is fused to the C-terminus of S65T GFP. In S~GFP(S65T)~His_6 (bottom), S15 is fused to the N-terminus and six histidine residues are fused to C-terminus of S65T GFP. Residues that link the tags to GFP(S65T) are also indicated.

A

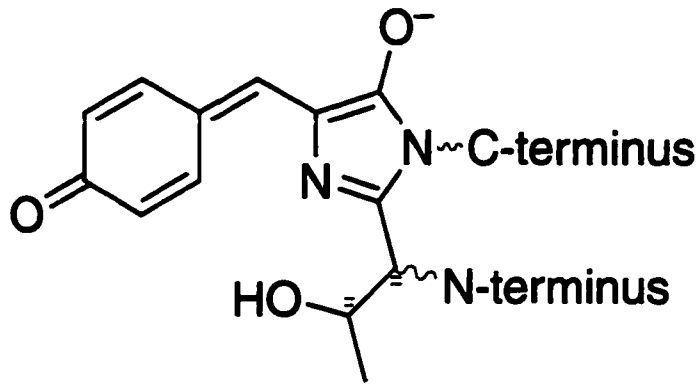
O⁻
N
C-terminus
N
O
HO
N-terminus

B


His6
GG
S65T GFP
NSGG
S15
S15
PD
S65T GFP
LE
His6

Figure 4.2 **A.** SDS-PAGE analysis of purified GFP fusion proteins. Lane M, molecular mass markers (14.4, 21.5, 31, 45, and 66 kDa); lane 1, S15~GFP(S65T)~His_6; lane 2, His_6~GFP(S65T)~S15.

B. Zymogram electrophoresis analysis of purified GFP fusion proteins. Lane 1, S15~GFP(S65T)~His_6; lane 2, His_6~GFP(S65T)~S15.

C. Fluorimager analysis of purified S15~GFP(S65T)~His_6. Lane 1 – 5, 10, 3.0, 1.0, 0.3, and 0.1 ng, respectively.

A

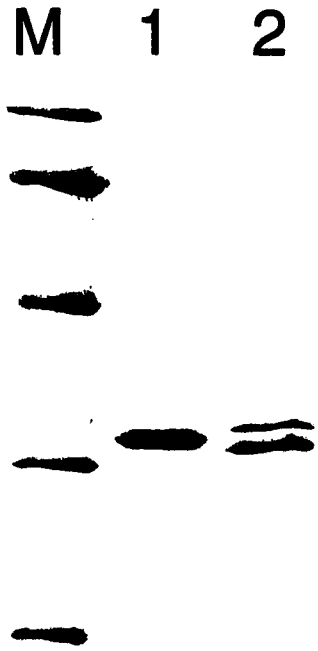

B

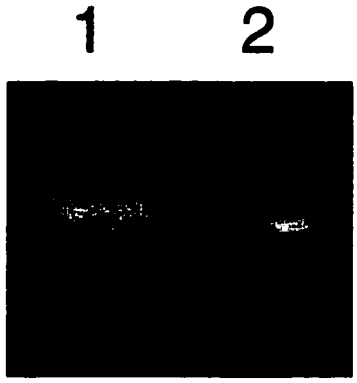

C

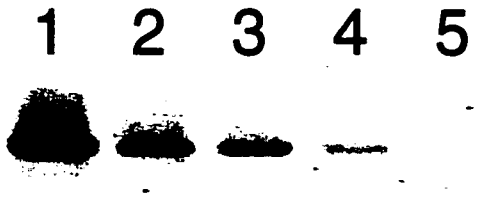

Figure 4.3 **A.** Fluorimager analysis of purified GFP fusion proteins after native PAGE. Lane 1, S15~GFP(S65T)~His_6; lane 2, His_6~GFP(S65T)~S15. **B.** Gel retardation assay demonstrating that S15~GFP(S65T)~His_6 and His_6~GFP(S65T)~S15 interact with S-protein. A GFP fusion protein was incubated with S-protein in 10 mM Tris-HCl buffer (pH 7.5) containing glycerol (5% v/v) for 20 min at 20 °C in a volume of 10 μL. The mixtures were then electrophoresed in a native 6% (w/v) polyacrylamide gel at 4 °C at 10 V/cm and scanned by a fluorimager using an internal filter set. Lane 1, 1 μM S15~GFP(S65T)~His_6 and no S-protein; lane 2, 1 μM S15~GFP(S65T)~His_6 and 1 μM S-protein ; lane 3, 1 μM His_6~GFP(S65T)~S15 and no S-protein; lane 4, 1 μM His_6~GFP(S65T)~S15 with 1 μM S-protein.

A

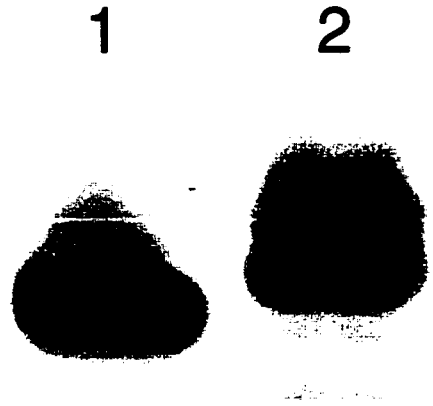

B

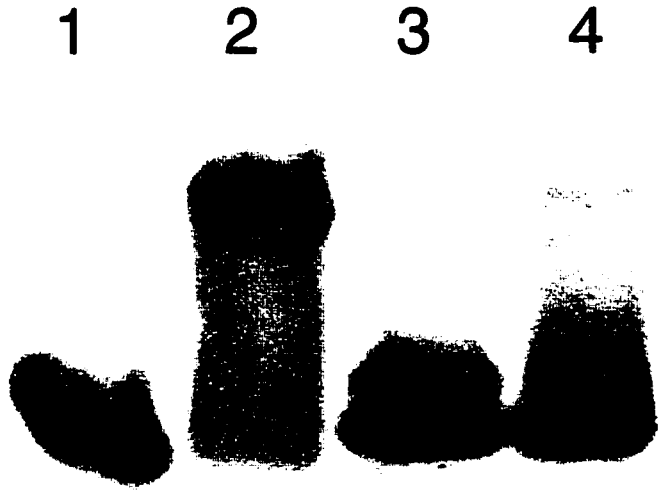

Figure 4.4 **A.** Gel retardation assay of the interaction of S15~GFP(S65T)~His_6 with S-protein. Assays were performed as in Figure 4.3B. Lanes 1 – 9, 1 μM S15~GFP(S65T)~His_6 and 0, 0.2, 0.3, 0.4, 0.5, 0.6, 0.7, 0.8, and 0.9 μM S-protein, respectively. The relative mobilities of free and bound S15~GFP(S65T)~His_6 were 0.72 and 0.47, respectively. The value of **R** was obtained for each lane, and values of K_d were calculated by using Equation 4.1.

B. Gel retardation assay demonstrating that S-peptide competes with S15~GFP(S65T)~His_6 for interaction with S-protein. S15~GFP(S65T)~His_6 was incubated with S-protein as in Figure 4.3B. After 20 min, S-peptide was added, and the mixtures were incubated for an additional 20 min at 20 °C. The mixtures were analyzed as in Figure 4.4A. Lane 1, 1 μM S15~GFP(S65T)~His_6 and no S-protein or S-peptide. Lane 2 – 6, 1 μM S15~GFP(S65T)~His_6, 1 μM S-protein, and 0, 0.3, 1.0, 3.0, and 10 μM S-peptide, respectively.

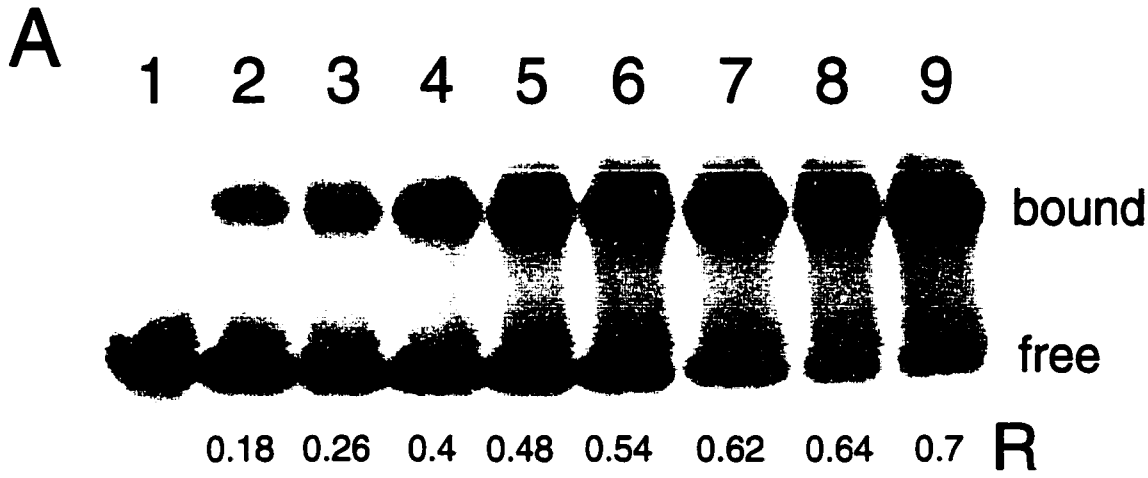
A
1 2 3 4 5 6 7 8 9
bound
free
0.18 0.26 0.4 0.48 0.54 0.62 0.64 0.7 R


B
1 2 3 4 5 6
bound
free

Figure 4.5 Fluorescence polarization assay of the interaction of S15~GFP(S65T)~His_6 with S-protein. S-protein was added to 20 mM Tris-HCl buffer in a volume of 1.0 mL. Each data point is an average of 5 – 7 measurements. Curves were obtained by fitting the data to Equation 4.3.

A. Effect of pH change on the interaction in the absence of added NaCl.

B. Effect of NaCl concentration on the interaction at pH 8.0.

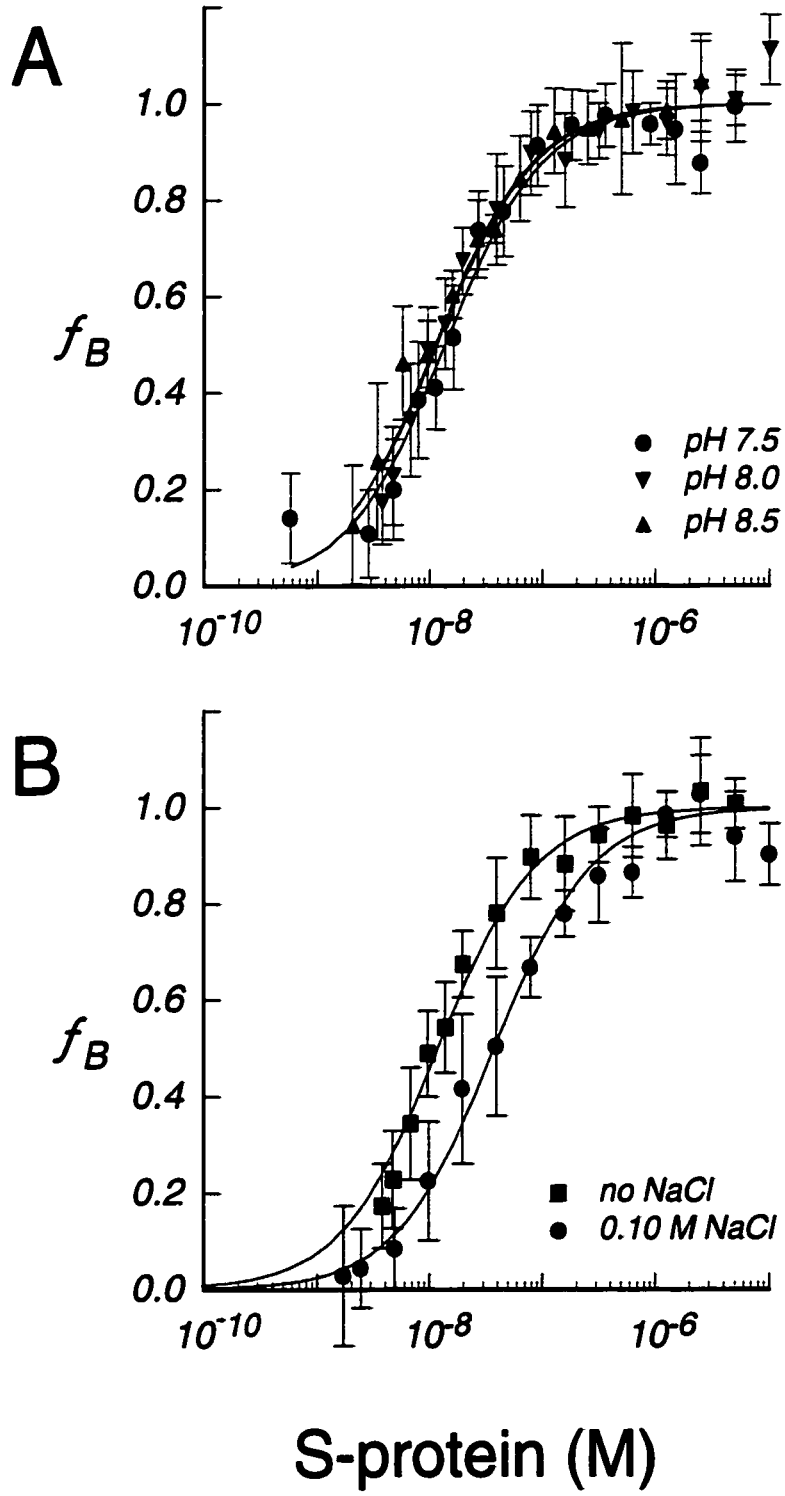
A
1.0
0.8
0.6
0.4
0.2
0.0
f_B
pH 7.5
pH 8.0
pH 8.5
10^{-10}
10^{-8}
10^{-6}
B
1.0
0.8
0.6
0.4
0.2
0.0
f_B
no NaCl
0.10 M NaCl
10^{-10}
10^{-8}
10^{-6}
S-protein (M)

APPENDIX

Kinetic analysis of dissociative inhibition;

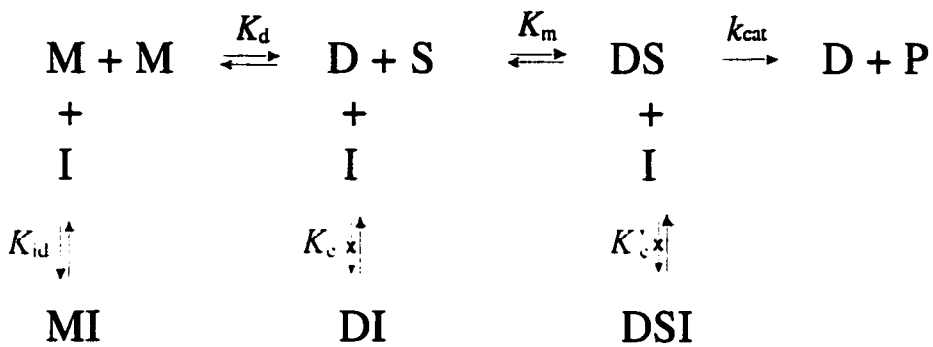

$$\frac{E_t}{\sqrt{k}} = \frac{K_m\left(1+\frac{I}{K_c}\right)}{k_{cat}+k'_{cat}\frac{I}{K'_c}}\sqrt{k} + \frac{\sqrt{K_d K_m}}{2\sqrt{k_{cat}+k'_{cat}\frac{I}{K'_c}}}\left(1+\frac{I}{K_{id}}\right)$$

If pure dissociative,

$$\frac{E_t}{\sqrt{k}} = \frac{K_m}{k_{cat}}\sqrt{k} + \frac{\sqrt{K_d K_m}}{2\sqrt{k_{cat}}}\left(1+\frac{I}{K_{id}}\right)$$

when I = 0,

$$\frac{E_t}{\sqrt{k}} = \frac{K_m}{k_{cat}}\sqrt{k} + \frac{\sqrt{K_d K_m}}{2\sqrt{k_{cat}}}$$

$$\frac{\frac{E_t}{\sqrt{k}} - \frac{\sqrt{K_d K_m}}{2\sqrt{k_{cat}}}}{\sqrt{k}} = \frac{K_m}{k_{cat}} + \frac{\sqrt{K_d K_m}}{2K_{id}\sqrt{k_{cat}}}\frac{I}{\sqrt{k}}$$

REFERENCES

Amann, E., Broker, M. & Wurm, F. (1984). Expression of Herpes simplex virus type 1 glycoprotein C antigens in *Escherichia coli*. *Gene* **32**, 203-215.

Anfinsen, C. B. (1973). Principles that govern the folding of protein chains. *Science* **181**, 223-230.

Ardelt, W., Mikulski, S. M. & Shogen, K. (1991). Amino acid sequence of an anti-tumor protein from *Rana pipiens* oocytes and early embryos. Homology to pancreatic ribonucleases. *J. Biol. Chem.* **266**, 245-251.

Argos, P. (1988). An investigation of protein subunit and domain interfaces. *Protein Eng.* **2**, 101-113.

Attie, A. D. & Raines, R. T. (1995). Analysis of receptor – ligand interactions. *J. Chem. Educ.* **72**, 119-124.

Ausubel, F. M., R., B., R., K., Moore, D. D., Seidman, J. G., Smith, J. A. & Struhl, K., Eds. (1994). *Current Protocols in Molecular Biololy*. New York: John Wiley & Sons.

Babe, L. M., Rose, J. & Craik, C. S. (1992). Synthetic "interface" peptides alter dimeric assembly of the HIV 1 and 2 proteases. *Protein Sci.* **1**, 1244-1253.

Babe, L. M., Rose, J. & Craik, C. S. (1995). Trans-dominant inhibitory human immunodeficiency virus type 1 protease monomers prevent protease activation and virion maturation. *Proc. Natl. Acad. Sci. USA* **92**, 10069-10073.

Baldwin, R. L. (1996). How Hofmeister ion interactions affect protein stability. *Biophys. J.* **71**, 2056-2063.

Barak, L. S., Ferguson, S. S., Zhang, J., Martenson, C., Meyer, T. & Caron, M. G. (1997). Internal trafficking and surface mobility of a functionally intact beta2-adrenergic receptor-green fluorescent protein conjugate. *Mol. Pharmacol.* **51**, 177-184.

Barnard, E. A. (1969). Biological function of pancreatic ribonuclease. *Nature* **221**, 340-344.

Beintema, J. J., Schuller, C., Irie, M. & Carsana, A. (1988). Molecular evolution of the ribonuclease superfamily. *Prog. Biophys. Mol. Biol.* **51**, 165-192.

Benfenati, F., Onofri, F. & Giovedi, S. (1999). Protein-protein interactions and protein modules in the control of neurotransmitter release. *Philos. Trans. R. Soc. Lond. B. Biol. Sci.* **354**, 243-257.

Boix, E., Wu, Y., Vasandani, V. M., Saxena, S. K., Ardelt, W., Ladner, J. & Youle, R. J. (1996). Role of the N terminus in RNase A homologues: differences in catalytic activity, ribonuclease inhibitor interaction and cytotoxicity. *J. Mol. Biol.* **257**, 992-1007.

Bokman, S. H. & Ward, W. W. (1981). Renaturation of *Aequorea* green fluorescent protein. *Biochem. Biophys. Res. Comm.* **101**, 1372-1380.

Bolivar, F., Rodriguez, R. L., Greene, P. J., Betlach, M. C., Heyneker, H. L. & Boyer, H. W. (1977). Construction and characterization of new cloning vehicles. II. A multipurpose cloning system. *Gene* **2**, 95-113.

Bouras, A., Boggetto, N., Benatalah, Z., de Rosny, E., Sicsic, S. & Reboud-Ravaux, M. (1999). Design, synthesis, and evaluation of conformationally constrained tongs, new inhibitors of HIV-1 protease dimerization. *J. Med. Chem.* **42**, 957-962.

Brosius, J., Dull, T. J., Sleeter, D. D. & Noller, H. F. (1981). Gene organization and primary structure of a ribosomal RNA operon from *Escherichia coli*. *J. Mol. Biol.* **148**, 107-127.

Campbell, V. W. & Jackson, D. A. (1980). The effect of divalent cations on the mode of action of DNase I. The initial reaction products produced from covalently closed circular DNA. *J. Biol. Chem.* **255**, 3726-3735.

Carey, J. (1991). Gel retardation. *Methods Enzymol.* **208**, 103-117.

Carpiro, L. A. & Han, G. Y. (1972). The 9-fluorenyl-methoxycarbonyl amino-protecting group. *J. Org. Chem.* **37**, 3404-3409.

Carr, D. W. & Scott, J. D. (1992). Blotting and band-shifting: techniques for studying protein-protein interactions. *Trends Biochem Sci.* **17**, 246-249.

Cayley, S., Lewis, B. A., Guttman, H. J. & Record, M. T., Jr. (1991). Characterization of the cytoplasm of *Escherichia coli* K-12 as a function of external osmolarity. Implications for protein-DNA interactions in vivo. *J. Mol. Biol.* **222**, 281-300.

Cecchini, D. J., Ehrat, M. & Giese, R. W. (1986). Substrate-leash amplification of ribonuclease activity. *J. Am. Chem. Soc.* **108**, 7841-7843.

Chalfie, M., Tu, Y., Euskirchen, G., Ward, W. W. & Prasher, D. C. (1994). Green fluorescent protein as a marker for gene expression. *Science* **263**, 802-805.

Chang, A. C. & Cohen, S. N. (1978). Construction and characterization of amplifiable multicopy DNA cloning vehicles derived from the P15A cryptic miniplasmid. *J. Bacteriol.* **134**, 1141-1156.

Chien, C. T., Bartel, P. L., Sternglanz, R. & Fields, S. (1991). The two-hybrid system: a method to identify and clone genes for proteins that interact with a protein of interest. *Proc. Natl. Acad. Sci. USA* **88**, 9578-9582.

Chivers, P. T., Prehoda, K. E., Volkman, B. F., Kim, B. M., Markley, J. L. & Raines, R. T. (1997). Microscopic pKa values of *Escherichia coli* thioredoxin. *Biochemistry* **36**, 14985-14991.

Cody, C. W., Prasher, D. C., Westler, W. M., Prendergast, F. G. & Ward, W. W. (1993). Chemical structure of the hexapeptide chromophore of the *Aequorea* green- fluorescent protein. *Biochemistry* **32**, 1212-1218.

Cohen, A. S. (1994). Clinical aspects of amyloidosis, including related proteins and central nervous system amyloid. *Curr. Opin. Rheumatol.* **6**, 68-77.

Colby, S., Dohner, K., Gunn, D. & Mayo, K. (1995). Purified GFP and anti-rGFP antiserum. *CLONTECHniques* **10**, 16-17.

Condra, J. H. (1998). Resistance to HIV protease inhibitors. *Haemophilia* **4**, 610-615.

Condra, J. H., Schleif, W. A., Blahy, O. M., Gabryelski, L. J., Graham, D. J., Quintero, J. C., Rhodes, A., Robbins, H. L., Roth, E., Shivaprakash, M. & et al. (1995). In vivo emergence of HIV-1 variants resistant to multiple protease inhibitors. *Nature* **374**, 569-571.

Connelly, P. R., Varadarajan, R., Sturtevant, J. M. & Richards, F. M. (1990). Thermodynamics of protein – peptide interactions in the ribonuclease S system studied by titration calorimetry. *Biochemistry* **29**, 6108-6114.

Cooper, A. (1998). Microcalorimetry of protein-protein interactions. *Methods Mol. Biol.* **88**, 11-22.

Corpet, F. (1988). Multiple sequence alignment with hierarchical clustering. *Nucleic Acids Res.* **16**, 10881-10890.

Crameri, A., Whitehorn, E. A., Tate, E. & Stemmer, W. P. C. (1996). Improved green fluorescent protein by molecular evolution using DNA shuffling. *Nat. Biotechnol.* **14**, 315-319.

Crameri, R., Jaussi, R., Menz, G. & Blaser, K. (1994). Display of expression products of cDNA libraries on phage surfaces. A versatile screening system for selective isolation of genes by specific gene-product/ligand interaction. *Eur. J. Biochem.* **226**, 53-58.

Cubitt, A. B., Heim, R., Adams, S. R., Boyd, A. E., Gross, L. A. & Tsien, R. Y. (1995). Understanding, improving and using green fluorescent proteins. *Trends Biochem. Sci.* **20**, 448-455.

Cubitt, A. B., Woollenweber, L. A. & Heim, R. (1999). Understanding structure-function relationships in the *Aequorea victoria* green fluorescent protein. *Methods Cell Biol.* **58**, 19-30.

Cull, M. G., Miller, J. F. & Schatz, P. J. (1992). Screening for receptor ligands using large libraries of peptides linked to the C terminus of the lac repressor. *Proc. Natl. Acad. Sci. USA* **89**, 1865-1869.

Cwirla, S. E., Peters, E. A., Barrett, R. W. & Dower, W. J. (1990). Peptides on phage: a vast library of peptides for identifying ligands. *Proc. Natl. Acad. Sci. USA* **87**, 6378-6382.

D'Alessio, G. & Riordan, J. F., Eds. (1998). *Ribonuclease: Structures and Functions.* New York: Academic Press.

Darke, P. L., Jordan, S. P., Hall, D. L., Zugay, J. A., Shafer, J. A. & Kuo, L. C. (1994). Dissociation and association of the HIV-1 protease dimer subunits: equilibria and rates. *Biochemistry* **33**, 98-105.

Delagrave, S., Hawtin, R. E., Silva, C. M., Yang, M. M. & Youvan, D. C. (1995). Red-shifted excitation mutants of the green fluorescent protein. *Bio/Technology* **13**, 151-154.

delCardayre, S. B., Ribo, M., Yokel, E. M., Quirk, D. J., Rutter, W. J. & Raines, R. T. (1995). Engineering ribonuclease A: production, purification and characterization of wild-type enzyme and mutants at Gln11. *Protein Eng.* **8**, 261-273.

Deng, W. P. & Nickoloff, J. A. (1992). Site-directed mutagenesis of virtually any plasmid by eliminating a unique site. *Anal. Biochem.* **200**, 81-88.

Divita, G., Restle, T., Goody, R. S., Chermann, J. C. & Baillon, J. G. (1994). Inhibition of human immunodeficiency virus type 1 reverse transcriptase dimerization using synthetic peptides derived from the connection domain. *J. Biol. Chem.* **269**, 13080-13083.

Domachowske, J. B., Dyer, K. D., Adams, A. G., Leto, T. L. & Rosenberg, H. F. (1998). Eosinophil cationic protein/RNase 3 is another RNase A-family ribonuclease with direct antiviral activity. *Nucleic Acids Res.* **26**, 3358-3363.

Durfee, T., Becherer, K., Chen, P. L., Yeh, S. H., Yang, Y., Kilburn, A. E., Lee, W. H. & Elledge, S. J. (1993). The retinoblastoma protein associates with the protein phosphatase type 1 catalytic subunit. *Genes Dev.* **7**, 555-569.

Dutia, B. M., Frame, M. C., Subak-Sharpe, J. H., Clark, W. N. & Marsden, H. S. (1986). Specific inhibition of herpesvirus ribonucleotide reductase by synthetic peptides. *Nature* **321**, 439-441.

Ehrig, T., O'Kane, D. J. & Prendergast, F. G. (1995). Green-fluorescent protein with altered fluorescence excitation spectra. *FEBS Lett.* **367**, 163-166.

Eichler, D. C., Tatar, T. F. & Lasater, L. S. (1981). Effect of human placental ribonuclease inhibitor in cell-free ribosomal RNA synthesis. *Biochem. Biophys. Res. Comm.* **101**, 396-403.

Evans, M. D. & Pryor, W. A. (1994). Cigarette smoking, emphysema, and damage to alpha 1-proteinase inhibitor. *Am. J. Physiol.* **266**, L593-611.

Fatkenheuer, G., Theisen, A., Rockstroh, J., Grabow, T., Wicke, C., Becker, K., Wieland, U., Pfister, H., Reiser, M., Hegener, P., Franzen, C., Schwenk, A. & Salzberger, B. (1997). Virological treatment failure of protease inhibitor therapy in an unselected cohort of HIV-infected patients. *AIDS* **11**, F113-116.

Fett, J. W., Strydom, D. J., Lobb, R. R., Alderman, E. M., Bethune, J. L., Riordan, J. F. & Vallee, B. L. (1985). Isolation and characterization of angiogenin, an angiogenic protein from human carcinoma cells. *Biochemistry* **24**, 5480-6.

Fields, S. & Song, O. (1989). A novel genetic system to detect protein-protein interactions. *Nature* **340**, 245-246.

Fleischmann, M., Bloch, W., Kolossov, E., Andressen, C., Muller, M., Brem, G., Hescheler, J., Addicks, K. & Fleischmann, B. K. (1998). Cardiac specific expression of the green fluorescent protein during early murine embryonic development. *FEBS Lett.* **440**, 370-376.

Flexner, C. (1998). HIV-protease inhibitors. *N. Engl. J. Med.* **338**, 1281-1292.

Franciskovich, J., Houseman, K., Mueller, R. & Chmielewski, J. (1993). A systematic evaluation of the inhibition of HIV-1 protease by its C- and N-terminal peptides. *Bioorg. Med. Chem. Lett.* **3**, 165-168.

Frankel, A. D. & Young, J. A. (1998). HIV-1: fifteen proteins and an RNA. *Annu. Rev. Biochem.* **67**, 1-25.

Gallo, R. C., Salahuddin, S. Z., Popovic, M., Shearer, G. M., Kaplan, M., Haynes, B. F., Palker, T. J., Redfield, R., Oleske, J., Safai, B. & et al. (1984). Frequent detection and isolation of cytopathic retroviruses (HTLV-III) from patients with AIDS and at risk for AIDS. *Science* **224**, 500-503.

Gleich, G. J., Loegering, D. A., Bell, M. P., Checkel, J. L., Ackerman, S. J. & McKean, D. J. (1986). Biochemical and functional similarities between human eosinophil- derived neurotoxin and eosinophil cationic protein: homology with ribonuclease. *Proc. Natl. Acad. Sci. USA* **83**, 3146-3150.

Gosink, M. M. & Vierstra, R. D. (1995). Redirecting the specificity of ubiquitination by modifying ubiquitin- conjugating enzymes. *Proc. Natl. Acad. Sci. USA* **92**, 9117-9121.

Gossen, J. A., Molijn, A. C., Douglas, G. R. & Vijg, J. (1992). Application of galactose-sensitive E. coli strains as selective hosts for LacZ- plasmids. *Nucleic Acids Res.* **20**, 3254.

Grant, S. K., Deckman, I. C., Culp, J. S., Minnich, M. D., Brooks, I. S., Hensley, P., Debouck, C. & Meek, T. D. (1992). Use of protein unfolding studies to determine the conformational and dimeric stabilities of HIV-1 and SIV proteases. *Biochemistry* **31**, 9491-9501.

Gyuris, J., Golemis, E., Chertkov, H. & Brent, R. (1993). Cdi1, a human G1 and S phase protein phosphatase that associates with Cdk2. *Cell* **75**, 791-803.

Hedtke, B., Meixner, M., Gillandt, S., Richter, E., Borner, T. & Weihe, A. (1999). Green fluorescent protein as a marker to investigate targeting of organellar RNA polymerases of higher plants in vivo. *Plant J.* **17**, 557-561.

Heim, R., Cubitt, A. B. & Tsien, R. Y. (1995). Improved green fluorescence. *Nature* **373**, 663-664.

Heim, R., Prasher, D. C. & Tsien, R. Y. (1994). Wavelength mutations and posttranslational autoxidation of green fluorescent protein. *Proc. Natl. Acad. Sci. USA* **91**, 12501-12504.

Heyduk, T., Ma, Y., Tang, H. & Ebright, R. H. (1996). Fluorescence anisotropy: rapid, quantitative assay for protein-DNA and protein-protein interaction. *Methods Enzymol.* **274**, 492-503.

Hochuli, E., Bannwarth, W., Döbeli, H., Gentz, R. & Stüber, D. (1988). Genetic approach to facilitate purification of recombinant proteins with a novel metal chelate adsorbent. *Bio/Technology* **6**, 1321-1325.

Houghten, R. A. (1993). Peptide libraries: criteria and trends. *Trends Genet.* **9**, 235-239.

Hu, J. C., O'Shea, E. K., Kim, P. S. & Sauer, R. T. (1990). Sequence requirements for coiled-coils: analysis with lambda repressor- GCN4 leucine zipper fusions. *Science* **250**, 1400-1403.

Huang, Z., Olson, N. A., You, W. & Haugland, R. P. (1992). A sensitive competitive ELISA for 2,4-dinitrophenol using 3,6-fluorescein diphosphate as a fluorogenic substrate. *J. Immunol. Methods* **149**, 261-266.

Ido, E., Han, H. P., Kezdy, F. J. & Tang, J. (1991). Kinetic studies of human immunodeficiency virus type 1 protease and its active-site hydrogen bond mutant A28S. *J. Biol. Chem.* **266**, 24359-24366.

Ingram, D. V. (1957). Gene mutations in human hemoglobin: Difference between normal and sickle cell hemoglobin. *Nature* **180**, 326.

Inouye, S. & Tsuji, F. I. (1994). *Aequorea* green fluorescent protein. Expression of the gene and fluorescence characteristics of the recombinant protein. *FEBS Lett.* **341**, 277-280.

Jameson, D. M. & Sawyer, W. H. (1995). Fluorescence anisotropy applied to biomolecular interactions. *Methods Enzymol.* **246**, 283-300.

Janin, J. & Chothia, C. (1990). The structure of protein-protein recognition sites. *J. Biol. Chem.* **265**, 16027-16030.

Janin, J., Miller, S. & Chothia, C. (1988). Surface, subunit interfaces and interior of oligomeric proteins. *J. Mol. Biol.* **204**, 155-164.

Jappelli, R. & Brenner, S. (1996). Interaction between cAMP-dependent protein kinase catalytic subunit and peptide inhibitors analyzed with lambda repressor fusions. *J. Mol. Biol.* **259**, 575-578.

Johnson, D. & Travis, J. (1979). The oxidative inactivation of human alpha-1-proteinase inhibitor. Further evidence for methionine at the reactive center. *J. Biol. Chem.* **254**, 4022-4026.

Jolley, M. E. (1996). Fluorescence polarization assays for the detection of proteases and their inhibitors. *J. Biomol. Screening* **1**, 33-38.

Jones, S. & Thornton, J. M. (1995). Protein-protein interactions: a review of protein dimer structures. *Prog. Biophys. Mol. Biol.* **63**, 31-65.

Jones, S. & Thornton, J. M. (1996). Principles of protein-protein interactions. *Proc. Natl. Acad. Sci. USA* **93**, 13-20.

Kameshita, I., Ishida, A. & Fujisawa, H. (1998). Analysis of protein-protein interaction by two-dimensional affinity electrophoresis. *Anal. Biochem.* **262**, 90-92.

Kamiya, Y., Oyama, F., Oyama, R., Sakakibara, F., Nitta, K., Kawauchi, H., Takayanagi, Y. & Titani, K. (1990). Amino acid sequence of a lectin from Japanese frog (Rana japonica) eggs. *J. Biochem. (Tokyo)* **108**, 139-143.

Kartha, G., Bello, J. & Harker, D. (1967). Tertiary structure of ribonuclease. *Nature* **213**, 862-865.

Katoh, I., Yasunaga, T., Ikawa, Y. & Yoshinaka, Y. (1987). Inhibition of retroviral protease activity by an aspartyl proteinase inhibitor. *Nature* **329**, 654-656.

Katoh, I., Yoshinaka, Y., Rein, A., Shibuya, M., Odaka, T. & Oroszlan, S. (1985). Murine leukemia virus maturation: protease region required for conversion from "immature" to "mature" core form and for virus infectivity. *Virology* **145**, 280-292.

Keegan, L., Gill, G. & Ptashne, M. (1986). Separation of DNA binding from the transcription-activating function of a eukaryotic regulatory protein. *Science* **231**, 699-704.

Kim, J. S. & Raines, R. T. (1993). Ribonuclease S-peptide as a carrier in fusion proteins. *Protein Sci.* **2**, 348-356.

Kim, J. S., Soucek, J., Matousek, J. & Raines, R. T. (1995). Mechanism of ribonuclease cytotoxicity. *J. Biol. Chem.* **270**, 31097-31102.

Kim, J.-S. & Raines, R. T. (1994). Peptide tags for a dual affinity fusion system. *Anal. Biochem.* **219**, 165-166.

Klabe, R. M., Bacheler, L. T., Ala, P. J., Erickson-Viitanen, S. & Meek, J. L. (1998). Resistance to HIV protease inhibitors: a comparison of enzyme inhibition and antiviral potency. *Biochemistry* **37**, 8735-8742.

Klotz, I. M. (1997). *Ligand – Receptor Energetics: A Guide for the Perplexed*, John Wiley & Sons, New York.

Kobe, B. & Deisenhofer, J. (1995). A structural basis of the interactions between leucine-rich repeats and protein ligands. *Nature* **374**, 183-186.

Koch, W. J., Inglese, J., Stone, W. C. & Lefkowitz, R. J. (1993). The binding site for the beta gamma subunits of heterotrimeric G proteins on the beta-adrenergic receptor kinase. *J. Biol. Chem.* **268**, 8256-8260.

Kohl, N. E., Emini, E. A., Schleif, W. A., Davis, L. J., Heimbach, J. C., Dixon, R. A., Scolnick, E. M. & Sigal, I. S. (1988). Active human immunodeficiency virus protease is required for viral infectivity. *Proc. Natl. Acad. Sci. USA* **85**, 4686-4690.

Kraulis, P. J. (1991). MOLSCRIPT: a program to produce both detailed and schematic plots of protein structures. *J. Appl. Crystallogr.* **24**, 946-950.

Krause, G., Lundstrom, J., Barea, J. L., Pueyo de la Cuesta, C. & Holmgren, A. (1991). Mimicking the active site of protein disulfide-isomerase by substitution of proline 34 in *Escherichia coli* thioredoxin. *J. Biol. Chem.* **266**, 9494-9500.

LaBean, T. H. & Kauffman, S. A. (1993). Design of synthetic gene libraries encoding random sequence proteins with desired ensemble characteristics. *Protein Sci.* **2**, 1249-1254.

Laemmli, U. K. (1970). Cleavage of structural proteins during the assembly of the head of bacteriophage T4. *Nature* **227**, 680-685.

Lakey, J. H. & Raggett, E. M. (1998). Measuring protein-protein interactions. *Curr. Opin. Struct. Biol.* **8**, 119-123.

Lang, T., Wacker, I., Steyer, J., Kaether, C., Wunderlich, I., Soldati, T., Gerdes, H. H. & Almers, W. (1997). Ca^{2+}-triggered peptide secretion in single cells imaged with green fluorescent protein and evanescent-wave microscopy. *Neuron* **18**, 857-863.

Lapatto, R., Blundell, T., Hemmings, A., Overington, J., Wilderspin, A., Wood, S., Merson, J. R., Whittle, P. J., Danley, D. E., Geoghegan, K. F. & et al. (1989). X-ray analysis of HIV-1 proteinase at 2.7 A resolution confirms structural homology among retroviral enzymes. *Nature* **342**, 299-302.

Lee, F. S., Fox, E. A., Zhou, H. M., Strydom, D. J. & Vallee, B. L. (1988). Primary structure of human placental ribonuclease inhibitor. *Biochemistry* **27**, 8545-8553.

Lee, F. S. & Vallee, B. L. (1989). Binding of placental ribonuclease inhibitor to the active site of angiogenin. *Biochemistry* **28**, 3556-3561.

Lee, F. S. & Vallee, B. L. (1993). Structure and action of mammalian ribonuclease (angiogenin) inhibitor. *Prog. Nucleic Acid Res. Mol. Biol.* **44**, 1-30.

Leland, P. A., Schultz, L. W., Kim, B. M. & Raines, R. T. (1998). Ribonuclease A variants with potent cytotoxic activity. *Proc. Natl. Acad. Sci. USA* **95**, 10407-10412.

LeTilly, V. & Royer, C. A. (1993). Fluorescence anisotropy assays implicate protein–protein interactions in regulating *trp* repressor DNA binding. *Biochemistry* **32**, 7753-7758.

Li, J. J. & Herskowitz, I. (1993). Isolation of ORC6, a component of the yeast origin recognition complex by a one-hybrid system. *Science* **262**, 1870-1874.

Li, T. S., Tubiana, R., Katlama, C., Calvez, V., Ait Mohand, H. & Autran, B. (1998). Long-lasting recovery in CD4 T-cell function and viral-load reduction after highly active antiretroviral therapy in advanced HIV-1 disease. *Lancet* **351**, 1682-1686.

Liao, Y. D. (1992). A pyrimidine-guanine sequence-specific ribonuclease from *Rana catesbeiana* (bullfrog) oocytes. *Nucleic Acids Res.* **20**, 1371-1377.

Lowman, H. B., Bass, S. H., Simpson, N. & Wells, J. A. (1991). Selecting high-affinity binding proteins by monovalent phage display. *Biochemistry* **30**, 10832-10838.

Lu, T., Van Dyke, M. & Sawadogo, M. (1993). Protein-protein interaction studies using immobilized oligohistidine fusion proteins. *Anal Biochem.* **213**, 318-322.

Lu, Z., Murray, K. S., Van Cleave, V., LaVallie, E. R., Stahl, M. L. & McCoy, J. M. (1995). Expression of thioredoxin random peptide libraries on the *Escherichia coli* cell surface as functional fusions to flagellin: a system designed for exploring protein-protein interactions. *Bio/Technology* **13**, 366-372.

Lundblad, J. R., Laurance, M. & Goodman, R. H. (1996). Fluorescence polarization analysis of protein-DNA and protein-protein interactions. *Mol. Endocrinol.* **10**, 607-612.

Mahajan, N. P., Linder, K., Berry, G., Gordon, G. W., Heim, R. & Herman, B. (1998). Bcl-2 and Bax interactions in mitochondria probed with green fluorescent protein and fluorescence resonance energy transfer. *Nat. Biotechnol.* **16**, 547-552.

Maletic-Savatic, M., Malinow, R. & Svoboda, K. (1999). Rapid dendritic morphogenesis in CA1 hippocampal dendrites induced by synaptic activity. *Science* **283**, 1923-1927.

Marchetti, A., Abril-Marti, M., Illi, B., Cesareni, G. & Nasi, S. (1995). Analysis of the Myc and Max interaction specificity with lambda repressor-HLH domain fusions. *J. Mol. Biol.* **248**, 541-550.

Matayoshi, E. D., Wang, G. T., Krafft, G. A. & Erickson, J. (1990). Novel fluorogenic substrates for assaying retroviral proteases by resonance energy transfer. *Science* **247**, 954-958.

Matousek, J. (1973). The effect of bovine seminal ribonuclease (BS RNase) on cells of Crocker tumour in mice. *Experientia* **29**, 858-859.

Mattheakis, L. C., Bhatt, R. R. & Dower, W. J. (1994). An in vitro polysome display system for identifying ligands from very large peptide libraries. *Proc. Natl. Acad. Sci. USA* **91**, 9022-9026.

Matthews, D. J. & Wells, J. A. (1993). Substrate phage: selection of protease substrates by monovalent phage display. *Science* **260**, 1113-1117.

Meyer, B. J. & Ptashne, M. (1980). Gene regulation at the right operator (OR) of bacteriophage lambda. III. lambda repressor directly activates gene transcription. *J. Mol. Biol.* **139**, 195-205.

Mikulski, S. M., Ardelt, W., Shogen, K., Bernstein, E. H. & Menduke, H. (1990). Striking increase of survival of mice bearing M109 Madison carcinoma treated with a novel protein from amphibian embryos. *J. Natl. Cancer Inst.* **82**, 151-153.

Miller, J. H., Ed. (1972). *Experiments in Molecular Genetics*. New York: Cold Spring Harbor Laboratory.

Miller, M., Jaskolski, M., Rao, J. K., Leis, J. & Wlodawer, A. (1989). Crystal structure of a retroviral protease proves relationship to aspartic protease family. *Nature* **337**, 576-579.

Mitra, R. D., Silva, C. M. & Youvan, D. C. (1996). Fluorescence resonance energy transfer between blue-emitting and red-shifted excitation derivatives of the green fluorescent protein. *Gene* **173**, 13-17.

Mitsui, Y., Satow, Y., Watanabe, Y., Hirono, S. & Iitaka, Y. (1979). Crystal structures of *Streptomyces* subtilisin inhibitor and its complex with subtilisin BPN'. *Nature* **277**, 447-52.

Miyawaki, A., Llopis, J., Heim, R., McCaffery, J. M., Adams, J. A., Ikura, M. & Tsien, R. Y. (1997). Fluorescent indicators for Ca^{2+} based on green fluorescent proteins and calmodulin. *Nature* **388**, 882-887.

Moore, S. & Stein, W. H. (1973). Chemical structures of pancreatic ribonuclease and deoxyribonuclease. *Science* **180**, 458-464.

Morin, J. G. & Hastings, J. W. (1971). Energy transfer in a bioluminescent system. *J. Cell Physiol.* **77**, 313-318.

Morise, H., Shimomura, O., Johnson, F. H. & Winant, J. (1974). Intermolecular energy transfer in the bioluminescent system of *Aequorea*. *Biochemistry* **13**, 2656-2662.

Muldoon, R. R., Levy, J. P., Kain, S. R., Kitts, P. A. & Link, C. J., Jr. (1997). Tracking and quantitation of retroviral-mediated transfer using a completely humanized, red-shifted green fluorescent protein gene. *Biotechniques* **22**, 162-167.

Nevalainen, L. T., Aoyama, T., Ikura, M., Crivici, A., Yan, H., Chua, N. H. & Nairn, A. C. (1997). Characterization of novel calmodulin-binding peptides with distinct inhibitory effects on calmodulin-dependent enzymes. *Biochem. J.* **321**, 107-115.

Olson, K. A., Fett, J. W., French, T. C., Key, M. E. & Vallee, B. L. (1995). Angiogenin antagonists prevent tumor growth in vivo. *Proc. Natl. Acad. Sci. USA* **92**, 442-446.

Ormö, M., Cubitt, A. B., Kallio, K., Gross, L. A., Tsien, R. Y. & Remington, S. J. (1996). Crystal structure of the *Aequorea victoria* green fluorescent protein. *Science* **237**, 1392-1395.

Pabo, C. O., Sauer, R. T., Sturtevant, J. M. & Ptashne, M. (1979). The lambda repressor contains two domains. *Proc. Natl. Acad. Sci. USA* **76**, 1608-1612.

Palella, F. J., Jr., Delaney, K. M., Moorman, A. C., Loveless, M. O., Fuhrer, J., Satten, G. A., Aschman, D. J. & Holmberg, S. D. (1998). Declining morbidity and mortality among patients with advanced human immunodeficiency virus infection. HIV Outpatient Study Investigators. *N. Engl. J. Med.* **338**, 853-860.

Palmer, S., Shafer, R. W. & Merigan, T. C. (1999). Highly drug-resistant HIV-1 clinical isolates are cross-resistant to many antiretroviral compounds in current clinical development. *AIDS* **13**, 661-667.

Papageorgiou, A. C., Shapiro, R. & Acharya, K. R. (1997). Molecular recognition of human angiogenin by placental ribonuclease inhibitor--an X-ray crystallographic study at 2.0 A resolution. *EMBO J.* **16**, 5162-5177.

Park, S.-H. & Raines, R. T. (1997). Green fluorescent protein as a signal for protein – protein interactions. *Protein Sci.* **6**, 2344-2349.

Patterson, G. H., Knobel, S. M., Sharif, W. D., Kain, S. R. & Piston, D. W. (1997). Use of the green fluorescent protein and its mutants in quantitative fluorescence microscopy. *Biophys. J.* **73**, 2782-2790.

Peng, C., Ho, B. K., Chang, T. W. & Chang, N. T. (1989). Role of human immunodeficiency virus type 1-specific protease in core protein maturation and viral infectivity. *J. Virol.* **63**, 2550-2556.

Perez, F., Diamantopoulos, G. S., Stalder, R. & Kreis, T. E. (1999). CLIP-170 highlights growing microtubule ends in vivo. *Cell* **96**, 517-527.

Perozzo, M. A., Ward, K. B., Thompson, R. B. & Ward, W. W. (1988). X-ray diffraction and time-resolved fluorescence analyses of *Aequorea* green fluorescent protein crystals. *J. Biol. Chem.* **263**, 7713-7716.

Picard, V., Ersdal-Badju, E., Lu, A. & Bock, S. C. (1994). A rapid and efficient one-tube PCR-based mutagenesis technique using *Pfu* DNA polymerase. *Nucleic Acids Res.* **22**, 2587-2591.

Piketty, C., Castiel, P., Belec, L., Batisse, D., Si Mohamed, A., Gilquin, J., Gonzalez-Canali, G., Jayle, D., Karmochkine, M., Weiss, L., Aboulker, J. P. & Kazatchkine, M. D. (1998). Discrepant responses to triple combination antiretroviral therapy in advanced HIV disease. *AIDS* **12**, 745-750.

Potts, J. T., Young, D. M. & Anfinsen, C. B. (1963). Reconstitution of fully active RNase S by carboxypeptidase-degraded RNase S-peptide. *J. Biol. Chem.* **238**, 2593-2594.

Pouli, A. E., Kennedy, H. J., Schofield, J. G. & Rutter, G. A. (1998). Insulin targeting to the regulated secretory pathway after fusion with green fluorescent protein and firefly luciferase. *Biochem. J.* **331**, 669-675.

Prasher, D. C., Eckenrode, V. K., Ward, W. W., Prendergast, F. G. & Cormier, M. J. (1992). Primary structure of the *Aequorea victoria* green-fluorescent protein. *Gene* **111**, 229-233.

Prendergast, F. G. & Mann, K. G. (1978). Chemical and physical properties of aequorin and the green fluorescent protein isolated from *Aequorea forskalea*. *Biochemistry* **17**, 3448-3453.

Presley, J. F., Cole, N. B., Schroer, T. A., Hirschberg, K., Zaal, K. J. & Lippincott-Schwartz, J. (1997). ER-to-Golgi transport visualized in living cells. *Nature* **389**, 81-85.

Radek, J. T., Jeong, J. M., Wilson, J. & Lorand, L. (1993). Association of the A subunits of recombinant placental factor XIII with the native carrier B subunits from human plasma. *Biochemistry* **32**, 3527-3534.

Raines, R. T. (1998). Ribonuclease A. *Chem. Rev.* **98**, 1045-1065.

Raines, R. T., McCormick, M., van Oosbree, T. R. & Mierendorf, R. C. (2000). The S-Tag fusion system. *Methods Enzymol.*, In Press.

Rajagopal, P., Waygood, E. B., Reizer, J., Saier, M. H., Jr. & Klevit, R. E. (1997). Demonstration of protein-protein interaction specificity by NMR chemical shift mapping. *Protein Sci.* **6**, 2624-2627.

Ratner, L., Josephs, S. F., Starcich, B., Hahn, B., Shaw, G. M., Gallo, R. C. & Wong-Staal, F. (1985). Nucleotide sequence analysis of a variant human T-cell leukemia virus (HTLV-Ib) provirus with a deletion in pX-I. *J. Virol.* **54**, 781-790.

Rebar, E. J. & Pabo, C. O. (1994). Zinc finger phage: affinity selection of fingers with new DNA-binding specificities. *Science* **263**, 671-673.

Ren, P., Lim, C.-S., Johnsen, R., Albert, P. S., Pilgrim, D. & Riddle, D. L. (1996). Control of *C. elegans* larval development by neuronal expression of TGF-β homolog. *Science* **274**, 1389-1391.

Richards, F. M. (1955). Titration of amino groups released during the digestion of ribonuclease by subtilisin. *Compt. rend. trav. lab. Carlsberg, Ser. Chim.* **29**, 322-328.

Richards, F. M. & Vithayathil, P. J. (1957). The preparation of subtilisin modified ribonuclease and the separation of the peptide and protein components. *J. Biol. Chem.* **234**, 1459-1465.

Richards, F. M. & Vithayathil, P. J. (1959). The preparation of subtilisin modified ribonuclease and separation of the peptide and protein components. *J. Biol. Chem.* **234**, 1459-1465.

Robey, R. B., Ruiz, O., Santos, A. V., Ma, J., Kear, F., Wang, L. J., Li, C. J., Bernardo, A. A. & Arruda, J. A. (1998). pH-dependent fluorescence of a heterologously expressed *Aequorea* green fluorescent protein mutant: in situ spectral characteristics and applicability to intracellular pH estimation. *Biochemistry* **37**, 9894-9901.

Rose, J. R., Salto, R. & Craik, C. S. (1993). Regulation of autoproteolysis of the HIV-1 and HIV-2 proteases with engineered amino acid substitutions. *J. Biol. Chem.* **268**, 11939-11945.

Rosenberg, H. F., Dyer, K. D., Tiffany, H. L. & Gonzalez, M. (1995). Rapid evolution of a unique family of primate ribonuclease genes. *Nat. Genet.* **10**, 219-223.

Roth, J. S. (1962). Ribonuclease. Further studies on ribonuclease inhibitor. *Biochim. Biophys. Acta* **61**, 903-915.

Sambrook, J., Fritsch, E. F. & Maniatis, T., Eds. (1989). *Molecular cloning: A laboratory manual.* Second edit. Cold Spring Harbor: Cold Spring Harbor Laboratory.

Santoro, J., Gonzalez, C., Bruix, M., Neira, J. L., Nieto, J. L., Herranz, J. & Rico, M. (1993). High-resolution three-dimensional structure of ribonuclease A in solution by nuclear magnetic resonance spectroscopy. *J. Mol. Biol.* **229**, 722-734.

Scheele, G. & Blackburn, P. (1979). Role of mammalian RNase inhibitor in cell-free protein synthesis. *Proc. Natl. Acad. Sci. USA* **76**, 1898-1902.

Schinazi, R. F., Larder, B. A. & Mellors, J. W. (1997). Mutations in retroviral genes associated with drug resistance. *Antivir. News* **5**, 129-142.

Schramm, H. J., Billich, A., Jaeger, E., Rucknagel, K. P., Arnold, G. & Schramm, W. (1993). The inhibition of HIV-1 protease by interface peptides. *Biochem. Biophys. Res. Comm.* **194**, 595-600.

Schramm, H. J., Boetzel, J., Buttner, J., Fritsche, E., Gohring, W., Jaeger, E., Konig, S., Thumfart, O., Wenger, T., Nagel, N. E. & Schramm, W. (1996). The inhibition of human immunodeficiency virus proteases by 'interface peptides'. *Antiviral Res.* **30**, 155-170.

Schramm, H. J., Breipohl, G., Hansen, J., Henke, S., Jaeger, E., Meichsner, C., Riess, G., Ruppert, D., Rucknagel, K. P., Schafer, W. & et al. (1992). Inhibition of HIV-1 protease by short peptides derived from the terminal segments of the protease. *Biochem. Biophys. Res. Comm.* **184**, 980-985.

Schramm, H. J., Nakashima, H., Schramm, W., Wakayama, H. & Yamamoto, N. (1991). HIV-1 reproduction is inhibited by peptides derived from the N- and C- termini of HIV-1 protease. *Biochem. Biophys. Res. Comm.* **179**, 847-851.

Schreier, A. A. & Baldwin, R. L. (1976). Concentration-dependent hydrogen exchange kinetics of ^{3}H-labeled S-peptide in ribonuclease S. *J. Mol. Biol.* **105**, 409-426.

Schreier, A. A. & Baldwin, R. L. (1977). Mechanism of dissociation of S-peptide from ribonuclease S. *Biochemistry* **16**, 4203-4209.

Scopes, R. K. (1994). *Protein Purification: Principles and Practice*, Springer-Verlag, New York.

Seelmeier, S., Schmidt, H., Turk, V. & von der Helm, K. (1988). Human immunodeficiency virus has an aspartic-type protease that can be inhibited by pepstatin A. *Proc. Natl. Acad. Sci. USA* **85**, 6612-6616.

SenGupta, D. J., Zhang, B., Kraemer, B., Pochart, P., Fields, S. & Wickens, M. (1996). A three-hybrid system to detect RNA-protein interactions in vivo. *Proc. Natl. Acad. Sci. USA* **93**, 8496-8501.

Shapira, S. K., Chou, J., Richaud, F. V. & Casadaban, M. J. (1983). New versatile plasmid vectors for expression of hybrid proteins coded by a cloned gene fused to *lacZ* gene sequences encoding an enzymatically active carboxy-terminal portion of beta-galactosidase. *Gene* **25**, 71-82.

Shapiro, R., Fox, E. A. & Riordan, J. F. (1989). Role of lysines in human angiogenin: chemical modification and site- directed mutagenesis. *Biochemistry* **28**, 1726-32.

Shapiro, R. & Vallee, B. L. (1989). Site-directed mutagenesis of histidine-13 and histidine-114 of human angiogenin. Alanine derivatives inhibit angiogenin-induced angiogenesis. *Biochemistry* **28**, 7401-8.

Sinha, N. D., Biernat, J., McManus, J. & Koster, H. (1984). Polymer support oligonucleotide synthesis XVIII: use of beta-cyanoethyl-N,N-dialkylamino-/N-morpholino phosphoramidite of deoxynucleosides for the synthesis of DNA fragments simplifying deprotection and isolation of the final product. *Nucleic Acids Res.* **12**, 4539-4557.

Sipe, J. D. (1992). Amyloidosis. *Annu. Rev. Biochem.* **61**, 947-975.

Smith, G. P. (1985). Filamentous fusion phage: novel expression vectors that display cloned antigens on the virion surface. *Science* **228**, 1315-1317.

Soncin, F., Shapiro, R. & Fett, J. W. (1994). A cell-surface proteoglycan mediates human adenocarcinoma HT-29 cell adhesion to human angiogenin. *J. Biol. Chem.* **269**, 8999-9005.

Soucek, J., Chudomel, V., Potmesilova, I. & Novak, J. T. (1986). Effect of ribonucleases on cell-mediated lympholysis reaction and on GM- CFC colonies in bone marrow culture. *Nat. Immun. Cell Growth Regul.* **5**, 250-258.

Soucek, J., Hruba, A., Paluska, E., Chudomel, V., Dostal, J. & Matousek, J. (1983). Immunosuppressive effects of bovine seminal fluid fractions with ribonuclease activity. *Folia Biol.* **29**, 250-261.

Souroujon, M. C. & Mochly-Rosen, D. (1998). Peptide modulators of protein-protein interactions in intracellular signaling. *Nat. Biotechnol.* **16**, 919-924.

Sternberg, M. J. & Gullick, W. J. (1989). Neu receptor dimerization. *Nature* **339**, 587.

Szeltner, Z. & Polgar, L. (1996). Conformational stability and catalytic activity of HIV-1 protease are both enhanced at high salt concentration. *J. Biol. Chem.* **271**, 5458-5463.

Tainer, J. A., Getzoff, E. D., Beem, K. M., Richardson, J. S. & Richardson, D. C. (1982). Determination and analysis of the 2 Å-structure of copper, zinc superoxide dismutase. *J. Mol. Biol.* **160**, 181-217.

Tian, Y., Adya, N., Wagner, S., Giam, C. Z., Green, M. R. & Ellington, A. D. (1995). Dissecting protein:protein interactions between transcription factors with an RNA aptamer. *RNA* **1**, 317-326.

Todd, M. J., Semo, N. & Freire, E. (1998). The structural stability of the HIV-1 protease. *J. Mol. Biol.* **283**, 475-488.

Topham, M. K., Bunting, M., Zimmerman, G. A., McIntyre, T. M., Blackshear, P. J. & Prescott, S. M. (1998). Protein kinase C regulates the nuclear localization of diacylglycerol kinase-zeta. *Nature* **394**, 697-700.

Tsai, C. J., Lin, S. L., Wolfson, H. J. & Nussinov, R. (1996). Protein-protein interfaces: architectures and interactions in protein- protein interfaces and in protein cores. Their similarities and differences. *Crit. Rev. Biochem. Mol. Biol.* **31**, 127-152.

Tsien, R. Y. (1998). The green fluorescent protein. *Annu. Rev. Biochem.* **67**, 509-544.

van den Pol, A. N. & Ghosh, P. K. (1998). Selective neuronal expression of green fluorescent protein with cytomegalovirus promoter reveals entire neuronal arbor in transgenic mice. *J. Neurosci.* **18**, 10640-10651.

Vescia, S., Tramontano, D., Augusti-Tocco, G. & D'Alessio, G. (1980). In vitro studies on selective inhibition of tumor cell growth by seminal ribonuclease. *Cancer Res.* **40**, 3740-3744.

Vicentini, A. M., Kieffer, B., Matthies, R., Meyhack, B., Hemmings, B. A., Stone, S. R. & Hofsteenge, J. (1990). Protein chemical and kinetic characterization of recombinant porcine ribonuclease inhibitor expressed in *Saccharomyces cerevisiae*. *Biochemistry* **29**, 8827-8834.

Vondrasek, J. & Wlodawer, A. (1997). Database of HIV proteinase structures. *Trends Biochem. Sci.* **22**, 183.

Wain-Hobson, S., Sonigo, P., Danos, O., Cole, S. & Alizon, M. (1985). Nucleotide sequence of the AIDS virus, LAV. *Cell* **40**, 9-17.

Ward, W. W. (1981). Properties of the coelenterate green-fluorescent proteins. In *Bioluminescence and Chemiluminescence* (DeLuca, M. & McElroy, W., eds.), pp. 235-242. Academic Press, New York.

Ward, W. W. (1997). *Green Fluorescent Protein: Properties, Applications and Protocols* (Chalfie, M. & Kain, S., Eds.), John Wiley & Sons, New York.

Ward, W. W. & Bokman, S. H. (1982). Reversible denaturation of *Aequorea* green-fluorescent protein: physical separation and characterization of the renatured protein. *Biochemistry* **21**, 4535-4540.

Watowich, S. J., Gross, L. J. & Josephs, R. (1993). Analysis of the intermolecular contacts within sickle hemoglobin fibers: effect of site-specific substitutions, fiber pitch, and double- strand disorder. *J. Struct. Biol.* **111**, 161-179.

Weber, I. T. (1990). Comparison of the crystal structures and intersubunit interactions of human immunodeficiency and Rous sarcoma virus proteases. *J. Biol. Chem.* **265**, 10492-10496.

Weinreich, M. D., Mahnke-Braam, L. & Reznikoff, W. S. (1994). A functional analysis of the Tn5 transposase. Identification of domains required for DNA binding and multimerization. *J. Mol. Biol.* **241**, 166-177.

Winzor, D. J. & Sawyer, W. H. (1995). *Quantitative Characterization of Ligand Binding*, Wiley-Liss, New York.

Wittmayer, P. K. & Raines, R. T. (1996). Substrate binding and turnover by the highly specific I-*Ppo*I endonuclease. *Biochemistry* **35**, 1076-1083.

Wlodawer, A., Miller, M., Jaskolski, M., Sathyanarayana, B. K., Baldwin, E., Weber, I. T., Selk, L. M., Clawson, L., Schneider, J. & Kent, S. B. (1989). Conserved folding in retroviral proteases: crystal structure of a synthetic HIV-1 protease. *Science* **245**, 616-621.

Wlodawer, A. & Vondrasek, J. (1998). Inhibitors of HIV-1 protease: a major success of structure-assisted drug design. *Annu. Rev. Biophys. Biomol. Struct.* **27**, 249-284.

Wondrak, E. M., Nashed, N. T., Haber, M. T., Jerina, D. M. & Louis, J. M. (1996). A transient precursor of the HIV-1 protease. Isolation, characterization, and kinetics of maturation. *J. Biol. Chem.* **271**, 4477-4481.

Wong-Staal, F. & Gallo, R. C. (1985). Human T-lymphotropic retroviruses. *Nature* **317**, 395-403.

Wu, Y., Mikulski, S. M., Ardelt, W., Rybak, S. M. & Youle, R. J. (1993). A cytotoxic ribonuclease. Study of the mechanism of onconase cytotoxicity. *J. Biol. Chem.* **268**, 10686-10693.

Wu, Y., Saxena, S. K., Ardelt, W., Gadina, M., Mikulski, S. M., De Lorenzo, C., D'Alessio, G. & Youle, R. J. (1995). A study of the intracellular routing of cytotoxic ribonucleases. *J. Biol. Chem.* **270**, 17476-17481.

Yang, F., Moss, L. G. & Phillips, G. N., Jr. (1996). The molecular structure of green fluorescent protein. *Nat. Biotechnol.* **14**, 1246-1251.

Zeng, M., Huang, B. R. & Lapeyre, J. N. (1996). Cloning strategies using a third irrelevant enzyme site (TIES) to overcome certain cloning problems. *Biotechniques* **20**, 69-78.

Zhang, B., Kraemer, B., SenGupta, D., Fields, S. & Wickens, M. (1999). Yeast three-hybrid system to detect and analyze interactions between RNA and protein. *Methods Enzymol.* **306**, 93-113.

Zhang, Z. Y., Poorman, R. A., Maggiora, L. L., Heinrikson, R. L. & Kezdy, F. J. (1991). Dissociative inhibition of dimeric enzymes. Kinetic characterization of the inhibition of HIV-1 protease by its COOH-terminal tetrapeptide. *J. Biol. Chem.* **266**, 15591-15594.

Zhu, X. G., Hanover, J. A., Hager, G. L. & Cheng, S. Y. (1998). Hormone-induced translocation of thyroid hormone receptors in living cells visualized using a receptor green fluorescent protein chimera. *J. Biol. Chem.* **273**, 27058-27063.

Zukermann, R. N. & Schultz, P. G. (1988). A hybrid sequence-selective ribonuclease S. *J. Am. Chem. Soc.* **110**, 6592-6594.

Zutshi, R., Brickner, M. & Chmielewski, J. (1998). Inhibiting the assembly of protein-protein interfaces. *Curr. Opin. Chem. Biol.* **2**, 62-66.

Zutshi, R., Franciskovich, J., Shultz, M., Schweitzer, B., Bishop, P., Wilson, M. & Chmielewski, J. (1997). Targeting the dimerization interface of HIV-1 protease: Inhibition with cross-linked interfacial peptides. *J. Amer. Chem. Soc.* **119**, 4841-4845.